

TECHNISCHE UNIVERSITÄT MÜNCHEN

Lehrstuhl für Bodenkunde

Dynamic (redox) interfaces in soil - Carbon turnover of microbial residues and their impact on soil properties

Jan Achtenhagen

Vollständiger Abdruck der von der Fakultät Wissenschaftszentrum Weihenstephan für Ernährung, Landnutzung und Umwelt der Technischen Universität München zur Erlangung des akademischen Grades eines

Doktors der Naturwissenschaften

genehmigten Dissertation.

Vorsitzender: Univ.-Prof. Dr. J. Geist

Prüfer der Dissertation: 1. Univ.-Prof. Dr. I. Kögel-Knabner

2. apl. Prof. Dr. M. Kästner (Universität Leipzig)

Die Dissertation wurde am 27.10.2014 bei der Technischen Universität München eingereicht und durch die Fakultät Wissenschaftszentrum Weihenstephan für Ernährung, Landnutzung und Umwelt am 17.12.2014 angenommen.

Summary

Soil is the worlds largest terrestrial C pool. More than 2400 Pg C is stored in the upper 2 m, while the amount of C stored in the atmosphere only accounts for 720 Pg. Soil organic matter (SOM) has a tremendous impact on soil properties and ecosystem functions, like nutrient cycle and soil water balance and therefore on the growth of microorganisms and plants. Understanding how SOM is formed and stabilized in soils and its general dynamics are central to the welfare of mankind, food security and crucial with respect to climate change.

The parent material of SOM has impact on its chemical composition and thus on turnover processes. Recent studies have shown a significant microbial contribution to SOM. In particular, microbial residues consisting of cell envelope fragments were shown to accumulate in soil and contribute to SOM formation. Cell envelope fragments are in principle readily degradable and thus needs to be stabilized in soil. Previous studies have shown that the occlusion of organic matter due to co-precipitation can be considered as a strong stabilization mechanism. This process may also be a significant stabilization mechanism for microbial residues, as they are actually incrustated by mineral particles showing in several studies. SOM also controls physico-chemical soil properties, including the wettability of soil particle surfaces. Soil water repellency (SWR) is a widely observed phenomenon with severe impacts on water availability, biological activity and organic matter decomposition. Microorganisms are also affected by SWR because it induces water and osmotic stress for the microorganisms and thus induces changes in microbial community composition and activity. However, microorganisms are able to adapt to changing environmental conditions by an increase in cell surface hydrophobicity upon exposure to water and osmotic stress. Despite a large body of previous research, the molecular basis of SWR is not yet mechanistically understood and a mechanistic framework to explain the process of SWR development

is still a major field of research. As microorganisms and their residues are an important source of SOM, the attachment of cells and their residues, e.g., cell envelope fragments, on mineral grains should decrease wettability of minerals.

This thesis focused on the formation and degradation of cell envelope fragments in liquid cultures, artificial soil and natural soil in general, their stabilization by occlusion with Fe and Al oxyhydroxides and the impact of microbial residues and microorganisms on soil surface properties, in particular wettability.

The formation of fragmented cell envelopes as well as humic substances during growth and decay of microorganisms was analyzed and visualized in pure cultures of bacteria by means of scanning electron microscopy. In addition, the formation of microbial cell envelope fragments was elucidated in incubation experiments with artificial soils amended with pure cultures of model microorganisms. Using test systems characterized by an increasing complexity, it was possible to elucidate and characterize the formation of cell envelope fragments in detail. The decay of cells and the formation of microbially derived humic substances was observable and measured in pure cultures, while the formation of cell fragments was only observed in the presence of an additional support phase, e.g., mineral surfaces. The fragmentation process was observable for actinomycetes in artificial soils, while the high complexity and heterogeneity even of this simplified system prevented the visualization of cell fragments from other bacteria. However, evidence for the death and decay of microorganisms and the subsequent formation of cell envelope fragments was given by analyzing the phospholipid fatty acids and total fatty acids, as proxies for the living and dead biomass. A decrease in the phospholipid fatty acid concentrations was shown for all organisms.

The degradation of cell envelope fragments and co-precipitation as a relevant stabilization mechanism was tested by incubating ^{14}C -labeled bacterial cells *Escherichia coli* and cell en-

velope fragments alone or as co-precipitates with Fe or Al oxyhydroxides in soil. Various conditions were applied to investigate the effect of redox conditions, water content and C supply. The mineralization of cell fragments (29 %) was lower than that of intact cells (36 %). Cell fragments therefore seemed to be more resistant to biodegradation than bulk cell C, resulting in selective enrichment of cell envelope material. Co-precipitation with Fe and Al decreased the mineralization of intact cells and cell fragments by a factor of 2 to 4, indicating a strong protection of biomass. While reduced oxygen contents had no clear effect, water saturation as well as nutrient and substrate addition accompanied by decreasing redox potentials increased the mineralization, in particular of samples occluded by redox-sensitive Fe oxyhydroxides. This emphasizes that dissolution of Fe minerals is an important destabilization mechanism. As cell wall fragments are important SOM precursors, the occlusion of this material into Fe or Al oxyhydroxides may have a significant impact on soil C cycling and thus on SOM accumulation and CO₂ release from soil.

The influence of bacteria and their cell envelope fragments on the wettability of a variety of soil model minerals was tested by using *Pseudomonas putida*. In order to evaluate the principal processes, the physico-chemical modifications of soil minerals due to attachment of cells exposed to environmental stress were analyzed by mixing osmotically stressed or unstressed bacterial pure cultures. The impact on surface wetting properties was investigated by determining the solid-water contact angles (CA), as measurement to characterize surface wettability, on macro- and micro-scale. By the CA measurement, evidence was found for changes in macroscopic and microscopic wettability of model minerals induced by bacteria, cell envelopes and cytosol. This effect was influenced by bacterial response to osmotic stress. Attachment of bacteria to quartz surfaces resulted in a significant increase in hydrophobicity of the surfaces. The CA increased by up to 90° in particular for stressed cells, emphasizing the impact of stress adaptation of microorganisms on mineral surface properties. Both cell envelope fragments and cytosol were found to decrease wettability significantly (CA of up

to 100°). The observations on the macro-scale were paralleled by those on the micro-scale. The findings may explain various phenomena related to SWR, like critical soil water content and may be one important explanation for the formation of SWR after irrigation with treated sewage effluents. The results also support the hypothesis of a microbial origin of SWR, in which macromolecular biological structures like cell envelope fragments may have a great impact.

Overall, the results of this dissertation emphasize the importance of microbial residues as source for SOM (including humic substances), the occlusion of microbial residues into Fe and Al oxyhydroxides as particularly relevant stabilization mechanism and thus for SOM formation and stress furthermore the significant impact of microorganisms and their residues on soil wetting properties.

Zusammenfassung

Der Boden ist der weltweit größte terrestrische Kohlenstoffspeicher. In den oberen 2 m sind mehr als 2400 Pg Kohlenstoff gespeichert, während die Atmosphäre nur 720 Pg enthält. Die organische Bodensubstanz hat weitreichende Auswirkungen auf die Eigenschaften von Böden und deren Ökosystemfunktionen, wie z. B. den Nährstoffkreislauf, sowie den Bodenwasserhaushalt und dadurch auf das Wachstum von Mikroorganismen und Pflanzen im Allgemeinen. Ein Prozessverständnis für die Bildung und Stabilisierung der Bodensubstanz ist vor allem im Hinblick auf die Versorgung der Menschheit mit Nahrungsmitteln und den Klimawandel essentiell.

Das Ausgangsmaterial der organischen Bodensubstanz bestimmt deren chemische Zusammensetzung und die biologische Umsetzung. Eine Vielzahl von Studien betonen den mikrobiellen Einfluss auf die Bildung der organischen Bodensubstanz. Es wurde gezeigt, dass vor allem Fragmente von mikrobiellen Zellen angereichert im Boden vorliegen und zur Bildung der organischen Bodensubstanz beitragen. Die Fragmente sind aufgrund ihrer chemischen Zusammensetzung jedoch potentiell biologisch abbaubar und müssen im Boden stabilisiert werden. Die Stabilisierung organischer Substanz durch die Co-Präzipitation mit Ionen wurde in diversen Studien gezeigt. Dieser Prozess könnte auch wichtig für die Stabilisierung von mikrobiellen Rückständen im Boden sein. So wurde in Studien gezeigt, dass mikrobielle Rückstände durch mineralische Substanz inkrustiert werden. Die organische Bodensubstanz übt zudem Einfluss auf physiko-chemische Bodeneigenschaften, wie etwa die Benetzbarkeit, aus. Wasserabweisende Böden stellen ein weltweites Problem dar, da die Hydrophobizität die Wasserverfügbarkeit sowie die biologische Aktivität beeinflusst und dadurch auch den Abbau von organischen Substanzen im Boden im Allgemeinen. Die geringe Benetzbarkeit hat aufgrund der Induzierung von osmotischem Stress sowie von

Wasserstress auch einen Einfluss auf Mikroorganismen und verändert damit die Zusammensetzung der mikrobiellen Gemeinschaft und deren Aktivität. Mikroorganismen sind jedoch in der Lage sich an verändernde Umweltbedingungen anzupassen. Die stressbedingte Erhöhung der Hydrophobizität der Zellhülle ist dabei ein oft beobachteter Prozess. Die molekularen Ursachen für die wasserabweisenden Eigenschaften von Böden sind trotz großer Anstrengungen noch nicht aufgeklärt. Zudem fehlt ein Verständnis für die Prozesse, die zur Ausprägung der Hydrophobizität führen. Da Mikroorganismen und deren Rückstände eine wichtige Quelle für die organische Bodensubstanz darstellen, sollten die Interaktionen zwischen Zellen bzw. Zellrückständen und mineralischen Oberflächen in Böden daher die Benetzbarkeit dieser Oberflächen verändern.

Die vorliegende Dissertation untersucht die Bildung und den Abbau von Zellhüllfragmenten in Flüssigkulturen sowie künstlichen und natürlichen Böden, deren Stabilisierung durch die Co-Präzipitation mit Fe- und Al-Oxyhydroxiden und die Auswirkung von mikrobiellen Rückständen auf die Benetzbarkeit von Bodenmineralen.

Die Bildung der Fragmente sowie von Huminstoffen beim Wachstum und Absterben von Mikroorganismen wurde in Flüssigkulturen untersucht und mittels Rasterelektronenmikroskopie visualisiert. Die Bildung von mikrobiellen Fragmenten der Zellhüllen wurde in Inkubationsexperimenten mit künstlichen Böden untersucht, die mit Reinkulturen unterschiedlicher Modell-Mikroorganismen versetzt waren.

Durch die Verwendung von unterschiedlich komplexen Testsystemen war es möglich, die Bildung der mikrobiellen Fragmente zu untersuchen und charakterisieren. Der Abbau von Bakterienzellen und die Bildung mikrobieller Huminstoffe wurde in Flüssigkulturen nachgewiesen. Der Zerfall der Zellhüllen in Fragmente wurde im Beisein einer zusätzlichen Oberfläche, wie der Oberfläche von Mineralen, gezeigt. Der Zerfallsprozess konnte in den künstlichen Böden bei Actinomyceten visualisiert werden, während dies bei den anderen

Modell-Bakterien durch den hohen Grad an Heterogenität und Komplexität der Böden nicht möglich war. Das Absterben und der anschließende Zerfall konnte jedoch durch die Analyse der Phospholipid- und Gesamtfettsäuren, welche stellvertretend für lebende und abgestorbene Mikroorganismen stehen, gezeigt werden. Es wurde für alle Organismen eine Verringerung der Phospholipid-Konzentrationen über die Zeit verzeichnet.

Der Abbau von mikrobiellen Zellfragmenten und der Einfluss der Co-Präzipitation auf den Abbau wurde in Experimenten mit ^{14}C -markierten *Escherichia coli* Zellen und Zellfragmenten untersucht. Die Biomasse wurde mit Fe- und Al-Oxyhydroxiden gefällt und im Boden inkubiert. Die Inkubation erfolgte mit unterschiedlichen Randbedingungen um den Einfluss von Redox-Bedingungen, Wassergehalt und zusätzlicher Zugabe von Kohlenstoff auf den Abbau zu ermitteln.

In den Experimenten wurden Zellfragmente (29 %) langsamer mineralisiert als intakte Bakterienzellen (36 %), was eine Akkumulation von Fragmenten im Boden zur Folge hat. Die Co-Präzipitation mit Al- und Fe-Oxyhydroxiden führte zu einer Verringerung der Mineralisierung um den Faktor 2 bis 4 im Vergleich zur Kontrolle ohne Minerale und stellt demnach einen effektiven Stabilisierungsmechanismus dar. Eine Verringerung des O_2 -Gehaltes hatte nur einen geringen Einfluss auf den Abbau, während die Wassersättigung des Bodens mit anschließender Zugabe von zusätzlichem Kohlenstoff (Glucose) und einer Senkung des Redoxpotentials, den Abbau beschleunigte. Dies wurde vor allem in Ansätzen mit redox-sensitiven Fe-Co-Präzipitaten beobachtet. Die Auflösung dieser Präzipitate stellt daher einen wichtigen Destabilisierungsmechanismus dar. Zellfragmente sind somit wichtige Ausgangsstoffe für die Bildung der organischen Bodensubstanz und die in dieser Arbeit beschriebenen Mechanismen haben einen signifikanten Einfluss auf den Kohlenstoffkreislauf im Boden und dadurch auf die Akkumulierung von organischer Bodensubstanz und des CO_2 -Ausstoßes von Böden im Allgemeinen.

Der Einfluss von Bakterienzellen und Zellresten auf die Benetzbarkeit unterschiedlicher Bodenminerale wurde mit *Pseudomonas putida* untersucht. Dabei wurden osmotisch gestresste oder ungestresste Zellen mit den Mineralen gemischt, um den Einfluss der Zellen und ihrer Stressadaption auf die Benetzbarkeit zu ermitteln. Die Benetzbarkeit der Modellminerale wurde durch die Messung des Kontaktwinkels auf der Mikro- und Makroskala untersucht. Durch die Messungen konnte gezeigt werden, dass die Benetzbarkeit der mineralischen Oberflächen durch die Interaktion mit Bakterienzellen, Zellfragmenten und Cytosol verringert wird. Zudem hatte die Erhöhung der Zellhydrophobizität von Bakterien, als Adaptionmechanismus in Gegenwart von osmotischem Stress, einen Einfluss auf die Benetzbarkeit der organo-mineralischen Assoziationen. Der Kontaktwinkel der Minerale erhöhte sich im Beisein von Bakterien auf bis zu 90°. Dies war vor allem bei gestressten Zellen ausgeprägt. Eine Erhöhung des Kontaktwinkels auf 100° war in der Gegenwart von Zellfragmenten und Cytosol zu verzeichnen. Beide Effekte ließen sich auf makroskopischer und mikroskopischer Ebene beobachten. Aufgrund dieser Ergebnisse lassen sich verschiedene Erscheinungen wasserabweisender Böden, wie z. B. der kritische Bodenwassergehalt oder die Ausbildung von Hydrophobizität nach Bewässerung mit behandeltem Abwasser, ganz oder teilweise erklären.

Die Ergebnisse der vorliegenden Dissertation zeigen, dass mikrobielle Rückstände eine wichtige Quelle für die organische Bodensubstanz und Huminstoffe darstellen. Sie zeigen zudem, dass der Einschluss der Rückstände in Fe- und Al-Oxyhydroxiden ein wichtiger Mechanismus zur Stabilisierung der organischen Bodensubstanz ist und die Ausprägung wasserabweisender Böden einen mikrobiellen Ursprung haben kann.

Contents

Summary	I
Zusammenfassung	V
List of Figures	XIII
List of Tables	XXI
List of abbreviations	XXIII
1 Introduction	1
1.1 Benefits and functions of soil organic matter	1
1.2 Molecular structure of soil organic matter	2
1.3 Soil organic matter stabilization and transformation	3
1.4 Contribution of microbial residues to soil organic matter formation	5
1.5 Soil water repellency	7
1.6 Artificial soils	10
2 Aims and Hypotheses	11
3 Materials and Methods	15
3.1 Chemicals and test organisms	15
3.2 Culture conditions	15
3.2.1 Growth media	15
3.2.2 Pure cultures for artificial soils incubation experiments	15
3.2.3 Culture conditions for osmotically stressed <i>Pseudomonas putida</i>	18
3.2.4 ¹⁴ C-labeling of <i>Escherichia coli</i>	18
3.3 Preparation of cell envelope fragments	19

3.4	pH and redox potential measurement	19
3.5	Model minerals	20
3.6	Preparation of ¹⁴ C-labeled organo-oxyhydroxide co-precipitates	21
3.7	Preparation of organo-mineral associations for wettability measurements . .	22
3.8	Artificial soils and natural soil under study	22
3.9	Preparation of soil extract	23
3.10	Incubation studies in liquid cultures, artificial and natural soil	24
3.10.1	Formation of humic substances in liquid cultures	24
3.10.2	Incubation of bacteria in liquid pure cultures	24
3.10.3	Incubation of bacterial cells and cell envelope fragments in artificial soils	25
3.10.4	Incubation of ¹⁴ C-labeled biomass in soil	25
3.11	Chemical analyses	27
3.11.1	Humic substances fractionation and total organic carbon measurement	27
3.11.2	Analysis of fatty acids	27
3.11.3	¹⁴ C activity measurement in liquid and soil samples	29
3.12	Visualization and surface characterization	29
3.12.1	Scanning electron microscopy	29
3.12.2	Macroscopic water contact angle measurement	30
3.12.3	Environmental scanning electron microscopy	31
3.13	Surface coverage determination, data analysis and statistics	31
4	Results and Discussion	33
4.1	Formation and turnover of cell envelope fragments	33
4.1.1	Formation of humic substances during growth and decay of bacteria in liquid cultures	33

4.1.2	Formation of cell envelope fragments during growth and decay of pure cultures of bacteria	38
4.1.3	Formation and stability of cell envelope fragments in artificial soils . .	48
4.1.4	Turnover of intact bacterial cells and their fragments in closed natural soil systems	61
4.2	Stabilization of microbial residues in soil	65
4.3	Impact of microbial residues on soil wettability	73
5	Conclusions and Synthesis	87
5.1	Formation and turnover of cell envelope fragments	87
5.2	Stabilization of microbial residues	87
5.3	Impact of microbial residues on soil wettability	88
5.4	Synthesis	89
	Appendix	91
	Bibliography	95
	Publications and Presentations	115
	Danksagung (Acknowledgements)	117
	Curriculum Vitae	119

List of Figures

Fig. 1	Conceptual models of soil organic matter: “Molecular aggregate” model (Wershaw, 2004) and “Humic Polymer” model; modified from Baldock and Nelson (2000) and Kleber and Johnson (2010).	3
Fig. 2	Conceptual model of organic matter stabilization according to von Lüt-zow et al. (2008).	4
Fig. 3	The cell envelope fragments formation cycle and the contribution to soil organic matter (SOM); modified from Miltner et al. (2012).	6
Fig. 4	Impact of soil water repellency on processes relevant for organic matter decomposition and water regime in soil (Goebel et al., 2011).	7
Fig. 5	Zonal model of organo-mineral associations (Kleber et al., 2007).	9
Fig. 6	Total organic carbon (TOC) of different fractions (fulvic acids (FA), humic acids (HA), humin (H)) in medium inoculated with a soil extract before (black bars) and after 2 weeks (grey bars) incubation. Different letters indicate significant differences between incubation time ($P < 0.05$). . . .	34
Fig. 7	Total organic carbon (TOC) of different fractions (fulvic acids (FA), humic acids (HA), humin (H)) in pure cultures of <i>E. coli</i> before (black bars), after 2 weeks (light grey bars) and 2 months (dark grey bars) incubation. Different letters indicate significant differences between incubation time ($P < 0.05$).	35
Fig. 8	Total organic carbon (TOC) of different fractions (fulvic acids (FA), humic acids (HA), humin (H)) in pure cultures of <i>B. subtilis</i> before (black bars), after 2 weeks (light grey bars) and 2 months (dark grey bars) incubation. Different letters indicate significant differences between incubation time ($P < 0.05$).	35

-
- Fig. 9 Different fractions of humic substance extraction: culture inoculated with soil extract before (a) and after (b) incubation; soil extract inoculum (c); fulvic acids (d), humic acids (e) and humin (f). Culture inoculated with *E. coli* after incubation (g), and humic acids (h) and culture inoculated with *B. subtilis* after incubation (i) and humic acids (j). 37
- Fig. 10 Scanning electron micrographs of cell envelope fragments of (a) *E. coli* and (b) *P. putida* attached to medium-grained quartz surfaces. 39
- Fig. 11 Scanning electron micrographs of *E. coli* at the (a) beginning and after (c) 1 d and (e) 16 d incubation and *P. putida* at the (a) beginning and after (d) 1 d and (f) 16 d incubation in liquid pure cultures. Cells are attached to Poly-D-lysine coated glass slides. 41
- Fig. 12 Scanning electron micrographs of *E. coli* at the (a) beginning and after (b) 6 d and (c) 13 d incubation in liquid pure cultures. 42
- Fig. 13 Scanning electron micrographs of *E. coli* after (a) 4.5 h, (c) 24 h and (e) 35 d and *P. putida* after (b) 4.5 h, (d) 24 h and (f) 35 d incubation in liquid pure cultures. Cells are attached to added medium-grained quartz surfaces (MQ). Micrographs (g, h) is MQ without attached biomass after 35 d incubation. Black circles indicate cell envelope fragments. 44
- Fig. 14 Scanning electron micrographs of *E. coli* after (a) 5 d and (b) 12 d incubation in liquid pure cultures supplemented with additional Mg^{2+} and Ca^{2+} . Cells are attached to added medium-grained quartz surfaces. Black circles indicate cell envelope fragments. 45
- Fig. 15 Scanning electron micrographs of *P. putida* at the (a, b) beginning and after (c, d) 16 d, (e, f) 35 d and (g, h) 98 d incubation on Poly-D-lysine coated glass slides. Black circles indicate cell envelope fragments. 46

-
- Fig. 16 Scanning electron micrographs of *E. coli* at the (a) beginning and after (c) 50 d, and *P. putida* at the (b) beginning and after (d) 50 d incubation on medium-grained quartz surfaces. 47
- Fig. 17 Scanning electron micrographs of artificial soil 1 (AS1) without biomass addition at the beginning and after (c) 8 weeks incubation. 49
- Fig. 18 Scanning electron micrographs of intact cells of *P. putida* at the (a) beginning and after (c) 8 weeks, and cell envelope fragments at the (b) beginning and after (d) 8 weeks incubation in artificial soil 1 (AS1). White circles indicate intact cells. 50
- Fig. 19 Relative percentages of different phospholipid fatty acids (PLFA) in incubation studies with (a) intact cells and (b) cell envelope fragments of *P. putida* before (black bars) and after (grey bars) 32 weeks incubation in artificial soil 1 (AS1). 52
- Fig. 20 Scanning electron micrographs of (a) intact cells of *B. subtilis* and (b) cell envelope fragments at incubation start in artificial soil 1 (AS1). 53
- Fig. 21 Relative percentages of different phospholipid fatty acids (PLFA) in incubation studies with (a) intact cells and (b) cell envelope fragments of *B. subtilis* before (black bars) and after (grey bars) 32 weeks incubation in artificial soil 1 (AS1). 54
- Fig. 22 Scanning electron micrographs of intact cells of *B. subtilis* at the (a) beginning and after (c) 8 weeks, and cell envelope fragments at the (b) beginning and after (d) 8 weeks incubation in artificial soil 2 (AS2). White circles indicate intact cells. 55
- Fig. 23 Relative percentages of different phospholipid fatty acids (PLFA) in incubation studies with a) intact cells and b) cell envelope fragments of *B. subtilis* before (black bars) and after (grey bars) 32 weeks incubation in artificial soil 2 (AS2). 56

-
- Fig. 24 Scanning electron micrographs of intact cells of *S. mirabilis* at the (a) beginning and after (c) 32 weeks, and cell envelope fragments at the (b) beginning and after (d) 32 weeks incubation in artificial soil 1 (AS1). White circles indicate intact cells or cell envelope fragments. 57
- Fig. 25 Relative percentages of different phospholipid fatty acids (PLFA) in incubation studies with (a) intact cells and (b) cell envelope fragments of *S. mirabilis* before (black bars) and after (grey bars) 32 weeks incubation in artificial soil 1 (AS1). 59
- Fig. 26 Cumulative mineralization of intact ¹⁴C-labeled *E. coli* cells (black circles) and cell envelope fragments (white circles) in soil incubation studies under (a) oxic and (b) O₂ depleted conditions. Arrows indicate time of nutrient and substrate addition (C, N, P) and the dotted areas water saturation. 63
- Fig. 27 Cumulative mineralization of intact ¹⁴C-labeled *E. coli* cells (black circles) and cell envelope fragments (white circles) with (a) co-precipitation with Fe oxyhydroxide or (b) co-precipitation with Al oxyhydroxide, in soil incubation studies under aerobic conditions. Arrows indicate additional nutrient and substrate addition (C, N, P). 66
- Fig. 28 Cumulative mineralization of intact ¹⁴C-labeled *E. coli* cells (black circles) and cell envelope fragments (white circles) with (a) co-precipitation with Fe oxyhydroxide or (b) co-precipitation with Al oxyhydroxide, in soil incubation studies under O₂ depleted conditions. Arrows indicate time of nutrient and substrate addition (C, N, P) and the dotted areas water saturation. 68

-
- Fig. 29 Occlusion and incrustation of microbial residues, e.g., cell envelope fragments, by co-precipitation with Al and Fe oxyhydroxides as a mechanism for soil organic matter stabilization. Reduced dissolved metal ions can migrate into the cell wall structures or accumulate at the surfaces, where they precipitate leading to strongly restricted access of potential degrading hydrolytic enzymes to the biomass. 72
- Fig. 30 Scanning electron micrographs of unstressed *P. putida* cells (a, b), osmotically stressed cells (c, d) and cell envelope fragments (e, f) attached to medium-grained quartz surfaces. In micrographs a, c and e, the concentration is 10^8 cells g^{-1} and in b, d and f, the concentration is 10^9 cells g^{-1} quartz. The smaller micrographs were taken at a higher magnification. 74
- Fig. 31 Contact angle of *P. putida* (Bac) and medium-grained quartz (MQ) and coarse-grained quartz (CQ)/*P. putida* (unstressed cells (black bars) and osmotically stressed cells (grey bars)) - associations after 2 h drying. Different letters indicate significant differences between cell concentrations (lower case letters apply to unstressed cells, upper case letters to stressed cells) and asterisks between unstressed and stressed cells of the same cell concentration ($P < 0.05$). 75
- Fig. 32 Contact angle of *P. putida*/mineral associations in relation to surface coverage with bacteria and corresponding fittings. (a) medium-grained quartz (MQ), unstressed cells; (b) MQ, osmotically stressed cells; (c) coarse-grained quartz (CQ), unstressed cells; (d) CQ, osmotically stressed cells. 76

-
- Fig. 33 Contact angle of *P. putida* (Bac) and fine-grained quartz (FQ) and kaolinite (KA)/*P. putida* (unstressed cells (black bars) and osmotically stressed cells (grey bars)) - associations after 2 h drying. Different letters indicate significant differences between cell concentrations (lower case letters apply to unstressed cells, upper case letters to stressed cells) and asterisks between unstressed and stressed cells of the same cell concentration ($P < 0.05$). 78
- Fig. 34 Contact angle of *P. putida* cell envelope fragments (CF), cytosol (CY), mixture of cell envelope fragments and cytosol (CF/CY) and bovine serum albumin (BSA; hatched bar)/medium-grained quartz (MQ) - associations after 2 h drying. Different bacteria concentrations were used (10^8 : black bars; 10^9 : light grey bars; 10^{10} cells g^{-1} mineral: dark grey bars). Different letters indicate significant differences between lowest cell concentration of each treatment and control (MQ) and asterisks between cell concentrations of the same treatment ($P < 0.05$). 79
- Fig. 35 Micrographs from condensation experiments in an environmental scanning electron microscope with unstressed *P. putida* cells (a, b), osmotically stressed cells (c, d), cell fragments (e, f) and cytosol (g, h) as organic coatings. The mineral phase is medium-grained quartz. In micrographs a, c, e and g, the concentration is 10^8 cells g^{-1} and in b, d, f and h, the concentration is 10^9 cells g^{-1} mineral. 81
- Fig. 36 Modified cell envelope fragments formation cycle from Miltner et al. (2012). The occlusion of cell envelope fragments is next to sorption of those on mineral surfaces an important stabilization mechanism, which is dependent on oxic and anoxic conditions in soil. The stabilized residues have influence on physical surface properties like soil water repellency. 90

-
- Fig. 37 Scanning electron micrographs of unstressed *P. putida* cells (a, b), and stressed cells (c, d). The mineral phase is coarse-grained quartz. In micrographs a and c, the concentration is 10^8 cells g^{-1} and in b and d, the concentration is 10^9 cells g^{-1} mineral. The smaller micrographs were taken with a higher magnification. 93
- Fig. 38 Micrographs from condensation experiments in an environmental scanning electron microscope with unstressed *P. putida* cells (a, b) and stressed cells (c, d) as organic coatings. The mineral phase is coarse quartz. In micrographs a and c, the concentration is 10^8 cells g^{-1} and in b and d, the concentration is 10^9 cells g^{-1} mineral. 94

List of Tables

Tab. 1	Composition of mineral medium 1 according to Hartmans et al. (1989). . .	16
Tab. 2	Composition of nutrient medium (DSMZ medium 1) (DSMZ, 2014). . . .	16
Tab. 3	Composition of GYM streptomyces medium (DSMZ medium 65) (DSMZ, 2014).	16
Tab. 4	Composition of modified M9 medium according to Studier and Moffatt (1986).	17
Tab. 5	Composition of optimized mineral medium according to Kindler et al. (2006).	17
Tab. 6	Properties of incubation studies in artificial soils.	26
Tab. 7	Concentrations of phospholipid fatty acids (PLFA) and total fatty acids (tFA) of the incubation studies with artificial soils after different times of incubation (n/a: not applicable).	60
Tab. 8	Residual activities (% of total activity) and recovery rates of the incubation experiments with ¹⁴ C-labeled <i>E. coli</i> (n/a: not applicable).	92

List of abbreviations

AS1:	artificial soil 1
AS2:	artificial soil 2
BSA:	bovine serum albumin
CA:	contact angles
CQ:	coarse-grained quartz
DOM:	dissolved organic matter
EPS:	extracellular polymeric substances
ESEM:	environmental scanning electron microscopy
FA:	fatty acids
FAME:	fatty acid methyl esters
FH:	ferrihydrite
FQ:	fine-grained quartz
GC-MS:	gas chromatography coupled to mass spectrometry
KA:	kaolinite
MON:	montmorillonite
MQ:	medium-grained quartz
NanoSIMS:	nano-scale secondary ion mass spectrometry
OM:	organic matter
PBS:	phosphate-buffered saline
PDL:	poly-D-lysine
PLFA:	phospholipid fatty acids
SEM:	scanning electron microscopy
SOM:	soil organic matter
SSA:	specific surface area
SWR:	soil water repellency

tFA: total fatty acids

TOC: total organic carbon

WHC: maximum water holding capacity

1 Introduction

1.1 Benefits and functions of soil organic matter

Soils carry the worlds largest terrestrial C pool. About 1500 Pg C is stored in the upper 100 cm of soil and another 910 Pg is stored between 100 and 200 cm (Batjes, 1996), while the amount of C stored in the atmosphere is only 720 Pg (Falkowski, 2000). Soil organic matter (SOM) has a tremendous impact on soil properties and ecosystem functions (Baldock and Nelson, 2000). It affects the growth of plant and microorganisms, provides structural stability of soil aggregates, directly influences soil water retention and contributes to the cation exchange capacity of soils (Baldock and Nelson, 2000). Understanding how SOM is stabilized in soils and its general dynamics is central to the welfare of mankind and crucial with respect to climate change (von Lützow et al., 2006; Kleber and Johnson, 2010; Schmidt et al., 2011). According to Kleber and Johnson (2010) there are three major reasons for the importance of understanding soil C dynamics. This knowledge will allow (1) predicting how the stored C responds to climate change (von Lützow et al., 2006; Heimann and Reichstein, 2008); (2) developing approaches to sequester atmospheric C in soil to mitigate climate change (Lal, 2004b) and (3) maintaining soil fertility by ensuring nutrient release and microbial activity and thus establishing strategies for a proper management of soils with respect to a sustainable agriculture and food security (Sleutel et al., 2003; Lal, 2004a; Bellamy et al., 2005; Stewart et al., 2007). In general, soil acts as regulatory center for the majority of ecosystem services, because it provides the substrate for most human activities (Barrios, 2007). For example, agricultural ecosystems are supported by soil services like nutrient cycling, soil structure and fertility, while the agriculture provides the provisioning services like food, fiber and fuel production (Zhang et al., 2007).

1.2 Molecular structure of soil organic matter

There are two general, but competing molecular models to describe the physical nature of SOM (Kleber and Johnson, 2010). The “humic polymer” model builds on the assumption that humic molecules of SOM are produced by secondary synthesis, i.e., humic macromolecules are polymerized from smaller molecules. These are metabolic products of plant litter decomposition, mainly breakdown products of proteins, polysaccharides or lignin (Oades, 1989; Hayes and Swift, 1990). An inherent stability, which is called recalcitrance, of the humic macromolecules due to their structure can be derived from the model (Kleber and Johnson, 2010). The so called humic substances can be characterized by a sequential extraction procedure, which is based on the solubility of the material under alkaline or acid conditions. The three fractions obtained are the fulvic acids, humic acids and humin (Sutton and Sposito, 2005). These fractions are only operationally defined and may be affected by artifacts. In addition, existence of three distinct compound classes has not been yet been proven (Baldock and Nelson, 2000; Kelleher and Simpson, 2006). There are furthermore arguments challenging the relevance of the extracted substances in natural soil environments (Baldock and Nelson, 2000). The competing and more recent model is the “molecular aggregate” model, which is proposed by Wershaw (2004). It implies that SOM is composed of partial degradation products of plant polymers like lignin. The “molecular aggregate” model disclaims the secondary synthesis and favors that SOM mainly consists of small molecules in supramolecular associations. Therefore, a recalcitrance of molecules cannot be derived by the model and other stabilization mechanisms are required. According to Wershaw (2004), SOM mainly consists of plant litter, living and dead microorganisms, organo-mineral associations, black C and metal-organic precipitates or complexes (Fig. 1).

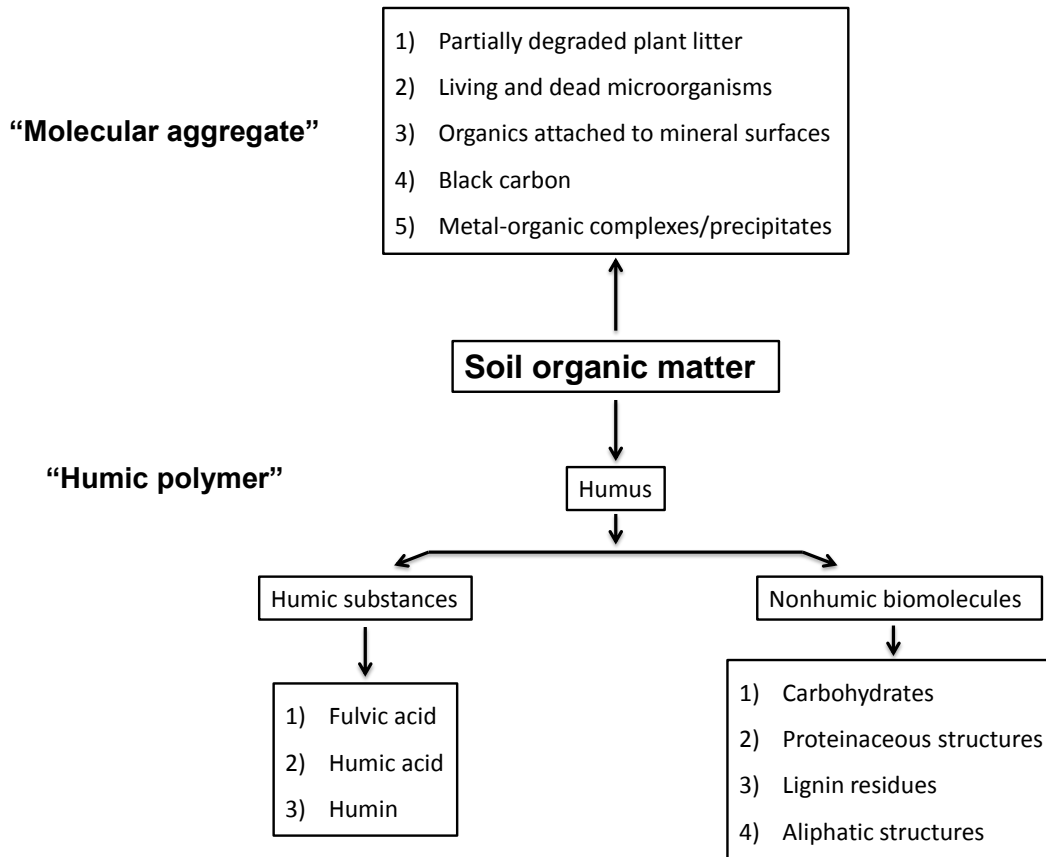


Fig. 1: Conceptual models of soil organic matter: "Molecular aggregate" model (Wershaw, 2004) and "Humic Polymer" model; modified from Baldock and Nelson (2000) and Kleber and Johnson (2010).

1.3 Soil organic matter stabilization and transformation

In general, the inputs for SOM are plant and microbial residues (Kögel-Knabner, 2002; Miltner et al., 2012). The residues are stabilized by different mechanisms such as interactions with mineral surfaces and complexation with metal ions and selective preservation and resynthesis, including primary and secondary recalcitrance (Sollins et al., 1996; von Lützow et al., 2006, 2008; Marschner et al., 2008) (Fig. 2). In particular, organo-mineral interactions were revealed as the main stabilization mechanism in incubation experiments because they reduce the attack by hydrolytic enzymes and reduce the availability of organic molecules

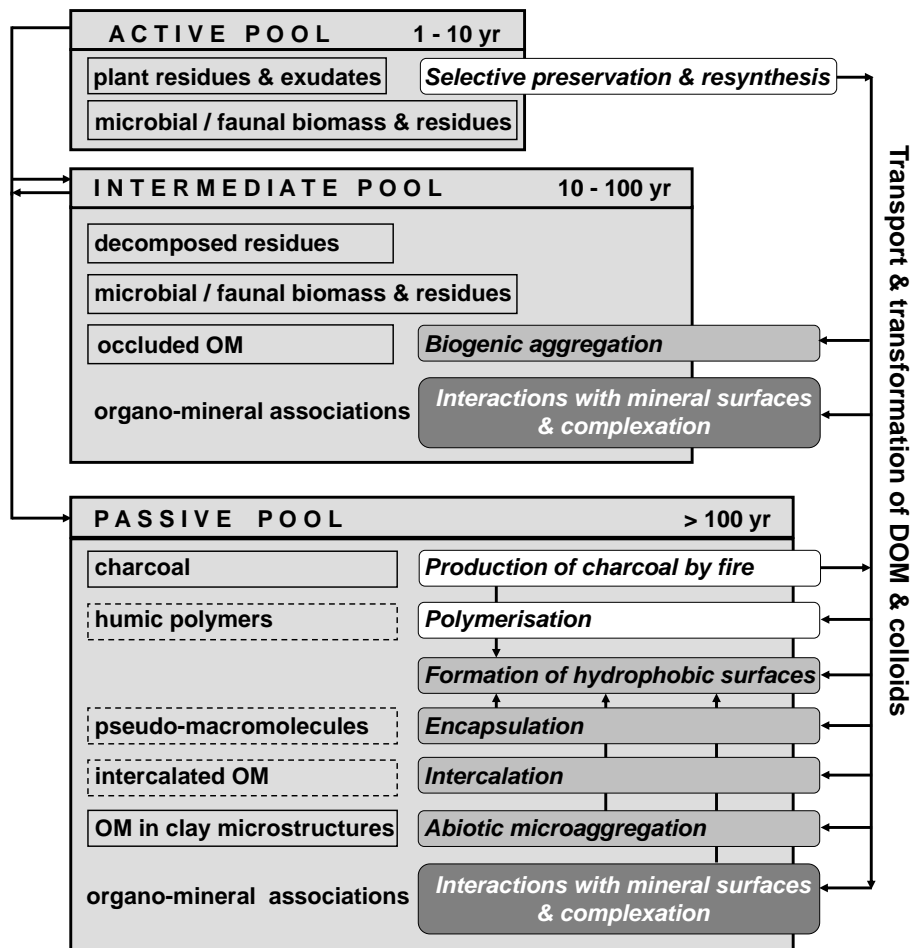


Fig. 2: Conceptual model of organic matter stabilization according to von Lützow et al. (2008).

(Miltner and Zech, 1999; Kalbitz et al., 2005; Kaiser and Guggenberger, 2007; Kögel-Knabner et al., 2008). The preservation of organic matter (OM) may occur via sorptive interactions due to strong multiple bonds of small organic molecules to mineral surfaces or via diffusion of OM into very small pores < 20 nm (Mayer, 1994; Kaiser and Guggenberger, 2007; Kögel-Knabner et al., 2008). Surfaces of oxides and hydroxides of Fe and Al are particularly able to create strong bonds with OM and therefore provide a strong protection against biodegradation (Kögel-Knabner et al., 2008). The importance of Fe and Al oxides and hydroxides were also shown for the stabilization of dissolved organic matter (DOM) by

sorptive interactions or co-precipitation (Kaiser and Guggenberger, 2000; Scheel et al., 2007). The protective effect of co-precipitation was shown for citric acid with non-crystalline Al hydroxide, allophane and imogolite as mineral phases (Boudot, 1992) and extracellular polymeric substances (EPS) with amorphous Al hydroxide as mineral phase (Mikutta et al., 2011). However, many previous studies dealing with EPS (Omoike and Chorover, 2006; Mikutta et al., 2011; Liu et al., 2013) are using *Bacillus subtilis* cultures that lyse during sporulation directly forming cell lysates and not EPS in a microbiological definition. Fe and Mn oxides and hydroxides are known to be redox-sensitive. At the same time, the redox potential also affects the activity of transformation processes by microorganisms, which can in turn adapt to fluctuations of redox potential (Mihelic and Luthy, 1988; Pett-Ridge et al., 2006; Thompson et al., 2006; DeAngelis et al., 2010). Oscillations of redox potential may even occur in microniches of oxic soils, because the interior of macroaggregates may become oxygen depleted due to microbial activity and low gas diffusivity in these aggregates (Zausig et al., 1993). The oscillation of the redox conditions affects Fe mineralogy by dissolution and precipitation (Pallud et al., 2010). The redox potential of soils is therefore an important factor for SOM stabilization and persistence (Schmidt et al., 2011). For the global C cycle destabilizing processes like dissolution of protecting minerals have been reported to be even more important than stabilizing mechanisms (Sollins et al., 2007).

1.4 Contribution of microbial residues to soil organic matter formation

Several studies emphasized the importance of the microbial impact on SOM formation (Schimel et al., 2007; Simpson et al., 2007; Miltner et al., 2012; Schurig et al., 2013; Schütze et al., 2013). Nearly 50 % of humic acids extracted from soil samples were shown to be of microbial origin (Simpson et al., 2007). It was estimated that 80 % of the soil organic C may

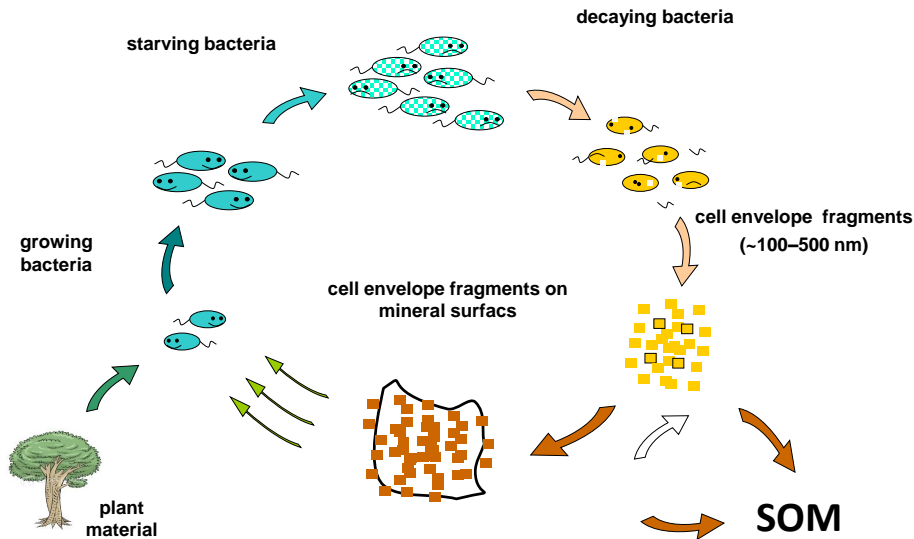


Fig. 3: The cell envelope fragments formation cycle and the contribution to soil organic matter (SOM); modified from Miltner et al. (2012).

be derived from microbial necromass, assuming microbial living biomass C is 2% of the total soil organic C and necromass amounts to 40 times the biomass (Liang and Balsler, 2011). The microbial contribution to the C pools and fluxes is therefore much higher than expected (Kästner, 2000). In particular, microbial residues consisting of cell envelope fragments were shown to contribute to SOM formation (Schimel et al., 2007; Miltner et al., 2012; Schurig et al., 2013; Schütze et al., 2013). The accumulation of cell envelope fragments during pedogenesis was visualized by scanning electron microscopy (Schurig et al., 2013). Miltner et al. (2012) proposed a conceptual mechanism describing the formation and stabilization of microbial cell envelope fragments in soil (Fig. 3). The contribution of cell envelope fragments to SOM formation is also supported by the observed accumulation of amino sugars, which are biomarkers for cell envelope residues, with depth in soil (Guggenberger et al., 1999). More evidence was given by incubation studies with ^{13}C -labeled bacterial cells (*Escherichia coli*), which showed a transfer of up to 40% of the label to non-living SOM (Kindler et al., 2006). Results from the same experiments also revealed the stability of peptides from intact microbial biomass emphasizing the contribution to SOM formation (Miltner et al., 2009).

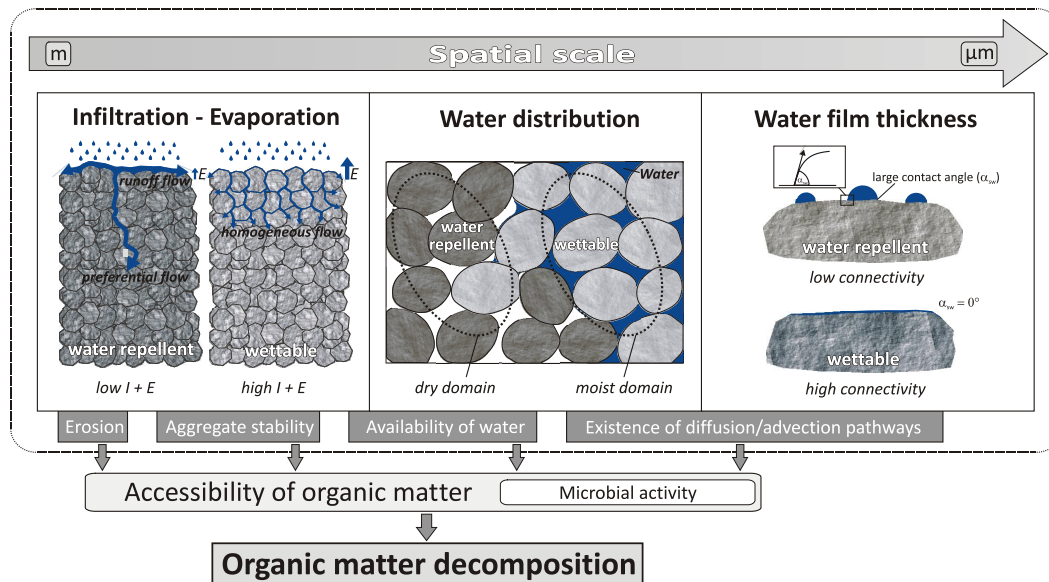


Fig. 4: Impact of soil water repellency on processes relevant for organic matter decomposition and water regime in soil (Goebel et al., 2011).

1.5 Soil water repellency

SOM also controls physico-chemical soil properties, including the wettability of soil particle surfaces (Bisdorf et al., 1993). The interactions between SOM and mineral surfaces may induce soil water repellency (SWR), a worldwide observed phenomenon, which has been reported for a vast variety of soils, e.g., silty clay or sandy loam soils (Dekker et al., 1999; Dekker and Ritsema, 2000; Doerr et al., 2000). SWR has macroscopic effects, like decreased water infiltration into topsoil and increased surface runoff, erosion and evaporation (Doerr et al., 2000; Goebel et al., 2011) (Fig.4). Due to its impact on the water availability and water film thickness on minerals, the biological activity and OM decomposition is influenced to a large extent (Churaev, 2000; Feeney et al., 2006; Goebel et al., 2011). SWR affects the water distribution on the micro-scale and can exclude large areas from water and nutrient flow on the macro-scale (Doerr et al., 2000; Goebel et al., 2005, 2007). If agricultural soils are affected, crop growth can be severely inhibited by SWR, resulting in enormous economic

damage (Blackwell, 2000). Microorganisms are also affected by SWR, because it induces water and osmotic stress with severe impact on the affected microbial community and its activity (Feeney et al., 2006; Schimel et al., 2007). However, microorganisms are able to adapt to changing environmental conditions by modifications of their surface properties, e.g., by an increase in cell surface hydrophobicity upon exposure to water stress, which is a widely observed and well described stress response (Lopez et al., 2000; Wick et al., 2003; Neumann et al., 2006; Baumgarten et al., 2012a,b). Changes in the structure of lipopolysaccharides and releases of membrane vesicles were described as underlying mechanisms (Al-Tahhan et al., 2000; Kulp and Kuehn, 2010; Baumgarten et al., 2012a). As mentioned before, microbial residues, in particular cell envelope fragments, were reported to be a significant part of SOM. The chemical components of the residues include various amphiphilic molecules (Miltner et al., 2012). Studies revealed amphiphilic molecules like phospholipid fatty acids (PLFA) and proteins to be effective in producing hydrophobic coatings and to be important constituents of SOM (Wershaw, 1993; Doerr et al., 2000; Horne and McIntosh, 2000; Hurrass and Schaumann, 2006; Kleber et al., 2007; Mayes et al., 2013). The main approach to study the chemical structure of substances inducing SWR is based on extraction of SWR affected soil material with organic solvents and subsequent application of the organic extract to hydrophilic minerals to induce SWR (Ma'Shum et al., 1988; Doerr et al., 2000). By this method, several compound classes like alkanes, alkanols, fatty acids (FA), sterols and waxes were identified to be able to induce SWR (Franco et al., 2000; Horne and McIntosh, 2000; Mainwaring et al., 2004). However, the origin of these compounds cannot be identified and were mostly considered to be plant derived. Based on the assumption that amphiphilic compounds are effective in producing hydrophobic surfaces, Horne and McIntosh (2000) proposed a zonal model, comprised of layers of amphiphilic compounds with either the polar or the apolar part of the molecule directed towards the surface, which explains the formation of hydrophobic coatings after drying. A structurally similar model was later suggested by Kleber et al. (2007) to describe the zonal structure of organo-mineral associations

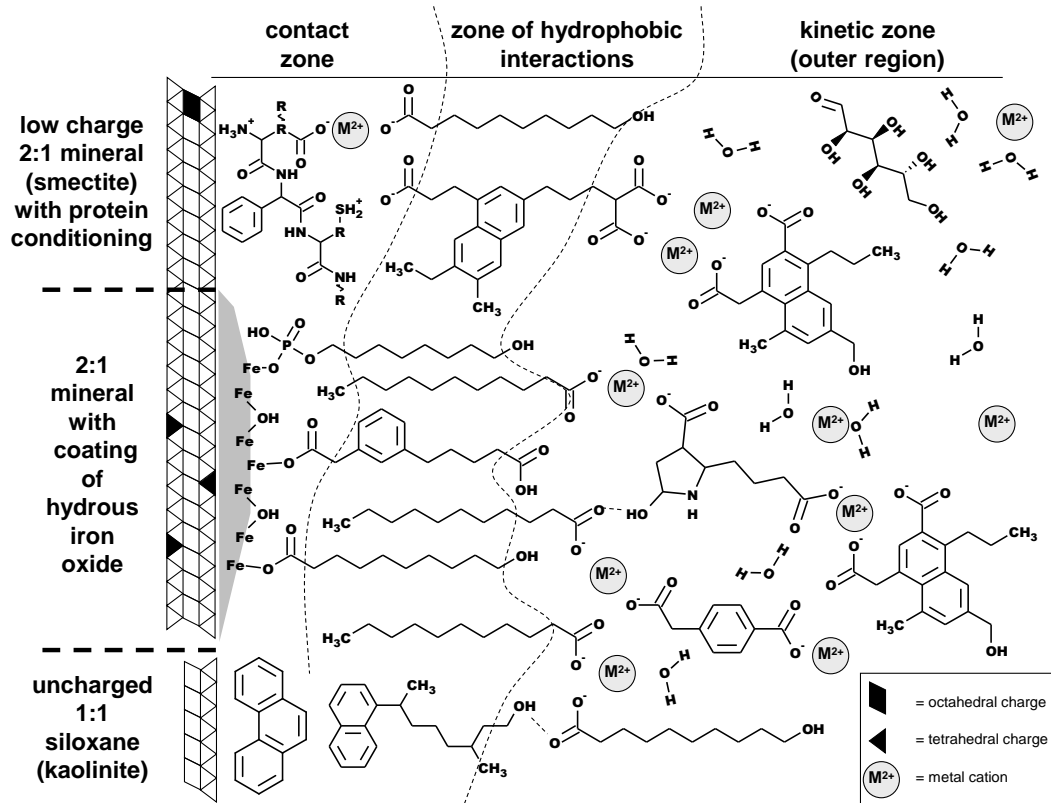


Fig. 5: Zonal model of organo-mineral associations (Kleber et al., 2007).

(Fig. 5). The structural arrangement of SOM components thus can inherently control soil particle surface wettability. In order to optimize soil management strategies to maintain soil functions and fertility, the development of a mechanistic framework to explain formation of SWR is desired. Despite high research efforts, up to now the molecular basis and the underlying mechanisms of SWR development is not yet mechanistically understood and still a major field in soil research (Mainwaring et al., 2004; Graber et al., 2009).

1.6 Artificial soils

Investigating processes such as SWR development in real soils is difficult because soil has a very complex structure and composition. In fact, it can be seen as the most complicated biogenic material on the planet (Young and Crawford, 2004). For a better mechanistic understanding of underlying processes of SOM formation and soil development, a reduction of complexity and exclusion of unpredictable abiotic factors and material can be helpful with regards to experimental approaches (Pronk et al., 2012). In addition to soil chronosequences, which allow studying initial interactions between minerals and OM during pedogenesis, artificial soils with pure minerals and defined microbial inoculum as well as OM can be useful to study the very initial stages of organo-mineral associations (Dümig et al., 2011; Pronk et al., 2012; Schurig et al., 2013). This approach was recently used to study the formation of organo-mineral associations and biogeochemical interfaces, aggregates, microbiological processes in general, the decomposition of OM and the response of microbial communities to polycyclic aromatic hydrocarbons (Totsche et al., 2010; Guenet et al., 2011; Pronk et al., 2012; Babin et al., 2013; Wei et al., 2014). In the present thesis, the concept of artificial soils was also used to study the formation of microbial residues, in particular the cell envelope fragments and to determine the contribution of different types of microorganisms to microbial necromass. A further reduction of complexity was obtained by exclusion of the mineral phase and the exclusive use of pure cultures of microorganisms.

2 Aims and Hypotheses

Based on the identification of research gaps in chapter 1, the aim of the present thesis was to evaluate (1) the formation and turnover of cell envelope fragments in general, (2) their stabilization in soil and (3) their impact on selected physical soil properties. In order to obtain these aims, the following research hypotheses were tested:

1. Formation and turnover of microbial cell envelope fragments
 - a) The growth and decay of microorganisms in artificial soils and in pure cultures is accompanied by the formation of cell envelope fragments and of humic substances.
 - b) Half-lives of fragmented cell envelopes are longer than those of intact bacterial cells, which may promote their accumulation.

Microbial necromass may originate from different groups of microorganisms, e.g., fungi, Gram-negative and Gram-positive bacteria, which cover the three principal types of cell walls. The formation of microbial cell envelope fragments from these major types of microbial cell wall structures was elucidated in incubation experiments with artificial soils amended with pure cultures of model microorganisms. PLFA and total fatty acids (tFA) were analyzed as proxies for the decay of microorganisms. The formation of cell envelope fragments was visualized by means of scanning electron microscopy (SEM). In addition, the formation of fragmented cell envelopes as well as humic substances during growth and decay of microorganisms was analyzed and visualized in pure cultures of bacteria. The turnover of cell envelope fragments as well as intact cells was tested using ^{14}C -labeled *E. coli* cells in incubation experiments in natural soils. Although their decay has already been investigated by various groups this was done only using freeze-dried fragments or non-native biomass enabling a

more rapid turnover compared to fresh biomass (Marumoto et al., 1977; Nakas and Klein, 1979; Cortez, 1989).

2. Stabilization of microbial biomass in soil

- a) Occlusion and incrustation of microbial cell envelope fragments and intact bacterial cells by co-precipitation with Al and Fe oxyhydroxides has a protective effect against degradation.
- b) Changes in redox condition affect the stabilization of biomass protected by redox-sensitive Fe oxyhydroxides.

Microbial cell envelope fragments themselves can act as matrix for the incrustation by Fe and Si. This process was already shown for fragments of *Streptomyces* spp., where the incrustation and occlusion of macromolecular cell architecture by inorganic material was clearly visible (Schütze et al., 2013). The occlusion due to co-precipitation can be considered as a strong stabilization mechanism. This process might be even more effective than sorptive interactions of organic molecules with mineral surfaces, which is the generally considered stabilization mechanism. The redox potential as an important factor for SOM stabilization and persistence may also affect the co-precipitated organo-mineral associations (Schmidt et al., 2011). The stabilizing effect of co-precipitation of microbial residues with Fe and Al oxyhydroxides was thus investigated in degradation experiments using ^{14}C -labeled biomass co-precipitated with the oxyhydroxides and incubated under various levels of oxygen.

3. Impact on soil surface properties (wettability)

- a) Interactions of intact bacterial cells and their envelope fragments with soil minerals change the surface wettability of the mineral particles.

-
- b) Osmotic-stress induced changes of bacterial surface properties are reflected in surface properties of organo-mineral associations and thus, when stabilized in soil, affect soil mineral wettability.

Microbial necromass and living bacterial cells may influence physical soil properties like the wettability of the mineral phase. Therefore, the influence of bacteria and their cell envelope fragments on the wettability of soil model minerals was tested. In order to evaluate the principal processes, the physico-chemical modifications of bacterial surfaces due to environmental stress were analyzed by exposing bacterial pure cultures to osmotic stress and subsequently mixing them with several model minerals. The microscopic and macroscopic contact angles (CA), a measure for SWR, of the organo-mineral associations were determined by environmental scanning electron microscopy (ESEM) and by the sessile drop method, respectively. In addition, SEM was used to characterize the surface coverage by structures in the sub- μm size range.

3 Materials and Methods

3.1 Chemicals and test organisms

All chemicals and organisms were obtained from commercial sources. *Pseudomonas putida* mt-2 (Gram-negative bacterium; DSM 3931), *B. subtilis* (Gram-positive bacterium; DSM 357) and *Streptomyces mirabilis* (Gram-positive actinomycete; DSM 40 553) were obtained from DSMZ (Braunschweig, Germany). *E. coli* K12 (Gram-negative bacterium) was obtained from the culture collection of the Department of Environmental Microbiology-UFZ (Leipzig, Germany).

3.2 Culture conditions

3.2.1 Growth media

Different media were used for the growth and incubation experiments with microorganisms (Tab. 1–Tab. 5). All media were prepared with demineralized water and sterilized before usage.

3.2.2 Pure cultures for artificial soils incubation experiments

For artificial soil incubation studies cells of *P. putida* (mineral medium 1 with 4 g L⁻¹ disodium succinate, Tab. 1), *B. subtilis* (nutrient medium, Tab. 2) and *S. mirabilis* (GYM streptomyces medium, Tab. 3) were grown until late stationary phase at 30 °C on a horizontal shaker in order to obtain high yields at defined growth conditions and harvested by centrifugation

Tab. 1: Composition of mineral medium 1 according to Hartmans et al. (1989).

Substance	Concentration
$(\text{NH}_4)_2\text{SO}_4$	2 g L^{-1}
K_2HPO_4	1.6 g L^{-1}
$\text{NaH}_2\text{PO}_4 \cdot 2\text{H}_2\text{O}$	0.85 g L^{-1}
$\text{MgCl}_2 \cdot 6\text{H}_2\text{O}$	0.1 g L^{-1}
EDTA	10 mg L^{-1}
$\text{FeSO}_4 \cdot 7\text{H}_2\text{O}$	5 mg L^{-1}
$\text{ZnSO}_4 \cdot 7\text{H}_2\text{O}$	2 mg L^{-1}
$\text{CaCl}_2 \cdot 2\text{H}_2\text{O}$	1 mg L^{-1}
$\text{MnCl}_2 \cdot 2\text{H}_2\text{O}$	1 mg L^{-1}
$\text{CoCl}_2 \cdot 6\text{H}_2\text{O}$	0.4 mg L^{-1}
$\text{CuSO}_4 \cdot 5\text{H}_2\text{O}$	0.2 mg L^{-1}
$\text{Na}_2\text{MoO}_4 \cdot 2\text{H}_2\text{O}$	0.2 mg L^{-1}

Tab. 2: Composition of nutrient medium (DSMZ medium 1) (DSMZ, 2014).

Substance	Concentration
Soya peptone	5 g L^{-1}
Meat extract	3 g L^{-1}

Tab. 3: Composition of GYM streptomycetes medium (DSMZ medium 65) (DSMZ, 2014).

Substance	Concentration
Malt extract	10 g L^{-1}
$\text{C}_6\text{H}_{12}\text{O}_6$	4 g L^{-1}
Yeast extract	4 g L^{-1}

Tab. 4: Composition of modified M9 medium according to Studier and Moffatt (1986).

Substance	Concentration
Na ₂ HPO ₄	6 g L ⁻¹
KH ₂ PO ₄	3 g L ⁻¹
NH ₄ Cl	1 g L ⁻¹
NaCl	0.5 g L ⁻¹
MgSO ₄ ·7H ₂ O	0.12 g L ⁻¹
CaCl ₂	10 mg L ⁻¹

Tab. 5: Composition of optimized mineral medium according to Kindler et al. (2006).

Substance	Concentration
Na ₂ HPO ₄	6.97 g L ⁻¹
K ₂ HPO ₄	3.42 g L ⁻¹
NH ₄ Cl	1 g L ⁻¹
NaCl	0.5 g L ⁻¹
MgCl ₂ ·7H ₂ O	0.2 g L ⁻¹
CaCl ₂	0.1 g L ⁻¹
FeSO ₄	10 mg L ⁻¹
MnSO ₄	0.2 mg L ⁻¹
ZnSO ₄	0.2 mg L ⁻¹

(5000 g, 15 min). The resulting cell pellet was washed three times with phosphate-buffered saline (PBS; 8 g NaCl, 0.2 g KCl, 1.44 g Na₂HPO₄, 0.24 g KH₂PO₄, 1 L demineralized water, pH 7.4). The cells were stored at 4 °C until start of incubation studies.

3.2.3 Culture conditions for osmotically stressed *Pseudomonas putida*

P. putida was cultivated in mineral medium 1 (Tab. 1) with 4 g L⁻¹ disodium succinate as sole C and energy source. Cells were grown in a baffled flask on a horizontal shaker at 30 °C. For inducing osmotic stress, 1.25 M NaCl (final concentration) was added at the early exponential growth phase. The control cells were obtained by growth without additional NaCl. After 2 h incubation, the cells were harvested by centrifugation (10 000 g, 10 min) and washed three times with 10 mM KNO₃. The cell pellet was finally resuspended with 10 mM KNO₃ and stored for further analysis.

3.2.4 ¹⁴C-labeling of *Escherichia coli*

Modified M9 medium (Tab. 4) amended with 2 g L⁻¹ D-glucose was used for growth of *E. coli*. For the labeling procedure, 1 L glass bottles containing 300 mL medium were inoculated with 5 % (v/v) of an overnight culture in the same medium. U-¹⁴C labeled D-glucose (Biotrend, Cologne, Germany) was used as a radiotracer. The specific activity of the tracer was 9.25–13.3 GBq mmol. The tracer was dissolved in EtOH:H₂O (9:1) to obtain an activity of 37 MBq mL⁻¹ and further dissolved in demineralized water to obtain the working standard with an activity of 4.2 MBq mL⁻¹. ¹⁴C glucose working standard was added in order to obtain an activity of 1.5–1.8 MBq per bottle. Cultures were incubated on a horizontal shaker at 30 °C. Labeled cells were grown until the late stationary phase was reached in

order to obtain high yields at defined growth conditions. Cells were harvested by centrifugation (2500 g, 15 min) and washed three times with sufficient 0.9 % NaCl to remove adhering nutrients and label. The harvested biomass contained 32 to 42 % of the added ^{14}C activity. Unlabeled cells as a control were prepared by the same procedure but without addition of ^{14}C glucose.

3.3 Preparation of cell envelope fragments

Cell envelope fragments were produced by ultrasonic disruption (Sonopuls HD 70, Bandelin electronics, Berlin, Germany). Briefly, portions of 500 μL cell suspensions of *E. coli*, *B. subtilis* or *P. putida* were ultrasonically disrupted (five steps, 1 min each step, on ice and 30 s cooling breaks between disruption cycles to prevent overheating, 30 % power, 50 % interval) and washed two times with demineralized water (10 000 g, 20 min). Preliminary tests with ^{14}C -labeled *E. coli* have shown a residual activity of about 10 % of the initially added activity in the remaining fragments (data not shown).

Fragments of *S. mirabilis* were produced by ultrasonic treatment (two steps, 10 min each step, 75 % power, 50 % interval) and additional glass beads. The fragments were then washed three times with demineralized water.

3.4 pH and redox potential measurement

The pH was measured according to ISO (2005). Briefly, 10 g soil was mixed with 50 mL of 0.01 M CaCl_2 . The suspension was shaken for 1 h on a horizontal shaker and left standing for 2 h without further shaking. The pH of the water saturated samples was directly measured using a pH electrode (SenTix[®] 41, WTW, Weilheim, Germany).

The device was calibrated with buffer solutions (pH 4 and pH 9) prior to measurements for quality assurance. All measurements were conducted in duplicate.

The redox potential of water saturated soil samples was measured using a redox electrode (SenTix® ORP, WTW, Weilheim, Germany). The testing time was 15 min and the device was calibrated using a redox buffer solution prior to measurement.

3.5 Model minerals

Coarse-grained quartz (CQ, Carl Roth GmbH, Karlsruhe, Germany) and a washed and calcined medium-grained quartz (MQ, Merck KGaA, Darmstadt, Germany) were chosen as representative material for two different sand fractions. Fine-grained quartz (FQ, Carl Roth GmbH, Karlsruhe, Germany), kaolinite (KA, Fluka, Sigma-Aldrich, St. Louis, USA) and montmorillonite (MON, Sigma-Aldrich, St. Louis, USA) were chosen as model minerals for the silt and clay fraction, respectively. For artificial soil incubation studies, MON was transferred into its Ca^{2+} form by a method modified from Rabung et al. (2005). Briefly, MON was mixed with 0.5 M CaCl_2 and subsequently stirred overnight. Then, the suspension was three times washed with demineralized water to get rid of excessive ions.

Ferrihydrite (FH) was chosen as a reactive and representative Fe mineral and synthesized according to the protocol for the synthesis of 2-line FH described by Schwertmann and Cornell (2000). Briefly, 10 g $\text{Fe}(\text{NO}_3)_3 \cdot 9\text{H}_2\text{O}$ was dissolved in 125 mL demineralized water. The pH was adjusted to 7–8 with 1 M KOH. Samples were centrifuged (2500 g, 5 min) and washed three times with demineralized water. Then, the suspension was dialyzed against demineralized water for 4 d, washed with demineralized water and freeze-dried. The specific surface area (SSA) of the minerals was determined by BET measurement with a Nova 4000e (Quantachrome, Odelzhausen, Germany) after drying of the minerals at 105 °C.

The corresponding areas were: CQ: $0.17 \text{ m}^2 \text{ g}^{-1}$, MQ: $0.35 \text{ m}^2 \text{ g}^{-1}$, FQ: $1.06 \text{ m}^2 \text{ g}^{-1}$, KA: $8.92 \text{ m}^2 \text{ g}^{-1}$. The SSA of MON was assumed to be $274 \text{ m}^2 \text{ g}^{-1}$ (Madurai et al., 2011).

3.6 Preparation of ^{14}C -labeled organo-oxyhydroxide co-precipitates

Four different precipitates were used for the incubation experiments. Fe oxyhydroxide precipitates were synthesized according to the protocol for the synthesis of 2-line FH described by Schwertmann and Cornell (2000). The protocol is described in 3.5. ^{14}C -labeled intact cells and cell fragments were added prior to pH adjustment. No further dialysis and drying was performed to prevent artifacts.

Al oxyhydroxides precipitates were synthesized according to Okada et al. (2002). Briefly, 50 mL 0.5 M $\text{Al}(\text{NO}_3)_3 \cdot 9\text{H}_2\text{O}$ was mixed with 50 mL 0.5 M NaAlO_2 . A suspension containing either intact cells or cell fragments was added and the pH adjusted to 9 with 5 M NaOH. The precipitates were aged at 60°C for 20 h. The samples were washed three times with demineralized water (2500 g, 5 min) to remove free bacteria, fragments and excessive ions, in particular nitrate. In order to prevent drying artifacts, the complexes were not dried. During the co-precipitation procedure, virtually the entire radioactive label remained within the precipitates (data not shown). All precipitates were used for incubation tests as described in 3.10.4.

3.7 Preparation of organo-mineral associations for wettability measurements

Unstressed and stressed cells of *P. putida*, prepared as described in 3.2.3, were diluted with 100 μL 10 mM KNO_3 and added to 500 mg of the mineral phase to be studied (CQ, MQ, FQ, KA) while gently stirring to prevent damage of the cells and release of cytosolic substances. The concentrations of cells used for the experiment were 10^8 , 10^9 and 10^{10} cells g^{-1} mineral. Cell numbers were previously estimated by optical density measurement and cross-checked by using a Coulter counter Multisizer 3 (Beckman Coulter, High Wycombe, U.K).

Cell fragments and cytosolic compounds from unstressed bacteria were separated by ultrasonic disruption, as described in 3.3. The pellet containing the cell envelope fragments was finally stored in 100 μL KNO_3 . For obtaining the cytosolic compounds, the supernatant of the first centrifugation step after ultrasonic disruption was collected (about 0.5 mL). Aliquots of 100 μL were used for the experiments. As a protein standard, bovine serum albumin (BSA, 100 $\mu\text{g mL}^{-1}$) was used. Cell envelope fragments, supernatant and BSA were finally mixed with 500 mg of the mineral phase. All organo-mineral associations (three replicates for each treatment) were air dried for 2 h at room temperature ($\sim 22^\circ\text{C}$, $\sim 60\%$ relative humidity) before further analysis as described in 3.12.2.

3.8 Artificial soils and natural soil under study

Two different artificial soils were chosen for incubation studies. Artificial soil 1 (AS1) consisted of 80 % CQ, 19 % MON and 1 % FH (w:w:w). The SSA was about $50 \text{ m}^2 \text{ g}^{-1}$. AS1 was supplemented with 0.2 % CaCO_3 to raise the pH (CaCl_2) to 6.5. The second artificial soil

(AS2) was a mixture of 59 % CQ, 35 % FQ, 5 % KA and 1 % FH (w:w:w:w) to get a soil with a lower SSA (about $0.9 \text{ m}^2 \text{ g}^{-1}$).

The incubation experiments with ^{14}C -labeled *E. coli* biomass were conducted with a silt loam soil collected from the A horizon of a Haplic Phaeozem at the agricultural long-term experiment “Statischer Düngungsversuch” in Bad Lauchstädt, Germany. Since 1902, this soil has been fertilized with farmyard manure (30 t ha^{-1} every second year). The plot was cropped with a rotation of winter wheat, sugar beet, summer barley and potatoes. The soil contained 21 % clay, 68 % silt, 11 % sand, 1.7 g kg^{-1} total N and 21 g kg^{-1} organic C (Blair et al., 2006). The pH (CaCl_2) was 6.6 and the maximum water holding capacity (WHC) was reached at a gravimetric water content of 37.5 %. Soil samples were stored at 4°C . Prior to incubation tests, samples were sieved through a 2 mm screen and preconditioned for 3 d at room temperature.

3.9 Preparation of soil extract

Soil extract was obtained by mixing “Bad Lauchstädt” soil with 0.2 % $\text{Na}_4\text{P}_2\text{O}_7$ 1:1 (w:w). Then, the suspension was shaken on an end-over-end shaker for 24 h at 60 rpm and subsequently centrifuged (960 g, 5 min) to remove coarse soil particles. The supernatant was centrifuged again for 15 min at 5000 g. The harvested cell pellet was dissolved in demineralized water and stored at 4°C . The soil extract was used as inoculum to investigate the formation of humic substances in liquid cultures (3.10.1) and as supplement for the artificial soils (3.10.3).

3.10 Incubation studies in liquid cultures, artificial and natural soil

3.10.1 Formation of humic substances in liquid cultures

E. coli, *B. subtilis* and soil extract were used as inoculums to investigate the formation of humic substances during the incubation of liquid cultures. 1 L baffled flasks containing 300 mL mineral medium (Tab. 1) were inoculated with 5% (v/v) of an overnight culture of *E. coli*, *B. subtilis* or 2% (v/v) with a soil extract. 5 g L⁻¹ glucose was used as sole C and energy source. The cultures were incubated on a horizontal shaker at 30 °C. Three 30 mL sample aliquots were taken after 2 weeks and 2 months incubation and sequentially fractionated into fulvo acids, humic acids and humin as described in 3.11.1.

3.10.2 Incubation of bacteria in liquid pure cultures

For incubation studies, *P. putida* and *E. coli* were cultivated in mineral medium 1 (Tab. 1) with 4 g L⁻¹ disodium succinate or 5 g L⁻¹ D-glucose as sole C and energy source, respectively. Cells were grown in baffled flasks with 200 mL growth medium on a horizontal shaker at 30 °C. 20 g L⁻¹ sterile MQ was added for testing the influence of a mineral phase on the formation of microbial cell envelope fragments. Sterile growth media without added cells was taken as a control. 0.5 mL sample aliquots were taken at every sampling point and fixed as described in 3.12.1. The fixed cells were transferred on Poly-D-lysine (PDL) coated glass slides and critical point dried as described in 3.12.1 after fixation. The samples with MQ were washed three times with PBS after fixation and stored. The same incubation studies were repeated with *E. coli* and optimized mineral medium with higher concentrations of Ca²⁺ and Mg²⁺ (Tab. 5). Furthermore, fixed cells were directly critical point dried without the transfer to PDL coated glass slides to prevent losses of cell envelope fragments.

In a further approach, 1.5 mL of early stationary phase *P. putida* cells were washed three times with 0.9 % NaCl and stored in 500 μ L NaCl. 20 μ L aliquots were put on PDL slides and incubated in closed glass petri dishes at 20 °C in darkness. The same test was repeated with 0.8 g MQ instead of PDL slides and *P. putida* or *E. coli* as test organisms. Furthermore, the cell-mineral associations were incubated without shaking at 30 °C. No washing step was performed after harvesting. All samples were further processed as described in 3.12.1.

3.10.3 Incubation of bacterial cells and cell envelope fragments in artificial soils

The test organisms, either as intact cells or cell envelope fragments were vigorously mixed with the artificial soils by using an agitating machine. Different combinations were performed, which are listed in Tab. 6. Soil extract was added dropwise to obtain an extracted soil:artificial soil ratio of 1:1 (w:w). The water contents of the mixtures were adjusted with 0.01 M CaCl₂ to ~60 % WHC. The bottles were aerated every week to obtain aerobic incubation conditions. Every 4 weeks, the water loss of the soils was compensated with demineralized water. Samples were taken after 0, 8, 16 and 32 weeks incubation.

3.10.4 Incubation of ¹⁴C-labeled biomass in soil

For incubation experiments, 25 g soil samples were mixed with ¹⁴C-labeled bacteria or cell fragments (6×10^8 cells g⁻¹ soil dry weight [dw]) or 1 % (w/w) organo-mineral coprecipitates, and the water content was adjusted to 60 % of the WHC with demineralized water. The soil samples with an activity of ~3 kBq (corresponding to 0.6 mg *E. coli* biomass g⁻¹ soil [dw]) were transferred into 500 mL glass bottles. Soil samples amended with unlabeled bacteria were used as controls. Test tubes with 10 mL 1 M NaOH were used to trap the ¹⁴CO₂. In order to maintain oxic conditions, the bottles of the oxic treatment were flushed

Tab. 6: Properties of incubation studies in artificial soils.

Organism	Cell status	Artificial soil ¹	Cells g ⁻¹ soil (dw) ²	C _{mic} [μg g ⁻¹ soil (dw)] ³
No organism	n/a ⁴	AS1	n/a	n/a
<i>P. putida</i>	intact	AS1	1.6 × 10 ¹⁰	2700
<i>P. putida</i>	fragments	AS1	n/a ⁵	1130
<i>B. subtilis</i>	intact	AS1	2.5 × 10 ⁹	208
<i>B. subtilis</i>	fragments	AS1	n/a	62.4
<i>B. subtilis</i>	intact	AS2	10 ¹⁰	856
<i>B. subtilis</i>	fragments	AS2	n/a	367
<i>S. mirabilis</i>	intact	AS1	4 × 10 ⁹	344
<i>S. mirabilis</i>	fragments	AS1	n/a	216

¹ see 3.8

² assuming 5.9 × 10¹⁰ cells nmol PLFA (Green and Scow, 2000)

³ dry weight

⁴ not applicable

⁵ cell envelope fragments were produced from the same number of intact cells

with humidified air weekly. In order to ensure an O₂ depleted atmosphere, the bottles for this treatment were flushed with humidified N₂. The degradation tests were run for 98 (Fe treatments) or 101 d (Al and control treatments). All treatments were run in triplicates. After 98 (Fe oxyhydroxide treatments) or 101 d (other treatments), 10 g soil samples (dw) were removed from the incubation bottles. The remaining soil samples of the N₂ atmosphere samples were mixed with 25 mL degassed demineralized water (dissolved O₂: 0.1 mg L⁻¹) in order to obtain a soil:water ratio of 1:1.7. Both the oxic and submerged samples were further incubated for another 182 d. After this incubation period, the effect of easily-available

substrates on the stability of the residual activity was tested. To this end, four portions of 25 mg D-glucose, $(\text{NH}_4)_2\text{SO}_4$ and K_2HPO_4 (8:1.3:0.2 [w:w:w], (ISO, 2003)) were added to the samples after 0, 11, 15 and 19 d. After the last amendment, the samples were incubated further 18 d .

3.11 Chemical analyses

3.11.1 Humic substances fractionation and total organic carbon measurement

For the fractionation of liquid cultures into fulvic acids, humic acids and humin a modified method of Swift (1996) was used. Briefly, 30 mL samples were mixed under N_2 with 100 mL freshly prepared 0.5 M NaOH and end-over-end shaken for 18 h at 60 rpm. Then, the samples were centrifuged at 15 min at 9600 g and the supernatants transferred into glass bottles. The remaining pellets (humic fraction) were resuspended in 40 mL demineralized water and stored frozen until further analysis. The supernatants were acidified to pH 1 with 6 M HCl, centrifuged (10 000 g, 20 min) and the precipitates (humic acid fraction) dissolved in 25 mL 0.1 M NaOH. The remaining supernatants were the fulvic acid fraction. The total organic carbon (TOC) was determined in a final step for all fractions by using a TOC analyzer (Shimadzu, TOC 600, Duisburg, Germany) and the “total C-inorganic C” method.

3.11.2 Analysis of fatty acids

The PLFA were extracted from 2 g soil samples by adding a mixture of 2 mL PBS, 5 mL MeOH and 2.5 mL chloroform (Bligh and Dyer, 1959; Zelles, 1997). Samples were shaken for 2 h, then additional 2.5 mL demineralized water and 2.5 mL chloroform were added. The organic phases were transferred to new glass vials and evaporated under N_2 . The samples

were resuspended in 1 mL chloroform and separated into glycolipids, neutral lipids and PLFA according to Frostegård et al. (1991) by chromatography over silica filled columns (Unisil, Clarkson Chromatography Products Inc., South Williamsport, USA) previously treated and washed with 0.02 M ammonium acetate in MeOH. The three FA fractions were eluted with 5 mL chloroform, 5 mL acetone and 15 mL MeOH. The PLFA-containing MeOH fraction was collected and evaporated under N₂ and the PLFA subsequently derivatized. Therefore, dried samples were resuspended in 500 µL MeOH/trimethylchlorosilane (9:1 [v:v]) and the PLFA methylated for 2 h at 60 °C to fatty acid methyl esters (FAME). The remaining supernatants were evaporated under N₂ and the residues dissolved in 100 µL hexane with 10 µg heneicosanoate methyl ester (FAME 21:0) as an internal standard. The tFA were directly methylated by adding 2 mL MeOH/trimethylchlorosilane (9:1 [v:v]) to air-dried soil samples and subsequent incubation for 2 h at 70 °C. The FAME were extracted from soil according to Miltner et al. (2004) with diethyl ether and purified over silica gel columns (Baker, Avantor Performance Materials, Center Valley, USA). The eluates were evaporated under N₂ and the residues dissolved in 200 µL hexane with 20 µg FAME 21:0. The FAME were analyzed by means of gas chromatography coupled to mass spectrometry (GC-MS) (Agilent GC7890A and MS5975C, Agilent Technologies, Santa Clara, USA). The temperature program for GC-MS (HP-5MS column) was: initial temperature at 50 °C for 1 min, heat to 250 °C at 4 °C min⁻¹, heat to 300 °C at 20 °C min⁻¹ and hold for 10 min. The inlet temperature was 280 °C and the injector at splitless mode and the MS-source at 230 °C. FAME were identified by comparison of mass spectra from a library and retention times of a standard mixture containing typical bacterial acid methyl esters (BAME Mix, Sigma-Aldrich, St. Louis, USA) and quantified in relation to the internal standard. All PLFA and tFA analyses were conducted in triplicates.

3.11.3 ^{14}C activity measurement in liquid and soil samples

The NaOH used for trapping the $^{14}\text{CO}_2$ was changed periodically. Aliquots of 0.5 mL were gently mixed with 5 mL Ultima Gold (PerkinElmer, Waltham, USA) and the activities measured with a Wallac 1414 scintillation counter (PerkinElmer, Waltham, USA; 5 min with chemiluminescence correction).

For measuring the radioactivity, solid samples were oxidized using a biological oxidizer (OX-500, Harvey Instrument Corporation, Tappan, USA). Dried and crushed soil (100 mg; two aliquots of each sample) was added to a ceramic sample holder and thoroughly mixed with 10 mg cellulose. The samples were combusted at 900 °C in an O_2 stream of 380 mL min^{-1} for 4 min. The evolved $^{14}\text{CO}_2$ was trapped in 15 mL scintillation cocktail (Oxysolve-C400, Zinsser Analytic GmbH, Frankfurt, Germany) and scintillation counted.

3.12 Visualization and surface characterization

3.12.1 Scanning electron microscopy

Aliquots of samples were fixed with 2.5 % (w/w) glutaraldehyde in PBS. After 6 h fixation, the fixative was replaced with fresh glutaraldehyde and subsequently fixed overnight at 4 °C. Samples from the incubation studies in liquid cultures (3.10.2) were fixed using freshly prepared 4 % formaldehyde/1 % glutaraldehyde (w/w) in PBS. Afterward the samples were washed three times with PBS and dehydrated by a graded acetone series. The solution was exchanged every 30 min by a solution with a higher acetone concentration (25, 25, 30, 50, 60, 70, 80, 90, 100, 100, 100 % [v/v]) (Schurig et al., 2013) and dried using critical point drying (Leica EM CPD300, Wetzlar, Germany or Emitech K850, Quorum Technologies Ltd., Ashford, UK). Samples on PDL coated glass slides were dehydrated by a graded EtOH

series (25, 50, 70, 90, 100, 100%[v/v]) and critical point dried as described above. All samples were coated with an Au layer (Sputtercoater SCD 50, Bal-Tec, Liechtenstein) and analyzed by means of SEM with an Ultra 55 (Carl Zeiss, Oberkochen, Germany) and the following settings: gun voltage: 1 kV, system vacuum: 10^{-8} Pa, detector: secondary electron 2, noise reduction: frame average/line average.

3.12.2 Macroscopic water contact angle measurement

As a measure for cell surface hydrophobicity, the CA of the bacteria was measured with the sessile drop method as described by van Loosdrecht et al. (1987). Briefly, bacterial cells were spread on 0.45 μm pore size filters (Schleicher & Schuell, Dassel, Germany) by means of filtration. The filters were air dried for 2 h at room temperature ($\sim 22^\circ\text{C}$, $\sim 60\%$ relative humidity) and analyzed by CA measurement (DSA 100, Krüss GmbH, Hamburg, Germany) with following settings: water drop volume: 3 μL , flow rate: 40 $\mu\text{L min}^{-1}$. The CA ($^\circ$) of four independently measured drops were evaluated by means of drop shape analysis.

The CA of the organo-mineral associations were determined using the sessile drop method as described by Bachmann et al. (2000). The dried samples were fixed with double-sided tape on glass slides by gentle pressing. Excessive material was removed by tapping to obtain a fixed monolayer. The CA was measured as described before. Samples with CA $> 0^\circ$ to 90° show reduced wettability, while values greater than 90° indicate extreme SWR (Goebel et al., 2011).

3.12.3 Environmental scanning electron microscopy

Condensation experiments in an ESEM (Quanta 200-ESEM, FEI Company, Eindhoven, Netherlands) were performed to characterize the micro-scale wettability of the organo-mineral associations (CQ and MQ as mineral compounds). For this, the samples were placed on a Peltier stage in a gaseous environment consisting of water vapour. The initial chamber pressure was 250 Pa and the gun voltage 20 kV. For a wettability experiment according to Goebel et al. (2007), the chamber pressure was increased until condensation of water on mineral surfaces was observable. The CA of the water droplets were analyzed by means of drop shape analysis with the software SCA20 (DataPhysics, Filderstadt, Germany). The amount of evaluated drops reached from two to five for each sample.

3.13 Surface coverage determination, data analysis and statistics

Mineral surface coverage was determined by multiplying the number of attached bacteria with their cross-section area, which was derived from scanning electron micrographs. The determined area was then related to the SSA of the minerals.

The macroscopic CA of the cell concentrations and the TOC of the different humic substance fractions over time was tested for significance using one way repeated-measures ANOVA followed by Holm-Sidak post hoc test for pairwise differences. Some data sets were $\sqrt{x + 0.5}$ transformed to obtain equal variance and normal distribution. The significance between unstressed and stressed cells without minerals was tested with t-test, while the effect of osmotic stress on the organo-mineral associations was tested using one way ANOVA followed by Dunnett's T3 post hoc test. For all tests, the significance level was set at 0.05. All curve fitting procedures and statistics were performed using SigmaPlot 12.5 (Systat Software, San Jose,

USA) and IBM SPSS Statistics 21 (IBM, Armonk, USA). The SEM and ESEM micrographs were cropped and scale bars added using ImageJ (Wayne Rasband, National Institute of Health, Bethesda, USA).

4 Results and Discussion

4.1 Formation and turnover of cell envelope fragments

4.1.1 Formation of humic substances during growth and decay of bacteria in liquid cultures

The microbial contribution to humic substances in soil was emphasized by previous studies (Simpson et al., 2007). That is why it was hypothesized that the growth and decay of bacteria is accompanied by the formation of humic substances. Therefore, their formation was investigated by incubation of a mixed culture obtained from a soil extract and of pure cultures of *E. coli* and *B. subtilis* and subsequent fractionation into operationally defined fulvic acids, humic acids and humin.

The results of the incubation of growth medium inoculated with a soil extract are shown in Fig. 6. After 2 weeks incubation, the $\text{TOC}_{\text{total}}$ significantly decreased from 1600 ± 400 to $530 \pm 28 \text{ mg L}^{-1}$. The same significant decrease was observed for the fulvic acid fraction (1800 ± 300 to $450 \pm 50 \text{ mg L}^{-1}$). In contrast, the humic acid fraction and humin fraction significantly increased three- to eightfold (11.3 ± 0.7 to $84 \pm 16 \text{ mg L}^{-1}$ and 17.8 ± 1.7 to $55 \pm 6 \text{ mg L}^{-1}$, respectively). These are 16 (humic acid) and 10% (humin) of the amount of $\text{TOC}_{\text{total}}$, while the major amount of TOC was recovered in the fulvic acid fraction.

The incubation experiment was repeated with pure cultures of *E. coli* and samples were taken after 2 weeks and 2 months incubation. Surprisingly, no significant decrease of $\text{TOC}_{\text{total}}$ was observed after 2 months incubation (1630 ± 150 to $1450 \pm 25 \text{ mg L}^{-1}$) (Fig. 7). The TOC of the fulvic acids significantly decreased from 1620 ± 60 to 1410 ± 28 after 2 weeks and to $1280 \pm 22 \text{ mg L}^{-1}$ after 2 months. The TOC of the humic acids and humin significantly

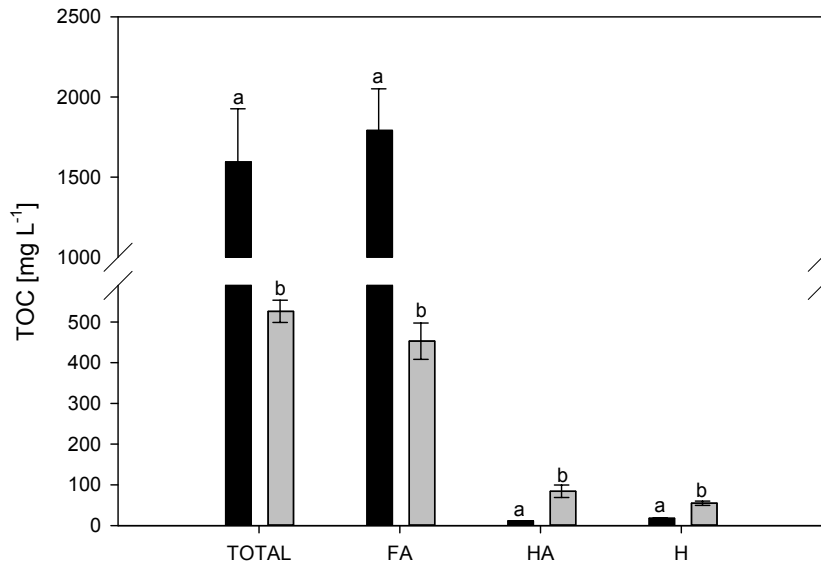


Fig. 6: Total organic carbon (TOC) of different fractions (fulvic acids (FA), humic acids (HA), humin (H)) in medium inoculated with a soil extract before (black bars) and after 2 weeks (grey bars) incubation. Different letters indicate significant differences between incubation time ($P < 0.05$).

increased five- to 13-fold from 7.0 ± 2.4 to $90 \pm 10 \text{ mg L}^{-1}$ and 9.7 ± 0.7 to $50 \pm 8 \text{ mg L}^{-1}$ after 2 months, which are 6 and 3 % of $\text{TOC}_{\text{total}}$, respectively.

The formation of humic-like substances during growth and decay was also analyzed with the Gram-positive bacterium *B. subtilis* (Fig. 8). In contrast to the incubation with *E. coli* (Fig. 7), the $\text{TOC}_{\text{total}}$ of *B. subtilis* pure cultures significantly decreased from 1630 ± 7 to $506 \pm 12 \text{ mg L}^{-1}$ after 2 months. A decrease was also observed for the fulvic acids (1660 ± 90 to $366 \pm 4 \text{ mg L}^{-1}$). The TOC of the humic acids and humin significantly increased four- to tenfold from 6.0 ± 0.4 to $60 \pm 30 \text{ mg L}^{-1}$ and 7 ± 1 to $27 \pm 1 \text{ mg L}^{-1}$ after 2 months, which are 12 and 5 % of $\text{TOC}_{\text{total}}$, respectively.

The formation of humic acids and humin during growth and decay of microorganisms was shown for all treatments. In this experiment with pure cultures of microorganisms the operationally defined fractions were clearly microbially derived. As the growth and decay

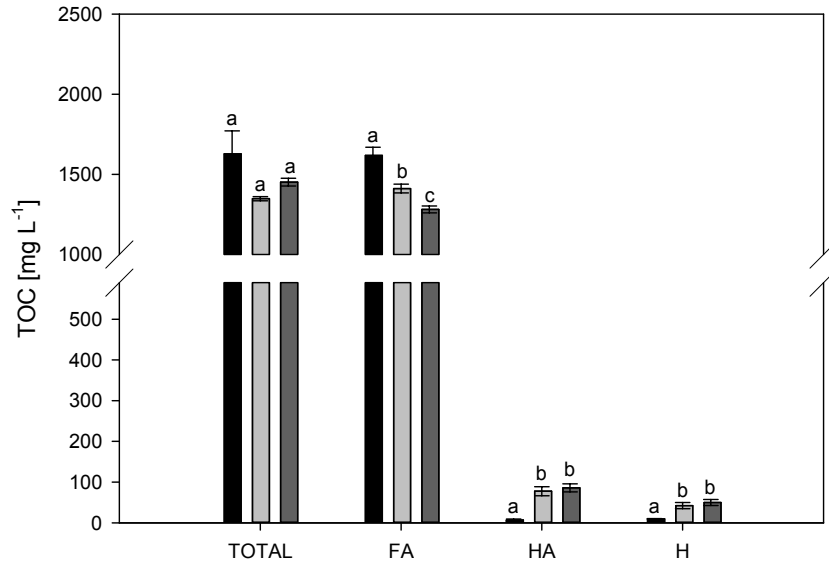


Fig. 7: Total organic carbon (TOC) of different fractions (fulvic acids (FA), humic acids (HA), humin (H)) in pure cultures of *E. coli* before (black bars), after 2 weeks (light grey bars) and 2 months (dark grey bars) incubation. Different letters indicate significant differences between incubation time ($P < 0.05$).

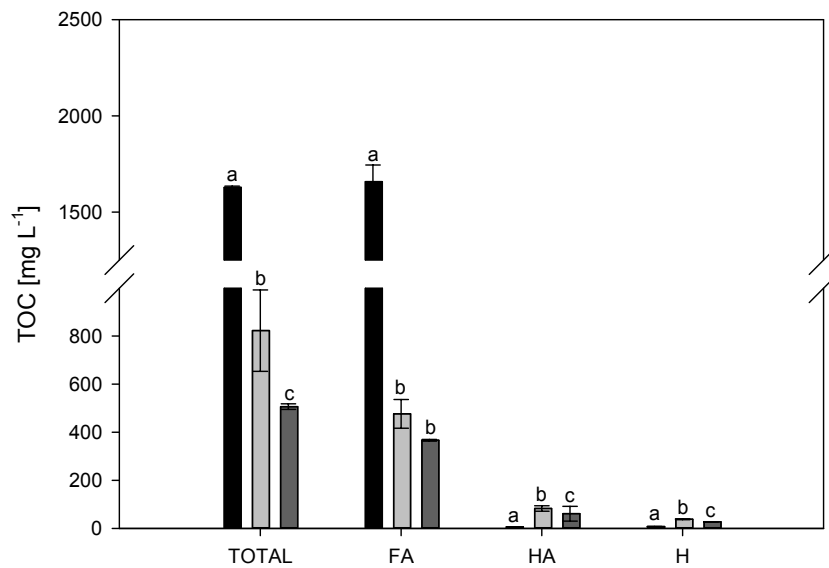


Fig. 8: Total organic carbon (TOC) of different fractions (fulvic acids (FA), humic acids (HA), humin (H)) in pure cultures of *B. subtilis* before (black bars), after 2 weeks (light grey bars) and 2 months (dark grey bars) incubation. Different letters indicate significant differences between incubation time ($P < 0.05$).

also take place in soil, these processes may be also valid for soils. The humin fraction of the present experiment consisted mainly of cells, fragmented cell envelopes or high pH precipitates, because the extraction procedure may have lysed intact bacterial cells and accumulate the broken envelopes during centrifugation. Although the amount of microbially derived humin and humic acids was relatively low, the substances may accumulate in soil due to repeated death and decay cycles and stabilized over a longer period, which may partially explain the 46 % contribution of microbial biomass to the humin fraction (Simpson et al., 2007). Therefore, no secondary synthesis, an assumption of the "humic polymer" model, is needed to explain the formation of humic substances (Hayes and Swift, 1990) in soil. Nevertheless, the secondary synthesis cannot be excluded based on the used experimental design.

The formation of humic-like substances was also shown for the incubation of pure and mixed cultures of aquatic microorganisms (Claus et al., 1999). 3 % of the initially added C was transferred into humic acids and fulvic acids. Similar results were shown for incubation of seawater amended with ^{14}C -glucose, where 3 % of initially added C was transferred into dissolved humic substances (Tranvik, 1993). The reason for the high amounts of fulvic acids in the present study compared to other studies is presumably that polystyrene resin for the isolation of the fulvic acid fraction was not used (Claus et al., 1999). Therefore, the fulvic acid fraction in this study does not only comprise high-molecular material, but also low-molecular compounds such as residual glucose, its metabolites and microbial exudates; this may have masked the formation of macromolecular fulvic acids. However, the resin has no influence on humic acids and humin concentrations; their formation thus has been shown clearly in this experiment. Previous studies focused on aquatic systems and microorganisms. The formation of humic substances during incubation of soil microorganisms in a growth medium with soil extract was demonstrated here for the first time.

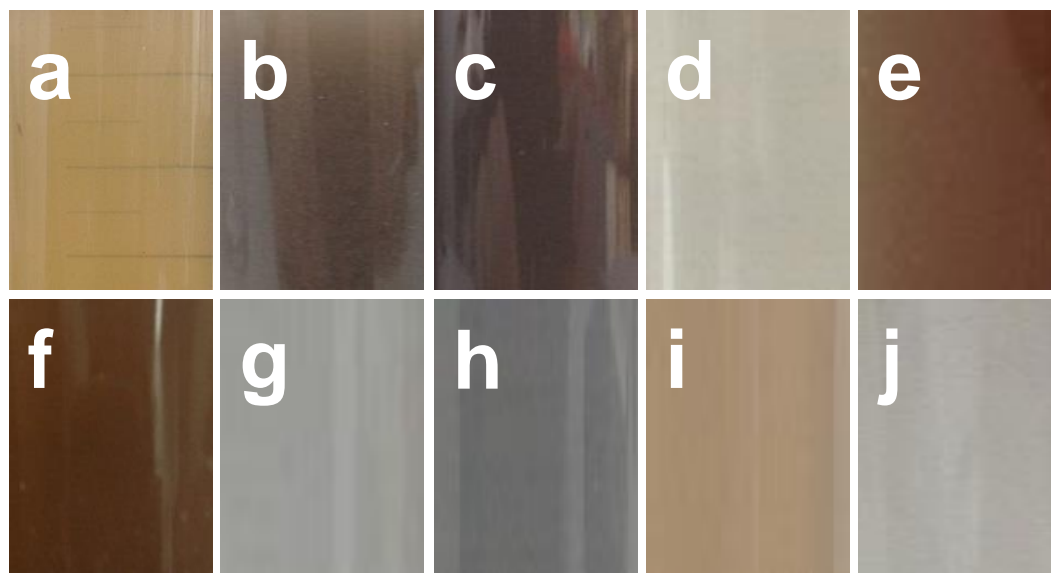


Fig. 9: Different fractions of humic substance extraction: culture inoculated with soil extract before (a) and after (b) incubation; soil extract inoculum (c); fulvic acids (d), humic acids (e) and humin (f). Culture inoculated with *E. coli* after incubation (g), and humic acids (h) and culture inoculated with *B. subtilis* after incubation (i) and humic acids (j).

In addition to the TOC concentrations, color and turbidity of the fractions were analyzed (Fig. 9). The color of the medium inoculated with soil extract turned from dark yellow to brown, which was similar to the used soil extract (Fig. 9a–c). The humic acids and humin were also brown, while the fulvic acids showed no color (Fig. 9d–f). The fulvic acid fractions of *E. coli* and *B. subtilis* were also clear (pictures not shown). In contrast, the humic acid and humin fractions were turbid (Fig. 9h, j). The pure culture of *B. subtilis* after incubation had a yellow-brownish color, while *E. coli* was whitish (Fig. 9g, i).

The change in color from light to dark after incubation was also reported for the incubation of growth medium inoculated with a population of groundwater microorganisms (Claus et al., 1999). One possible reason is dark colored fungal melanin, which was shown to be synthesized by various fungi in vitro (Paim et al., 1990). According to Sollins et al. (1996) the melanin may be incorporated into fungal cell walls or released during growth and decay.

According to their solubility, the melanin may therefore contribute to the TOC within the humic acid and humin fractions. However, the melanin can not contribute to the fulvic acids, humic acids and humin of the bacterial pure cultures. In these samples, the observed humic substances and the brown color have to be derived from bacteria.

The chemical structure of the fractions was not characterized further. Fourier transform infrared spectroscopy or nuclear magnetic resonance spectroscopy may be suitable techniques, which were used for the characterization of humic substances in previous studies (Claus et al., 1999; Simpson et al., 2007).

In summary, the results of the incubation experiment confirmed the hypothesis, that growth and decay of microorganisms is accompanied by formation of humic substances. By the accumulation of the substances over a long period, this process may be relevant in soils and therefore be responsible for the observed microbial contribution to humic substances.

4.1.2 Formation of cell envelope fragments during growth and decay of pure cultures of bacteria

According to several studies, the decay of microorganisms in soil is accompanied by the formation of cell envelope fragments, which contribute to SOM formation (Miltner et al., 2012; Schurig et al., 2013; Schütze et al., 2013). As the decay and fragmentation is difficult to directly observe in natural soils, a decrease in complexity may be helpful to study these processes more detailed. Therefore, it was hypothesized, that growth and decay of microorganisms in pure cultures is also accompanied by the formation of those fragments. Thus, the aim of the present study was to track and visualize their formation by SEM. For that reason, different experiments with pure cultures of *E. coli* and *P. putida* were performed. The experiments were conducted in liquid cultures, in quartz-bacteria mixtures and on PDL

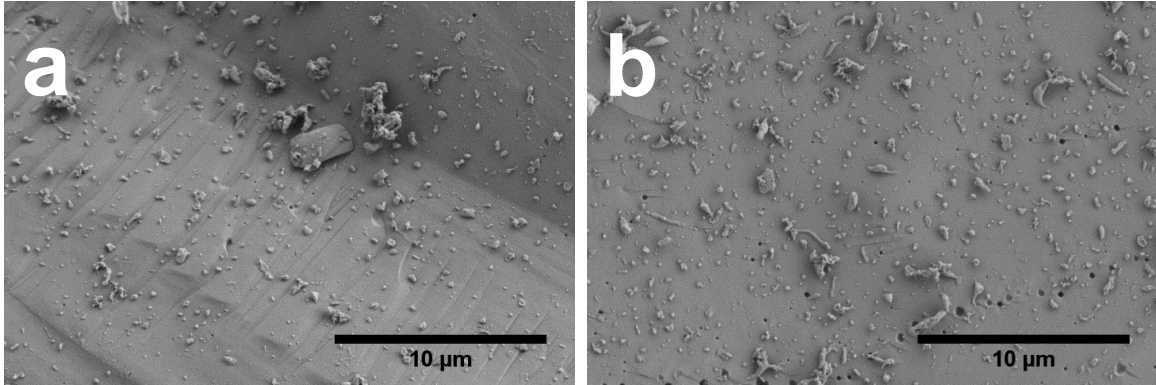


Fig. 10: Scanning electron micrographs of cell envelope fragments of (a) *E. coli* and (b) *P. putida* attached to medium-grained quartz surfaces.

coated glass slides to elucidate the impact of different soil phases and incubation conditions on the decay of bacteria and the formation of envelope fragments.

The fragmented cell envelopes of ultrasonically disrupted cells of *E. coli* and *P. putida* attached to MQ were first visualized as a reference sample for fragments to compare the artificially produced fragments with naturally formed fragments of the subsequent experiments (Fig. 10). Fragmented cell envelopes of *E. coli* and *P. putida* were either circular or filamentous (Fig. 10a, b). Some aggregation of biogenic material was observable. There were no differences between the microorganisms regarding the shape of the fragments. Rarely intact cells were observable indicating that the ultrasonic disruption method used was suitable. The shape of the fragmented cells was different from the one reported in previous studies, where fragments were more round, flat and patchy (Miltner et al., 2012; Schurig et al., 2013; Schütze et al., 2013). This may be due to the used ultrasonic disruption or differences in the preparation for SEM. The high abundance of fragments on the mineral surface indicates that the attachment of fragments is stable during the numerous preparation steps including fixation, dehydration and critical point drying.

Since it was possible to visualize cell envelope fragments, their formation during growth and decay of bacteria was studied in incubation experiments with pure cultures of *E. coli* and *P. putida*. Samples from liquid cultures were taken at different time steps, transferred to PDL slides and analyzed by SEM (Fig. 11). For both bacterial strains, no fragmentation over times was observable. Cells of *P. putida* were intact after 16 d incubation, while the envelope of *E. coli* cells was shriveled, which may be due to starting decay or be an artifact due to insufficient fixation or dehydration during sample preparation (Fig. 11e, f). However, the shriveling of cells became more severe during incubation and is therefore at least partly a cell decay. In contrast to these observations, the formation of fragmented cell envelopes during growth of *E. coli* in liquid pure cultures was shown before (Miltner et al., 2012). Reasons for the absence of fragments may be losses during sample preparation, e.g., the use of PDL slides causing adverse electrostatic interactions or during dehydration by the graded EtOH series. For the formation of fragments in soil, biotic factors, e.g., phages, micropredators or degradation by extracellular enzymes, may be important (Lueders et al., 2006; Burns et al., 2013).

The described incubation experiments were repeated with *E. coli* (Fig. 12). In contrast, no PDL slides were used to exclude losses of fragments due to adverse electrostatic interactions. However, the absence of PDL slides did not increase the accumulation of cell envelope fragments over time. After 6 d incubation, the cells were mainly shriveled, while further incubation increased the amount of broken and damaged cells (Fig. 12b, c). Nevertheless, the formation of cell envelope fragments was not observable. Reasons for that may be losses during sample preparation, e.g., during dehydration by the graded EtOH series or during critical-point drying. Furthermore, SEM only allows imaging the surfaces of cell aggregates and fragments may be hidden within aggregation of cells.

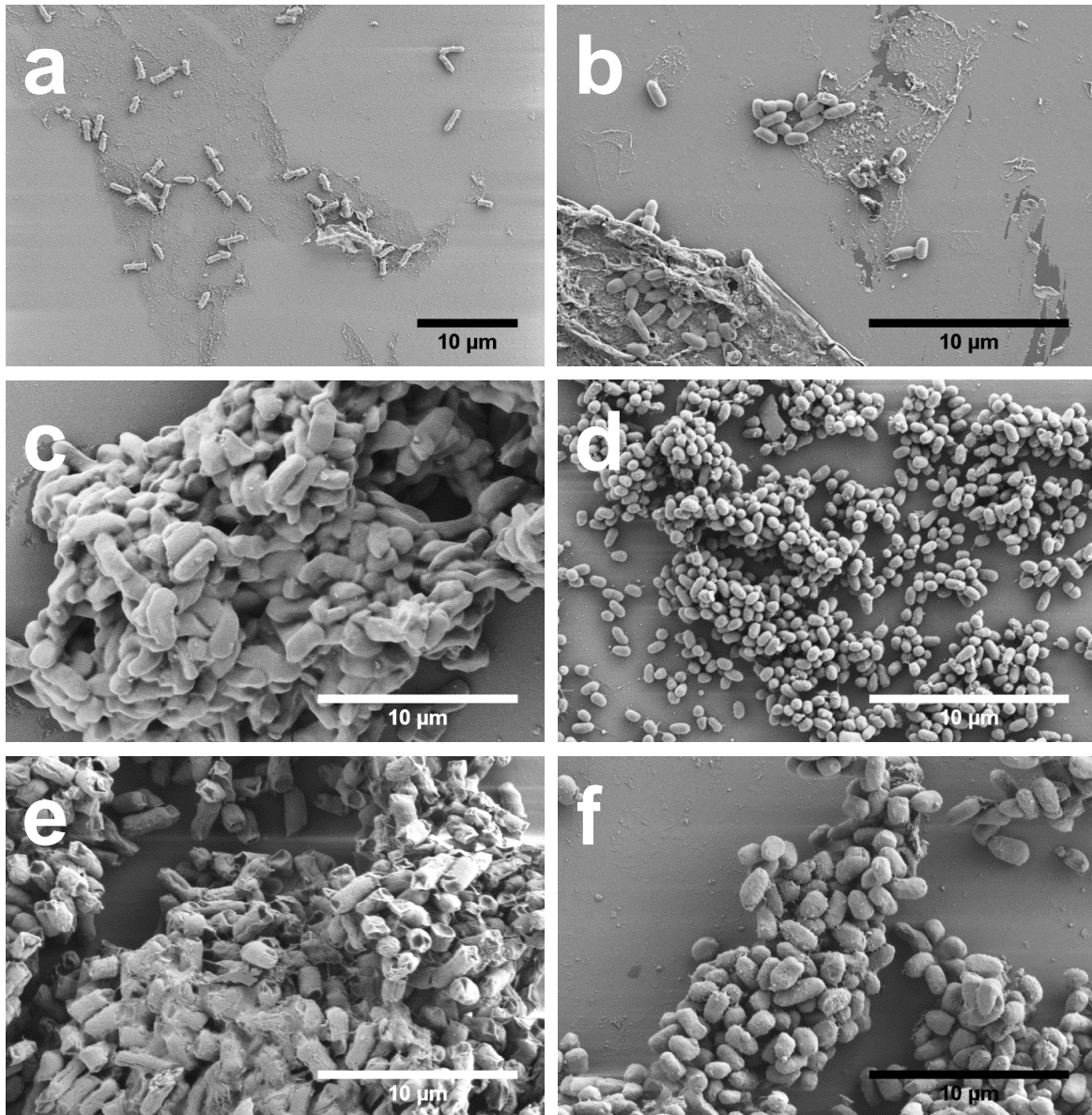


Fig. 11: Scanning electron micrographs of *E. coli* at the (a) beginning and after (c) 1 d and (e) 16 d incubation and *P. putida* at the (a) beginning and after (d) 1 d and (f) 16 d incubation in liquid pure cultures. Cells are attached to Poly-D-lysine coated glass slides.

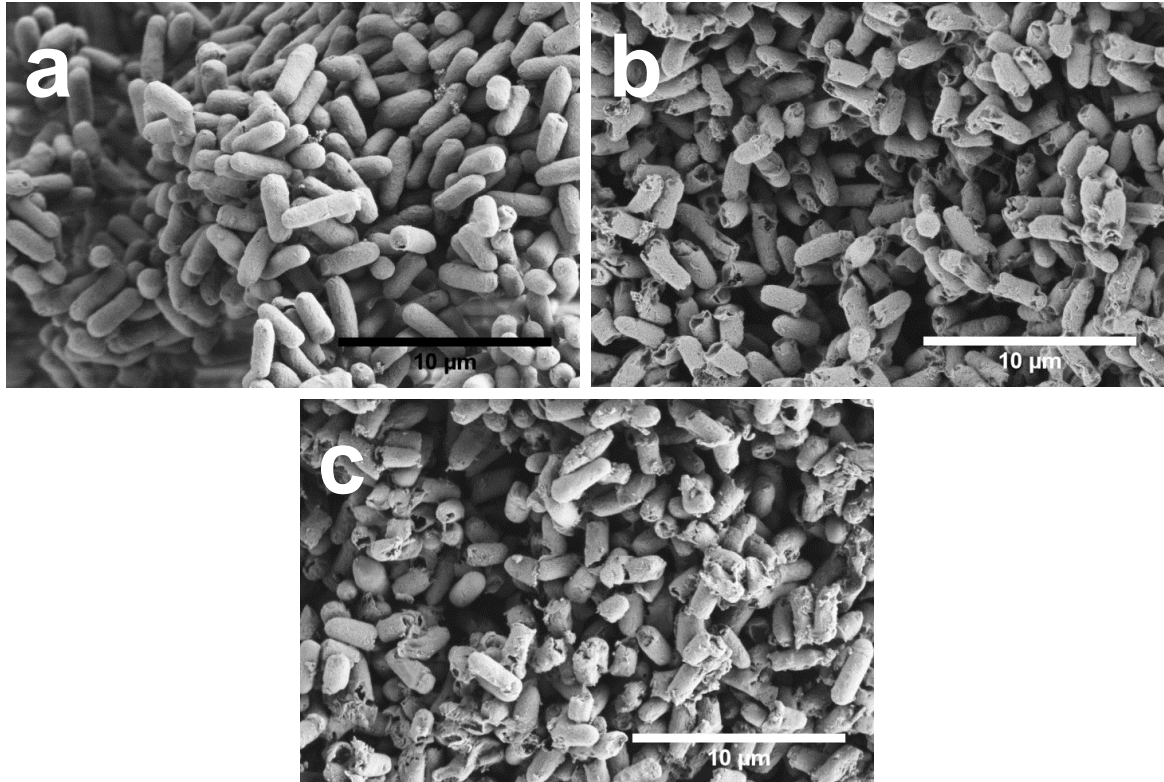


Fig. 12: Scanning electron micrographs of *E. coli* at the (a) beginning and after (b) 6 d and (c) 13 d incubation in liquid pure cultures.

The mineral phase may be a further crucial aspect for the accumulation of cell envelope fragments. Therefore, the formation of them during growth and decay of bacteria was also tested after addition of a mineral phase (MQ) to the pure cultures and subsequent incubation. Furthermore, the attachment of cells and fragments to mineral surfaces was analyzed (Fig. 13). After 35 d incubation, the amount of bacterial cells attached to the quartz surface was very low (Fig. 13e, f). The fragmentation of cells was observed after 35 d (Fig. 13; black circles). The surface of MQ without intact cells and fragments was smooth with some isolated small pieces of quartz (Fig. 13g, h). The low coverage of mineral surface with bacteria may be due to the low concentration of divalent cations, like Ca^{2+} or Mg^{2+} in the growth medium or the low cation exchange capacity of quartz, which were shown

to be important for bacterial adhesion on soil particles (McEldowney and Fletcher, 1986; Huysman and Verstraete, 1993). This may also have an influence on the adhesion of cell envelope fragments in soil.

For analyzing the impact of divalent cation on bacterial and fragments adhesion, the same experiment setup was repeated with *E. coli* grown in an Mg^{2+} and Ca^{2+} enriched medium (Fig. 14). After 5 and 12 d incubation, the number of cells attached to mineral surface was higher compared to cells growing in a Mg^{2+} and Ca^{2+} poor medium (compare Fig. 13, Fig. 14). Furthermore, cell envelope fragments were attached to intact cells of *E. coli* (Fig. 14b; black circles). Therefore, the higher concentration of divalent cations resulted in an increased cell adhesion, cell envelope fragment formation and their attachment, which may also be an important process for natural soils.

The decay and formation of fragmented cell envelopes from surface-attached bacteria under no-growth conditions was studied with *P. putida* attached to PDL slides (Fig. 15). After growth in liquid culture, cells were transferred to the slides and incubated at room temperatures. Cells of *P. putida* became more and more damaged over time (Fig. 15a–d). Fibrous networks of EPS were observable after 16 d (Fig. 15c, d). Fragmented cell wall envelopes as known from previous experiments were mainly bound to those networks (Fig. 15e, f, h; black circles). Therefore, the visualization of the formation of fragments was possible by using PDL slides and attached bacterial cells. After 35 and 98 d, porous and damaged cells rather than intact ones were dominant. The fibrous EPS formation and aggregation of fragmented structures was also observed for *Rhodococcus opacus* subjected to slow air-drying (Alvarez et al., 2004). Similar results were found for *Pseudomonas* sp. cultures growing on quartz sand after desiccation (Roberson and Firestone, 1992; Roberson et al., 1993). As the cells were not incubated in a closed system, the observed EPS-like networks and cell fragmentation may be attributed to the air-drying.

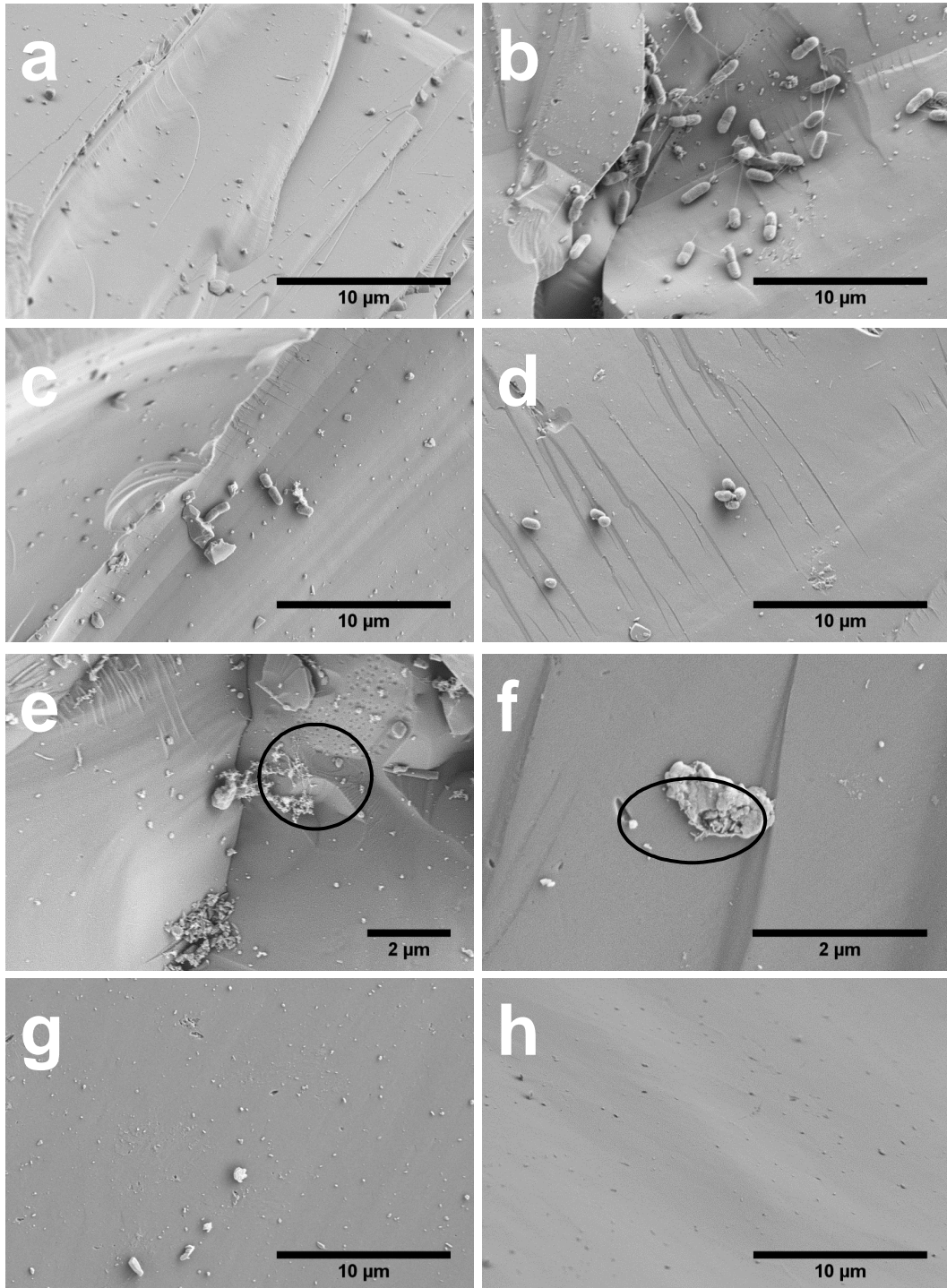


Fig. 13: Scanning electron micrographs of *E. coli* after (a) 4.5 h, (c) 24 h and (e) 35 d and *P. putida* after (b) 4.5 h, (d) 24 h and (f) 35 d incubation in liquid pure cultures. Cells are attached to added medium-grained quartz surfaces (MQ). Micrographs (g, h) is MQ without attached biomass after 35 d incubation. Black circles indicate cell envelope fragments.

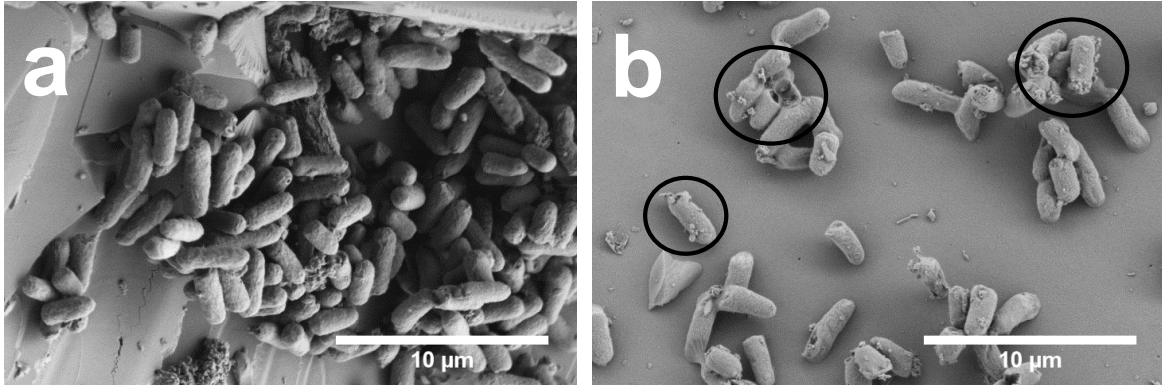


Fig. 14: Scanning electron micrographs of *E. coli* after (a) 5 d and (b) 12 d incubation in liquid pure cultures supplemented with additional Mg^{2+} and Ca^{2+} . Cells are attached to added medium-grained quartz surfaces. Black circles indicate cell envelope fragments.

As already mentioned, the mineral phase may play an important role in accumulation of cell envelope fragments. Therefore, the decay and formation of fragmented cell envelopes under no-growth conditions was also studied with *E. coli* and *P. putida* attached to MQ (Fig. 16). After growth in liquid culture, cells were homogeneously distributed on MQ surface and incubated at 30 °C. Cells of *E. coli* were still intact after 50 d incubation (Fig. 16c). In contrast, *P. putida* cells were damaged and aggregation of biomaterial, which may consist of cell envelope fragments, was observable (Fig. 16d).

In summary, the decay of cells was observable in pure cultures and the formation of cell envelope fragments was visualized on PDL coated slides or if an additional mineral phase was present confirming the initial hypothesis, that the death and decay of microorganisms is accompanied by the formation of cell fragments. Assuming that the growth, decay and formation of envelope fragments are general processes, they may be also valid for soils. Although the amount of fragments was low, they may accumulate in soil due to repeated death and decay cycles. Medium-grained sand was exclusively used as an additional mineral phase and therefore, the impact of clay minerals needs to be elucidated in further experiments. In the treatments where the fragmentation could not be shown, there had to be losses

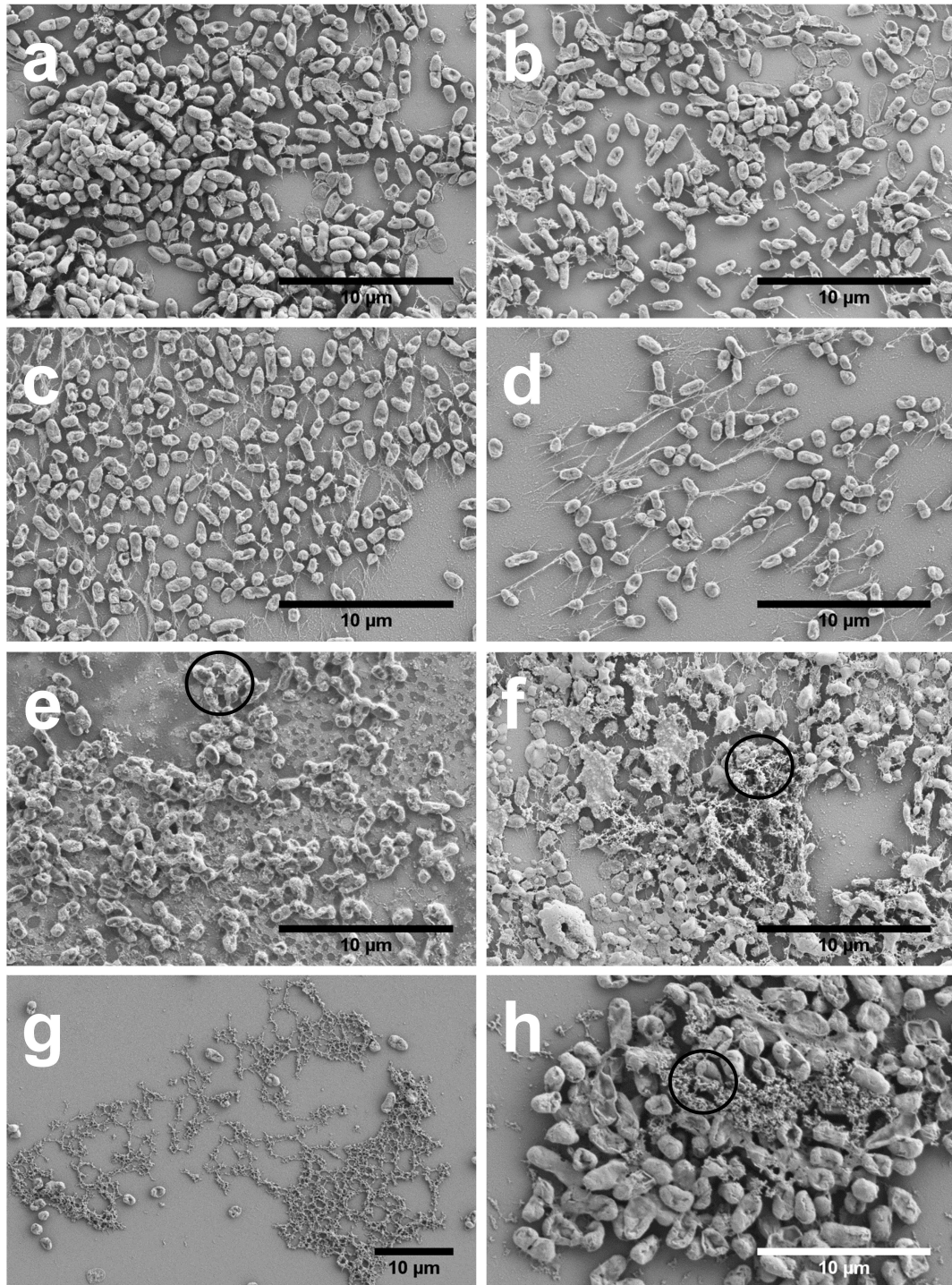


Fig. 15: Scanning electron micrographs of *P. putida* at the (a, b) beginning and after (c, d) 16 d, (e, f) 35 d and (g, h) 98 d incubation on Poly-D-lysine coated glass slides. Black circles indicate cell envelope fragments.

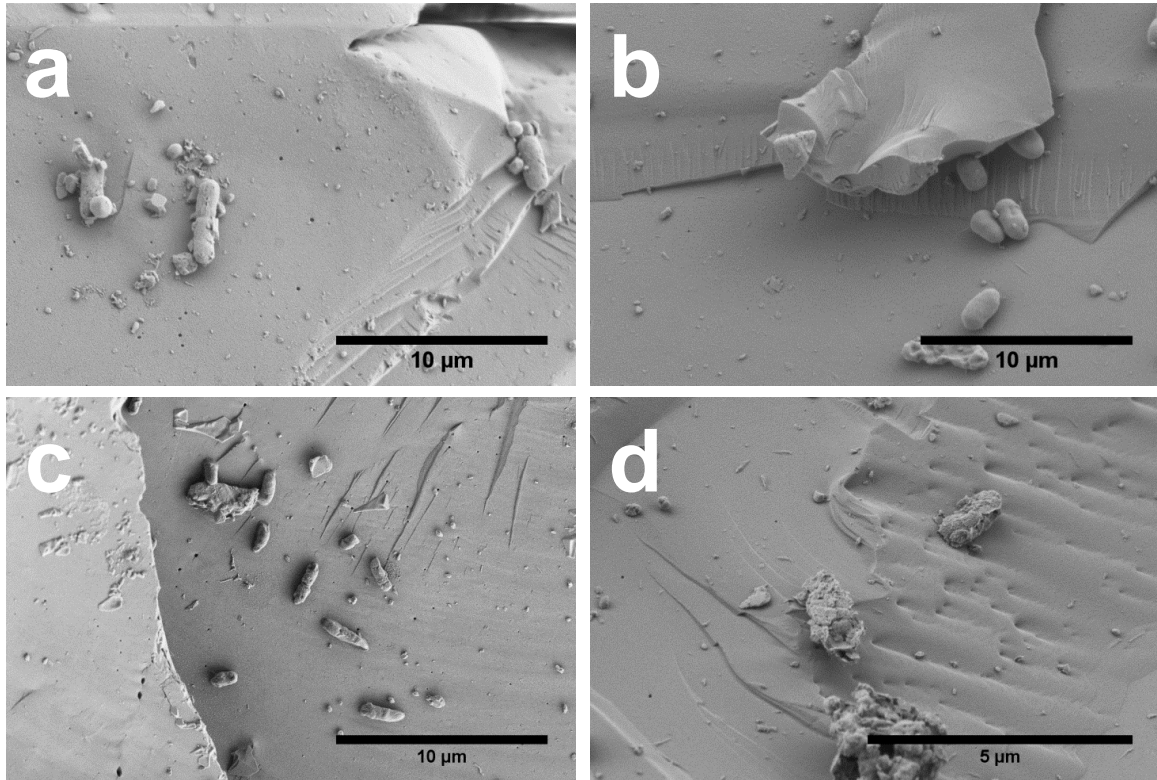


Fig. 16: Scanning electron micrographs of *E. coli* at the (a) beginning and after (c) 50 d, and *P. putida* at the (b) beginning and after (d) 50 d incubation on medium-grained quartz surfaces.

during preparation, i.e., centrifugation and dehydration. Furthermore, the fragments may be hidden in cell aggregates, which prevented its visualization. Unfortunately, the observed fragments had a different more globular shape than the fragments observed as known from other studies (Miltner et al., 2012; Schurig et al., 2013; Schütze et al., 2013), which may be due to differences in preparation. Furthermore, the importance of divalent cations for the attachment of cells and envelope fragments to mineral surfaces was also shown.

4.1.3 Formation and stability of cell envelope fragments in artificial soils

In a next step, the formation of cell envelope fragments was studied in more complex test systems. As the accumulation was shown in the presence of minerals and divalent cations, these factors seem to be important for a test systems suitable for the visualization of the fragmentation process. Artificial soil were chosen for the next experiments to meet these conditions and to mimic natural soil conditions more closely. As microbial residues may originate from different types of microorganisms, the experiments were conducted with Gram-negative and Gram-positive bacteria as well as with actinomycetes, which are Gram-positive bacteria, but tend to form hyphal structures like fungi. The bacterial cells and the envelope fragments were visualized by means of SEM. Furthermore, tFA and PLFA were analyzed as proxies for living and dead biomass. Two different artificial soils were used for the incubation studies and the test systems were incubated for 32 weeks under aerobic conditions.

At the beginning and after 8 weeks incubation no microbial cells were observed for the control using AS1 without biomass amendment (Fig. 17). A patchy layer was observable on mineral surface, which may be organic or inorganic, while differences between before and after incubation were not observable. The missing intact cells and dead biomass correspond with the low amounts of PLFA. The concentration of PLFA was only 9 ± 3 at the beginning and $1.6 \pm 0.6 \text{ nmol g}^{-1}$ soil after 32 weeks incubation (Tab. 7, page 60). The major PLFA were 16:0 and 18:0, ubiquitous FA for prokaryotes and eukaryotes, and may originate from the added soil extract (Zelles, 1997). Therefore, no formation of a microbial community was detected which is caused by the limitation in C and nutrients.

P. putida was chosen as a representative Gram-negative bacterium. The incubation was performed with intact cells and corresponding cell envelope fragments in AS1. At the beginning of incubation, intact cells of *P. putida* were visible, which was not the case after 8 weeks

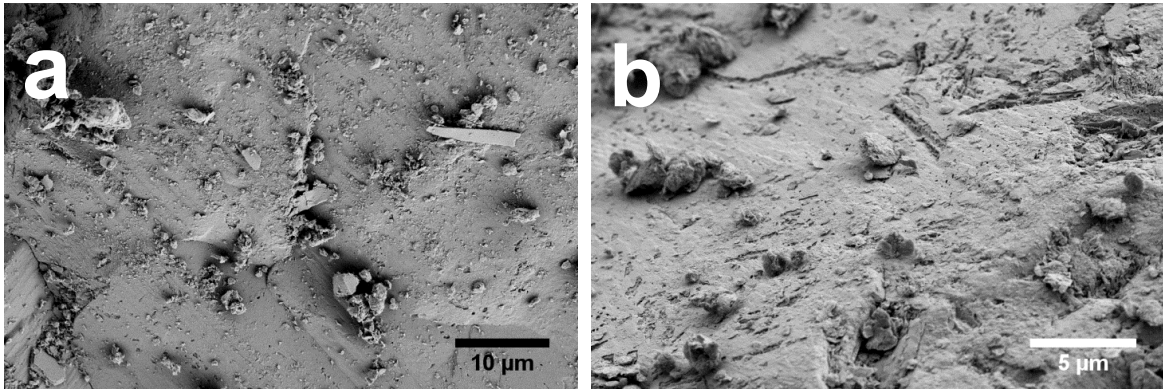


Fig. 17: Scanning electron micrographs of artificial soil 1 (AS1) without biomass addition at the beginning and after (c) 8 weeks incubation.

(Fig. 18a, c) indicating a rapid decay of the cells. In contrast, it was not possible to identify cell envelope fragments due to heterogeneous surfaces (Fig. 18b, d). Assuming a shape and size of the fragments as shown in Fig. 10 (page 39), the determination between fragments and abiotic structures is not possible by SEM. The PLFA concentration of the intact cells decreased from 270 ± 40 to 43.9 ± 2.2 nmol g⁻¹ soil after 32 weeks incubation, whereas the amount of tFA initially remained stable (270 ± 60 to 150 ± 28 nmol g⁻¹) (Tab. 7). Lower concentrations were determined for the cell envelope fragments, but the relative decrease was nearly the same (PLFA: 231 ± 25 to 25 ± 18 , tFA: 272 ± 6 to 108 ± 13 nmol g⁻¹). Assuming that PLFA are exclusively stable in living cells and non-existent in storage products or dead cells, a decrease in the amount of PLFA is a proxy for the death and decay of the bacterial cells (Zelles, 1997). The higher stability of tFA compared to PLFA is an evidence for the accumulation of less degradable cell envelope fragments, which contain neutral lipids or glycolipids rather than phospholipids. The same observations were made for the fate of the Gram-negative bacteria *E. coli* in soil bioreactors, where the amount of PLFA decreased to 25–35 % of the initial value after 224 d incubation (Kindler et al., 2006), while they decreased to about 16 % in the present study. The PLFA composition of intact cells and cell envelope fragments only changed slightly after incubation and the differences between

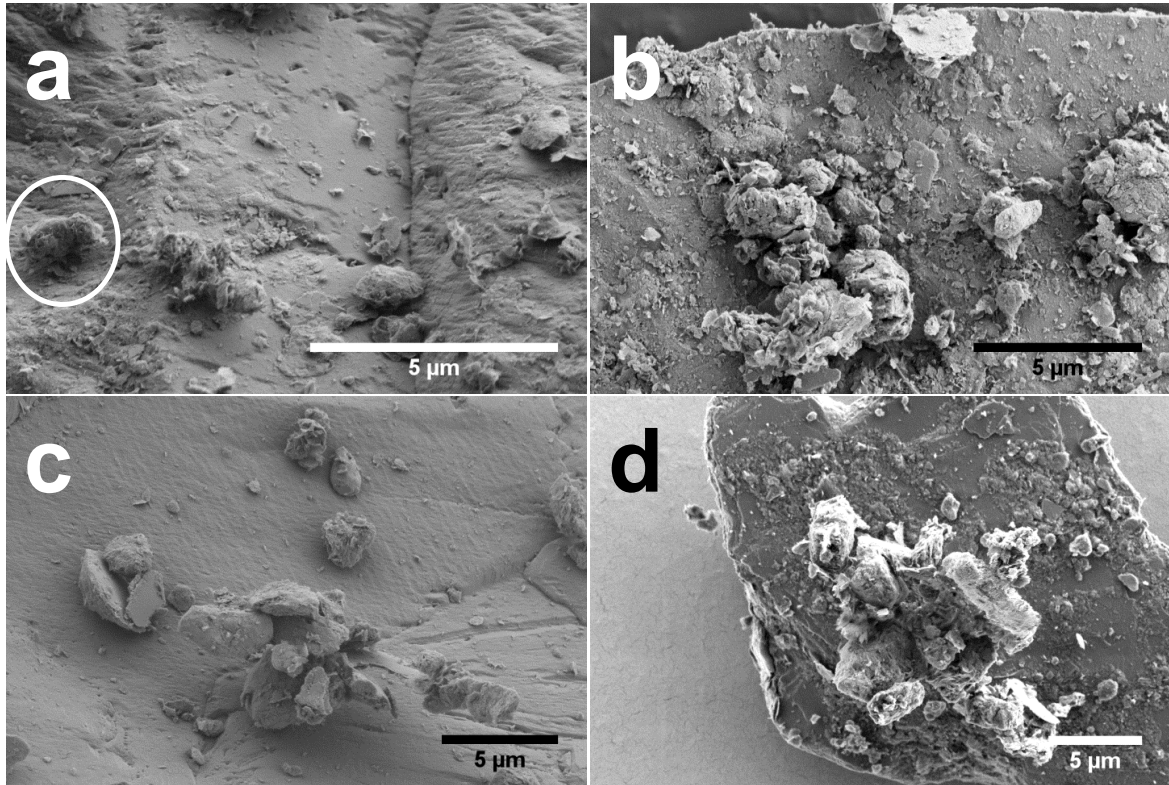


Fig. 18: Scanning electron micrographs of intact cells of *P. putida* at the (a) beginning and after (c) 8 weeks, and cell envelope fragments at the (b) beginning and after (d) 8 weeks incubation in artificial soil 1 (AS1). White circles indicate intact cells.

them were negligible (Fig. 19). The majority of detected PLFA were straight-chain (16:0, 18:0), cyclopropyl (cy17:0, cy19:0), monounsaturated (16:1, 18:1) and hydroxy FA (OH-18), which are characteristic for Gram-negative bacteria (Zelles, 1997). The high abundance of cyclopropyl FA, which are stress and starvation markers, may explain the decay of the bacterial cells caused by substrate limitation (Guckert et al., 1986). During incubation, the microbial community became more diverse, which was shown by the increase in branched-chain FA (a-15:0, i-15:0, i-16:0), typical biomarkers for Gram-positive bacteria (Zelles, 1997). These bacteria may originate from the added soil extract growing on *P. putida*. The higher diversity is therefore related to the death and decay of the initially added *P. putida* and to

the formation of cell envelope fragments by different mechanisms, e.g., micro-predation (Lueders et al., 2006).

The incubation studies were also conducted with *B. subtilis* as a representative for the Gram-positive bacteria. It was not possible to observe intact cells even directly after blending (Fig. 20a). This may be due to the high SSA of AS1 ($52 \text{ m}^2 \text{ g}^{-1}$) resulting in a low coverage of the surfaces by cells or to losses during preparation of the samples for SEM analysis, i.e., dehydration and centrifugation. Like in the study with *P. putida*, it was not possible to visualize cell envelope fragments due to the heterogeneous mineral surfaces (Fig. 20b).

Like in the incubation studies with *P. putida*, a decrease in the amount of PLFA was also found for *B. subtilis* (Tab. 7). After 32 weeks incubation, about 38 % of the initial PLFA amount was detected for the intact cells (42 ± 13 to $16 \pm 5 \text{ nmol g}^{-1}$) and cell fragments (13 ± 3 to $5 \pm 2 \text{ nmol g}^{-1}$ soil). Cells and envelope fragments of *B. subtilis* were thus more stable over time than *P. putida* cells and fragments, which may be related to the formation of spores and the different structure of the cell wall of Gram-positive bacteria. The PLFA composition only changed to a minor extent during 32 weeks incubation for both intact cells and cell envelope fragments (Fig. 21), while differences between both treatments were detectable. For the intact cells, branched-chain FA (i-15:0, a-15:0, i-17:0, a-17:0) were the dominant PLFA, while the major PLFA for the cell envelope fragments were the straight-chain FA 16:0 and 18:0. For intact cells and fragments, the PLFA composition became more diverse with incubation, indicating a formation of a diverse microbial community (i.e., increase in mono-saturated FA), similar to what was observed for *P. putida*.

Since it was not possible to detect intact cells and envelope fragments in the first experiments with *B. subtilis*, the experiment was repeated with higher cell numbers (10^{10} instead of 2.5×10^9 cells g^{-1} soil) and a different artificial soil (AS2, which is characterized by a

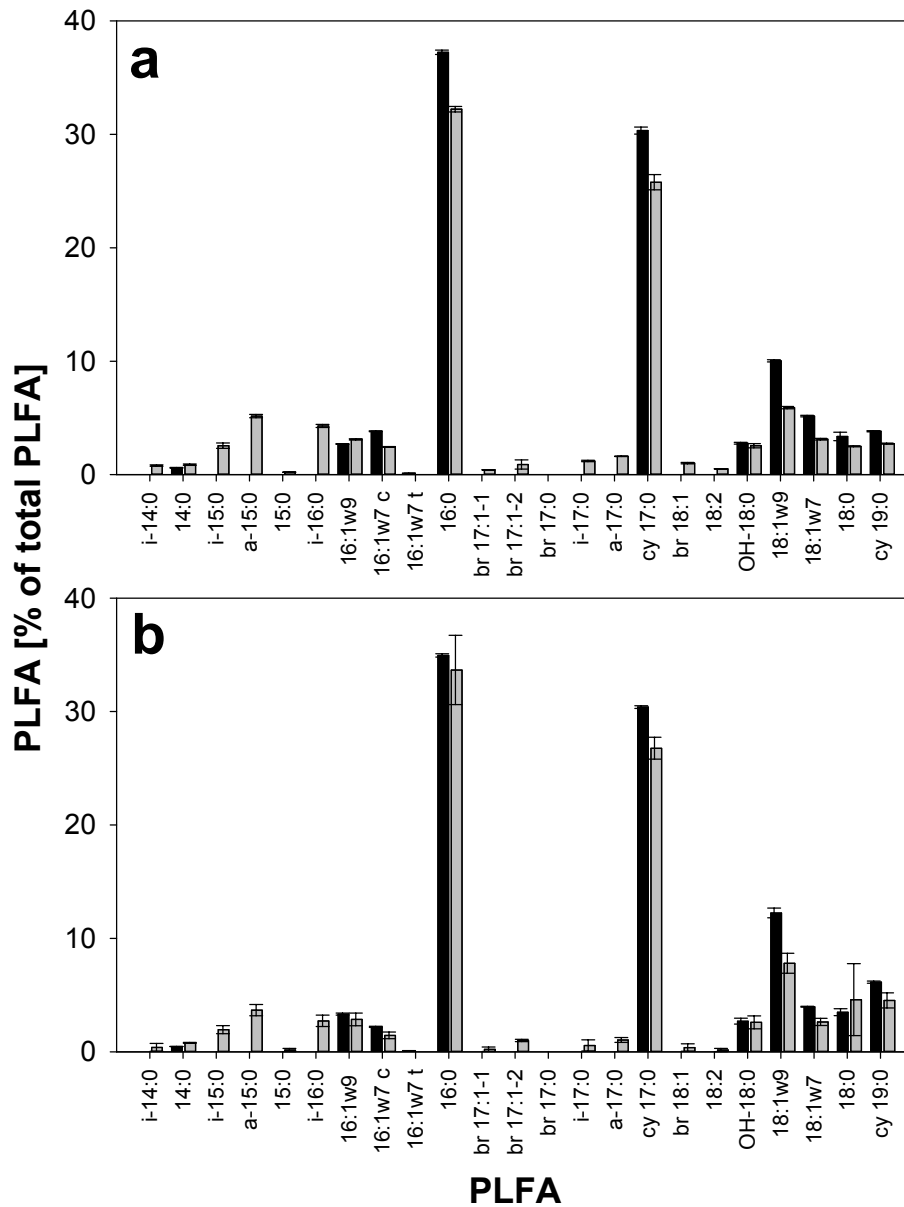


Fig. 19: Relative percentages of different phospholipid fatty acids (PLFA) in incubation studies with (a) intact cells and (b) cell envelope fragments of *P. putida* before (black bars) and after (grey bars) 32 weeks incubation in artificial soil 1 (AS1).

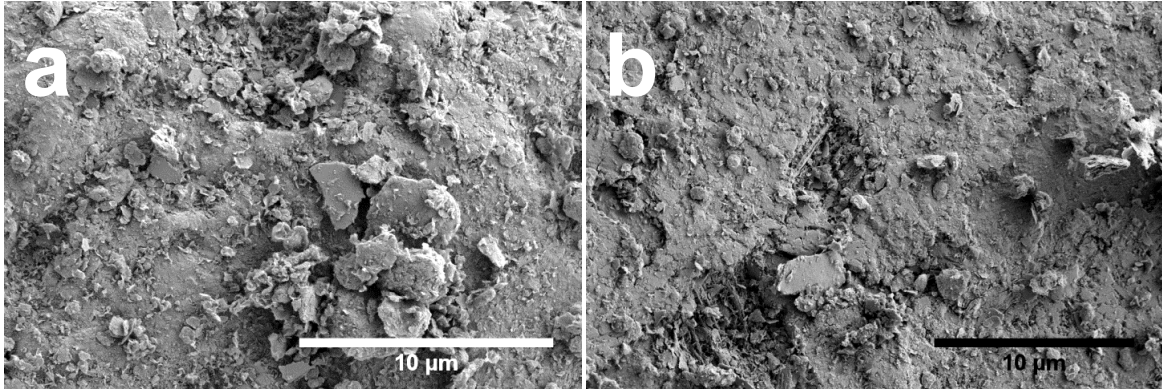


Fig. 20: Scanning electron micrographs of (a) intact cells of *B. subtilis* and (b) cell envelope fragments at incubation start in artificial soil 1 (AS1).

lower SSA than AS1 (SSA of AS1: $52 \text{ m}^2 \text{ g}^{-1}$, SSA of AS2: $0.9 \text{ m}^2 \text{ g}^{-1}$). Intact cells were observable directly after blending (Fig. 22a; white circle) but they rapidly disappeared after 8 weeks incubation (Fig. 22c) indicating a death and decay of the cells. However, also in this experiment the visualization of the cell envelope fragments was not possible due to the heterogeneous mineral surfaces. Patchy and flat structures were observable but the distinction between organic and inorganic was not possible by using SEM (Fig. 22b, d).

The PLFA and tFA concentrations decreased over time for intact cells (PLFA: 171 ± 23 to 9 ± 5 , tFA: 473.1 ± 2.5 to $49 \pm 11 \text{ nmol g}^{-1} \text{ soil}$) and fragments (PLFA: 70 ± 60 to 7 ± 7 , tFA: 149 ± 6 to $44 \pm 6 \text{ nmol g}^{-1}$) (Tab. 7). Therefore, next to the studies in AS1, the death and decay of the initially added bacterial biomass was performed in AS2. However, the decrease was more distinctive, because only 9–13 % of the initial PLFA concentrations were detected after 32 weeks incubation. The different texture of the artificial soil may cause less protection of microbial residues by mineral surfaces and be a reason for a more rapid turnover (Gregorich et al., 1991). The changes in PLFA composition were also different (Fig. 23). The percentage of the Gram-positive marker FA (branched chain: i-15:0, a-15:0, i-17:0, a-17:0) decreased to a large extent, while saturated straight-chain FA (16:0, 18:0), cyclopropyl FA (cy17:0, cy19:0) and mono-unsaturated FA (16:1w9, 18:1w7) increased.

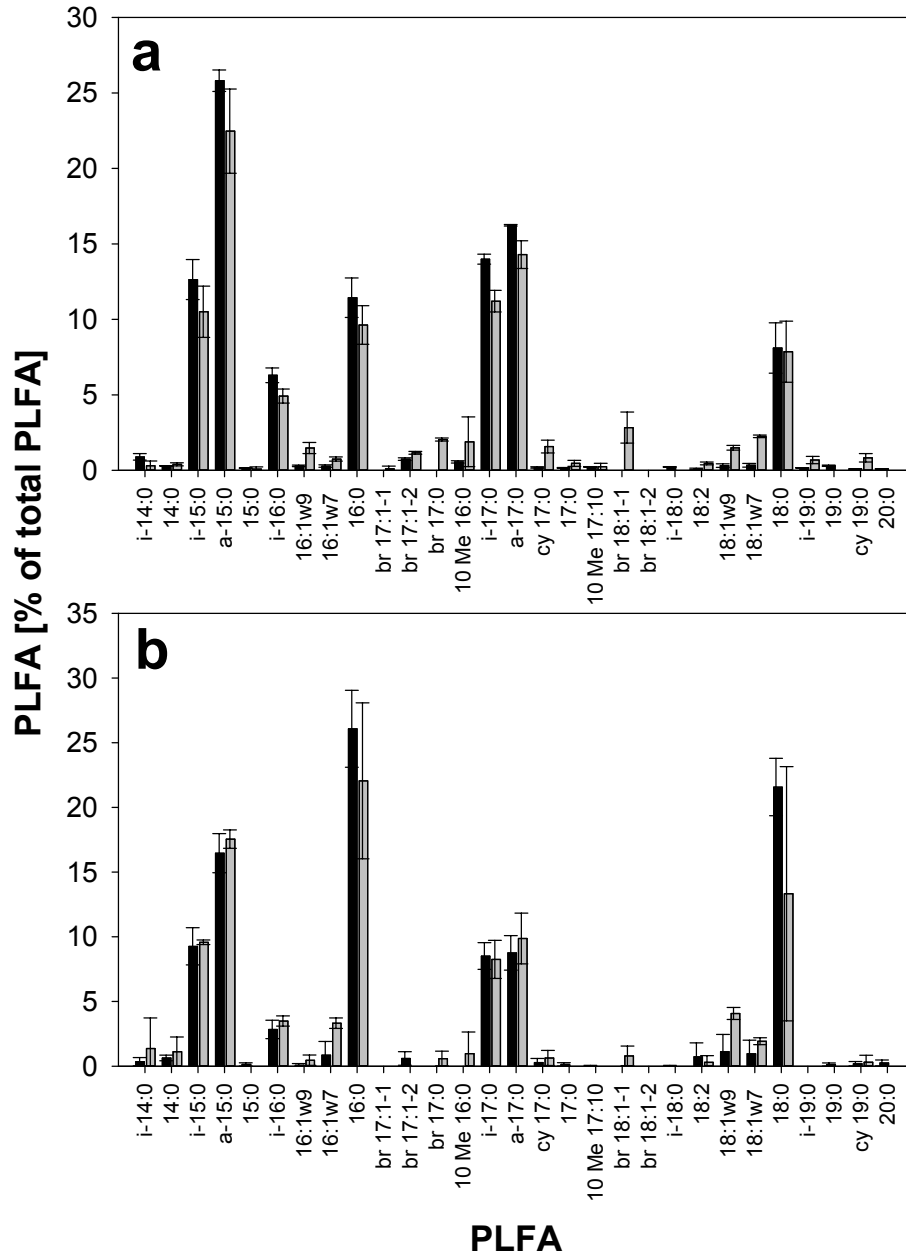


Fig. 21: Relative percentages of different phospholipid fatty acids (PLFA) in incubation studies with (a) intact cells and (b) cell envelope fragments of *B. subtilis* before (black bars) and after (grey bars) 32 weeks incubation in artificial soil 1 (AS1).

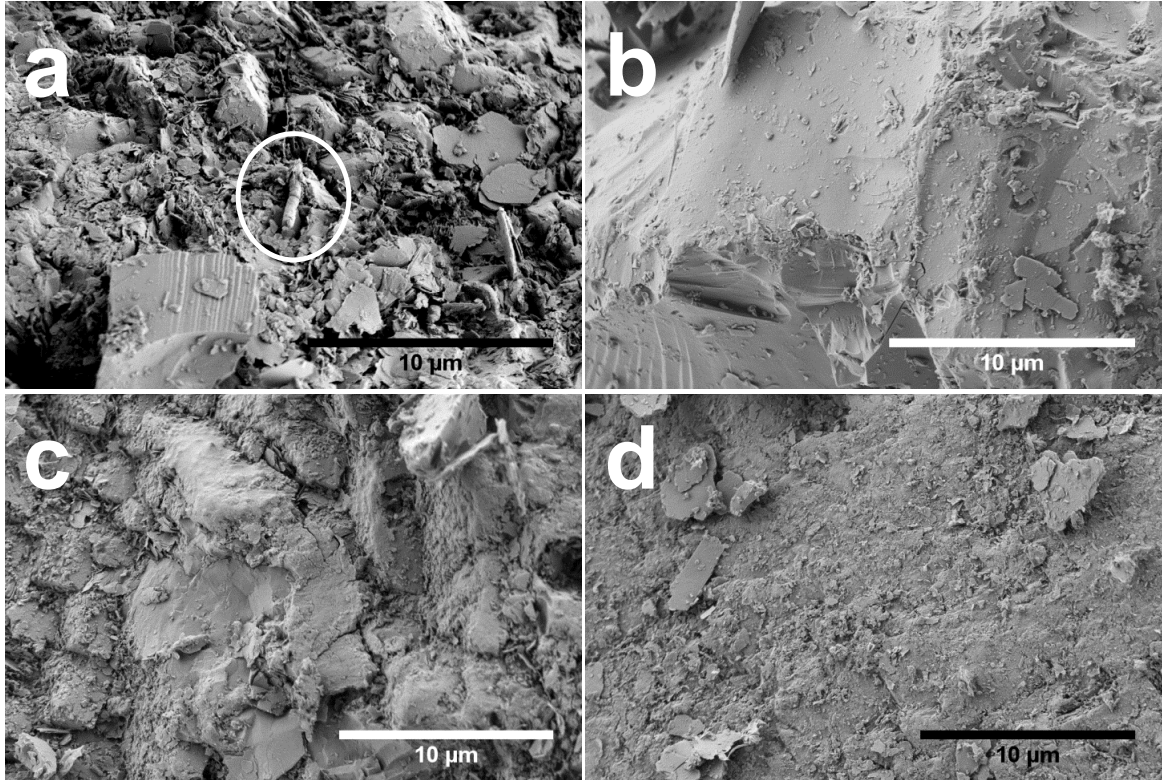


Fig. 22: Scanning electron micrographs of intact cells of *B. subtilis* at the (a) beginning and after (c) 8 weeks, and cell envelope fragments at the (b) beginning and after (d) 8 weeks incubation in artificial soil 2 (AS2). White circles indicate intact cells.

Cells and envelope fragments of *S. mirabilis*, an actinomycete, were observable during incubation although the cell number was lower compared to the studies with *P. putida* and *B. subtilis* (Fig. 24). The hyphal structures, which are considerably larger preventing the cells from dissipation and destruction during the mixing process, were responsible for these observations. These structures were smaller for the cell fragments than for the intact cells. The envelopes were already disintegrated into flaky and porous structures at 0 d, but their visual nature was preserved during incubation. After 32 weeks, the filamentous hyphal structures of the intact cells were still observable, but they were porous, fractured and flaky compared to the start of the incubation period. Furthermore, the hyphae were covered by small-sized minerals possibly protecting the biomass from further degradation. The structures were

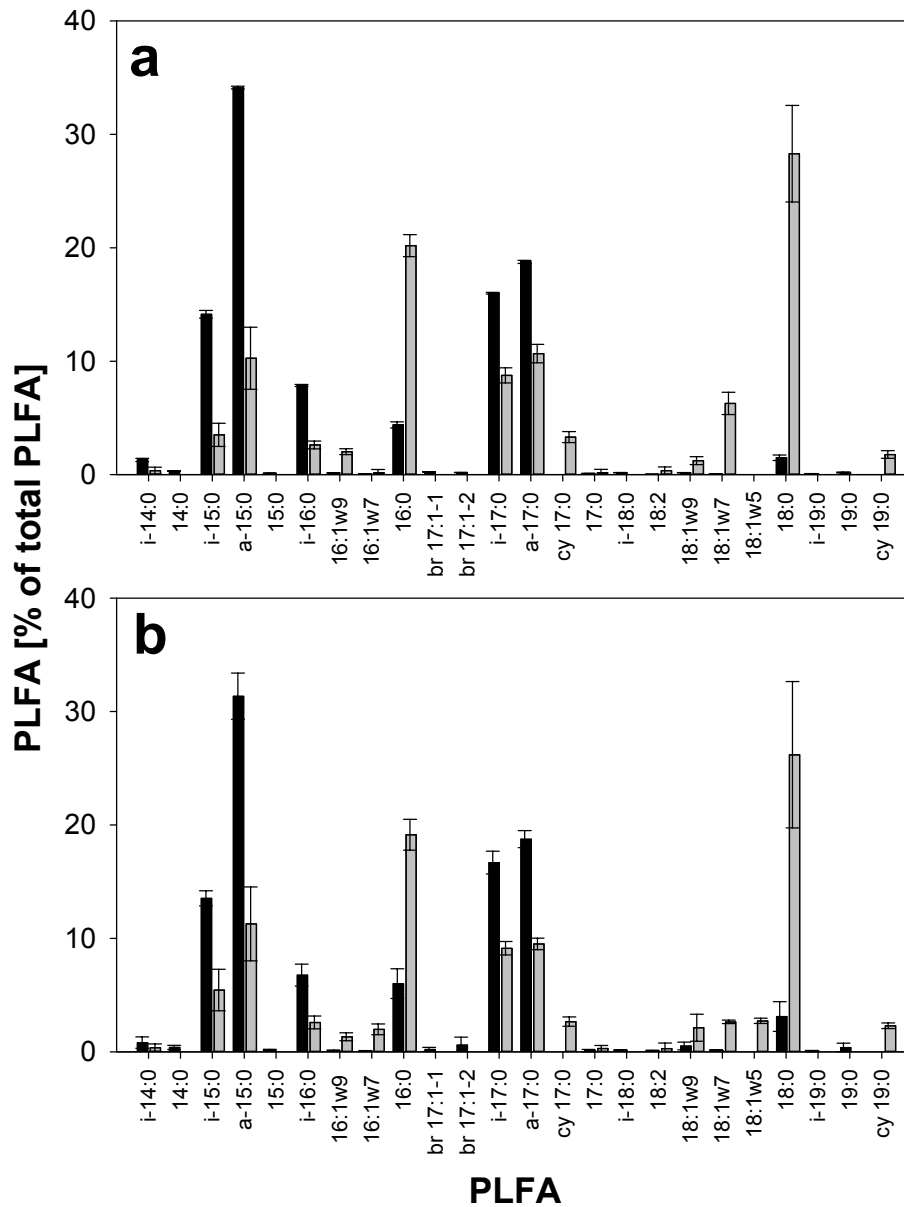


Fig. 23: Relative percentages of different phospholipid fatty acids (PLFA) in incubation studies with a) intact cells and b) cell envelope fragments of *B. subtilis* before (black bars) and after (grey bars) 32 weeks incubation in artificial soil 2 (AS2).

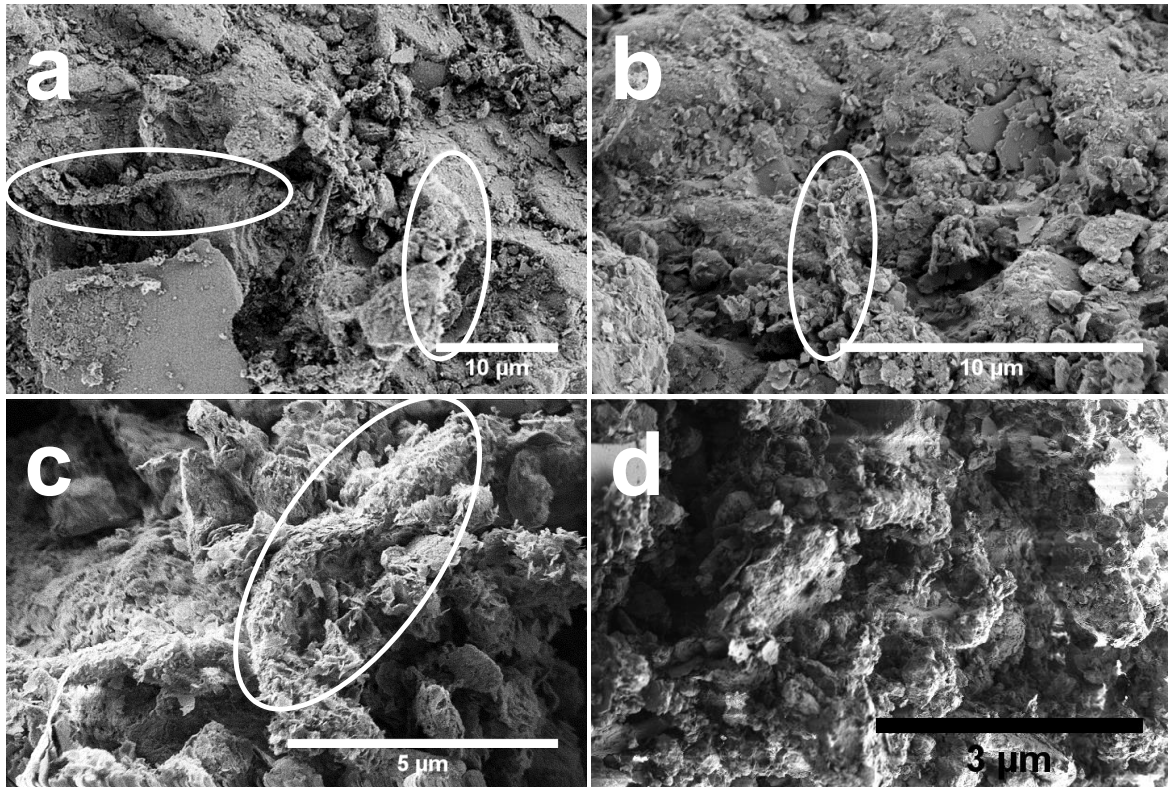


Fig. 24: Scanning electron micrographs of intact cells of *S. mirabilis* at the (a) beginning and after (c) 32 weeks, and cell envelope fragments at the (b) beginning and after (d) 32 weeks incubation in artificial soil 1 (AS1). White circles indicate intact cells or cell envelope fragments.

similar to the cell envelopes at incubation start. Therefore, the death and decay led to the formation of cell envelope fragments. The remaining hyphae and envelope fragments contribute therefore to SOM. The results of the present study are in accordance with previous ones, where the death and decay of *Streptomyces* spp. in heavy-metal contaminated soils and the formation of residual cell envelope fragments was also observed (Schütze et al., 2013).

The death and decay of *S. mirabilis* is supported by the results of the PLFA and tFA analysis. The PLFA of the intact cell treatment decreased from 69 ± 5 to 6.6 ± 2.9 and of the cell fragment treatment from 43 ± 9 to 6.4 ± 0.4 nmol g⁻¹ soil after 32 weeks incubation corresponding to 10 and 15% of the initial value, respectively (Tab. 7). The tFA concentrations

were higher than the PLFA even for the initial samples (intact cells: 850 ± 70 to 107.1 ± 2.9 , cell envelope fragments: 198 ± 23 to 45 ± 4 nmol g⁻¹ soil), but the decrease less pronounced supporting the stabilization of the FA within the non-living SOM fraction. The composition of the PLFA for intact cells and cell envelope fragments was similar (Fig. 25). At the beginning, the a-15:0 and a-17:0 FA, which are indicators for Gram-positive bacteria like *Streptomyces* sp., accounted for nearly 60% of the PLFA. Their abundance decreased during incubation, while the amount of 18:0 and several monounsaturated FA, e.g., br 17:1, 18:1w9 and 18:1w7 increased indicating the decay of the initially added *S. mirabilis* and growth of other species of bacteria.

In the present experiments, the degradation and the formation of cell envelope fragments of different types of microorganisms was analyzed. While the decrease in PLFA and tFA concentration was shown for all organisms, the visualization of the decay by means of SEM was only possible for *S. mirabilis*. The PLFA composition of the treatments with intact cells and fragments were similar and specific for the added bacterial strain. During incubation, the PLFA composition became more diverse indicating the development of a microbial community.

The use of ¹³C-labeled bacteria as described by Kindler et al. (2006) with subsequent analysis by means of nano-scale secondary ion mass spectrometry (NanoSIMS) (Vogel et al., 2014) may be helpful to detect cell envelope fragments and elucidate their spatial organization on mineral surfaces. Less complex systems, e.g., without clay minerals, would reduce the heterogeneity and the SSA of the artificial soils and thus make visualization of the cell envelope fragments possible, but would also decrease the adaptability of the results to natural soils.

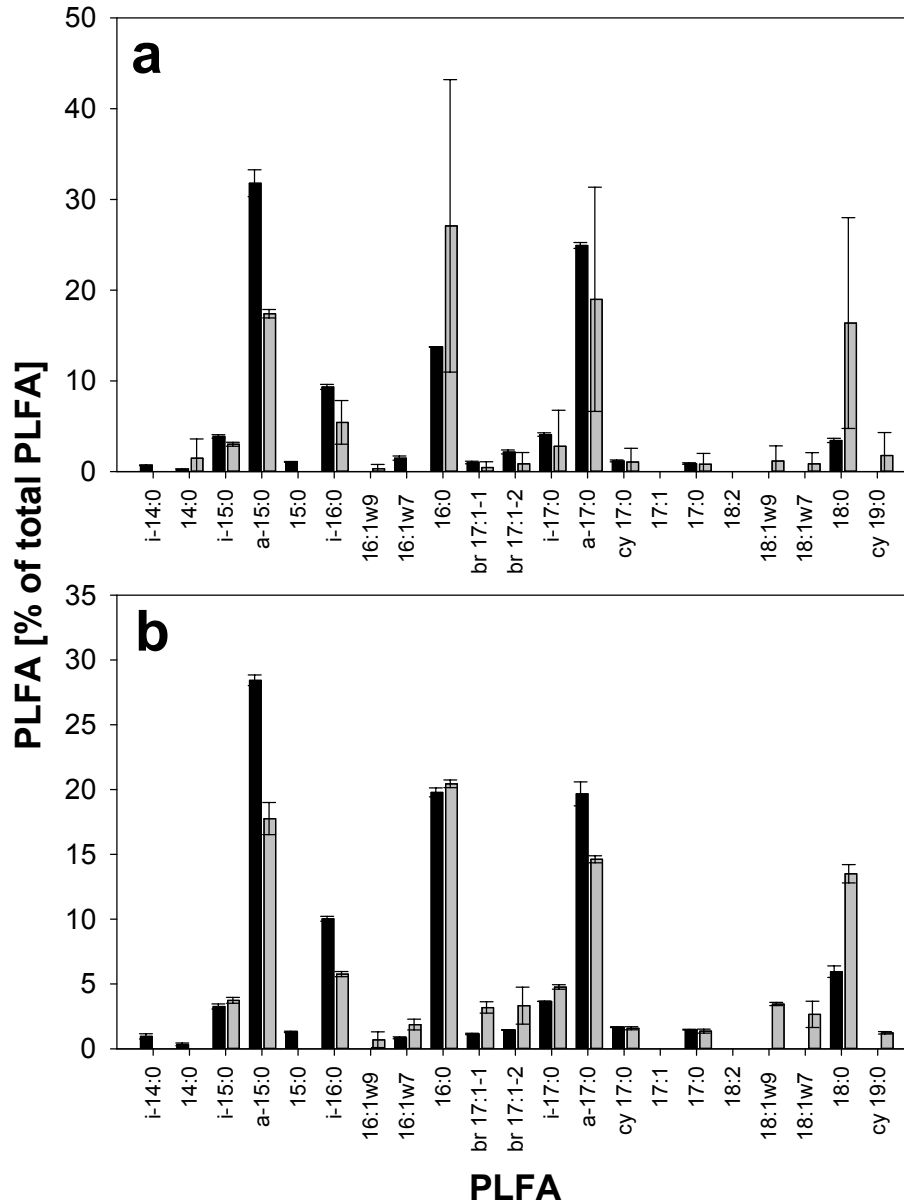


Fig. 25: Relative percentages of different phospholipid fatty acids (PLFA) in incubation studies with (a) intact cells and (b) cell envelope fragments of *S. mirabilis* before (black bars) and after (grey bars) 32 weeks incubation in artificial soil 1 (AS1).

Tab. 7: Concentrations of phospholipid fatty acids (PLFA) and total fatty acids (tFA) of the incubation studies with artificial soils after different times of incubation (n/a: not applicable).

Organism	Control		<i>Pseudomonas putida</i>		<i>Bacillus subtilis</i>		<i>B. subtilis</i>		<i>Streptomyces mirabilis</i>	
Artificial soil	AS1		AS1		AS1		AS2		AS1	
	PLFA	tFA	PLFA	tFA	PLFA	tFA	PLFA	tFA	PLFA	tFA
[nmol g ⁻¹ soil (dry weight)]										
Intact cells										
Week 0	9 ± 4	2.3 ± 0.7	270 ± 40	270 ± 60	42 ± 13	226 ± 14	171 ± 23	473.1 ± 2.5	69 ± 5	850 ± 70
Week 8	5.2 ± 0.7	2.6 ± 0.2	106 ± 21	230 ± 40	34.8 ± 2.5	117 ± 13	63 ± 18	230 ± 70	31 ± 7	174 ± 26
Week 16	1.9 ± 0.3	3.7 ± 0.2	75 ± 4	124 ± 27	21 ± 4	70 ± 9	14.9 ± 1.1	97 ± 28	13.8 ± 0.8	137 ± 8
Week 32	1.6 ± 0.6	3.1 ± 0.6	43.9 ± 2.2	150 ± 28	16 ± 5	38.7 ± 2.3	9 ± 5	49 ± 11	6.6 ± 2.9	107.1 ± 2.9
Cell fragments										
Week 0	n/a	n/a	231 ± 25	272 ± 6	13 ± 3	50 ± 8	70 ± 60	149 ± 6	43 ± 9	198 ± 23
Week 8	n/a	n/a	79 ± 14	230 ± 11	12.8 ± 0.5	47 ± 8	15 ± 7	37 ± 6	17.6 ± 2.9	109 ± 2
Week 16	n/a	n/a	55 ± 10	89.5 ± 0.8	9.30 ± 2.14	32 ± 5	4.5 ± 0.9	43 ± 5	9 ± 4	61 ± 4
Week 32	n/a	n/a	25 ± 18	108 ± 13	5 ± 2	14.6 ± 1.6	7 ± 7	44 ± 6	6.4 ± 0.4	45 ± 4

4.1.4 Turnover of intact bacterial cells and their fragments in closed natural soil systems

As the results of the previous experiments gave no information about the turnover and recalcitrance of cell envelope fragments, these aspects were further investigated. It was hypothesized that the turnover of fragmented cell envelopes is slower than those of intact bacterial cells, which may contribute to their accumulation. In order to test this, incubation studies with ^{14}C -labeled *E. coli* cells and corresponding cell envelope fragments were performed in natural soil to increase the degree of complexity once again. Various conditions were applied to investigate the effect of redox conditions, water content and additional C, N and P containing substrate on the turnover of cells and fragments.

$36.4 \pm 1.2\%$ of the initially added labeled intact *E. coli* cells were mineralized after 101 d incubation under aerobic conditions (Fig. 26a). In comparison, the mineralization of labeled cell envelope fragments was less ($29.1 \pm 0.5\%$), which indicates greater stability for the fragments. Further incubation and additional added C, N, and P containing substrate did not change the difference between the treatments (mineralization intact cells: $50.6 \pm 1.5\%$, mineralization cell envelope fragments: $43.9 \pm 0.7\%$). The addition of fresh nutrients and substrate thus led to a further increase in mineralization for both intact cells and cell wall fragments. The recovery ranged from 90 to 110 % (for residual activities and recoveries see Appendix Tab. 8, page 92).

The incubation was also performed under O_2 depleted conditions with subsequent water saturation. Therefore, the systems were incubated under a N_2 atmosphere and saturated with degassed demineralized water after 101 d incubation. $39.5 \pm 2.4\%$ of the initially labeled intact cells were recovered as $^{14}\text{CO}_2$ after 101 d incubation (Fig. 26b). In contrast, the extent of mineralization of the cell fragments was just 27.1 ± 1.0 From 101 d, the incubation systems were water saturated. This increased the mineralization of the cell fragments to

a large extent, while the nutrient addition had no effect. Therefore, at the end of the incubation after 346 d, the difference between cell fragments and intact cells was negligible (mineralization intact cells: $59.00 \pm 0.36\%$, mineralization cell fragments: $58.00 \pm 0.63\%$). At this time, the redox potential varied between -60 and -30 mV and the pH between 7.6 and 7.8. The recovery was between 90 and 110 % (Appendix Tab. 8).

Under the conditions studied, the cell envelope fragments had lower decomposition rates than intact cells. This may promote their accumulation in soil. Reasons for the reduced mineralization of the cell envelope fragments may be their structural flexibility and many different functional groups present in biomolecules such as proteins, or the smaller size of the fragments compared to intact cells, which may allow a better contact to mineral surfaces.

Kindler et al. (2006) found 65 % mineralization of ^{13}C -labeled *E. coli* cells after 224 d incubation in closed, aerated soil reactors. In earlier studies, the mineralization of various prokaryotic cells varied between 43 and 50 % after 56 d (Marumoto et al., 1982). After 130 d, mineralization of a mixture of soil bacteria was 54 %, independent of the added bacterial ^{14}C input (van Veen et al., 1987). Therefore, the mineralization rates of previous studies were higher compared to this study, which is presumably due to the specific experimental conditions, in particular the usage of lyophilized cell material enabling a much faster microbial metabolism, other soil types and the continuous aeration. Regarding the degradation of cell envelope fragments in soil systems, a previous study found that the mineralization was 60 % for *Saccharomyces cerevisiae* fragments after 6 weeks (Marumoto et al., 1977). For the degradation of microbial cell walls in a semi-arid grassland soil under various soil water contents, mineralization between 12 and 78 % after 7 d was observed (Nakas and Klein, 1979). In contrast to the results of this study, Cortez (1989) observed only negligible differences between the mineralization of cell envelope fragments (60 %) and intact cells (59 %) after

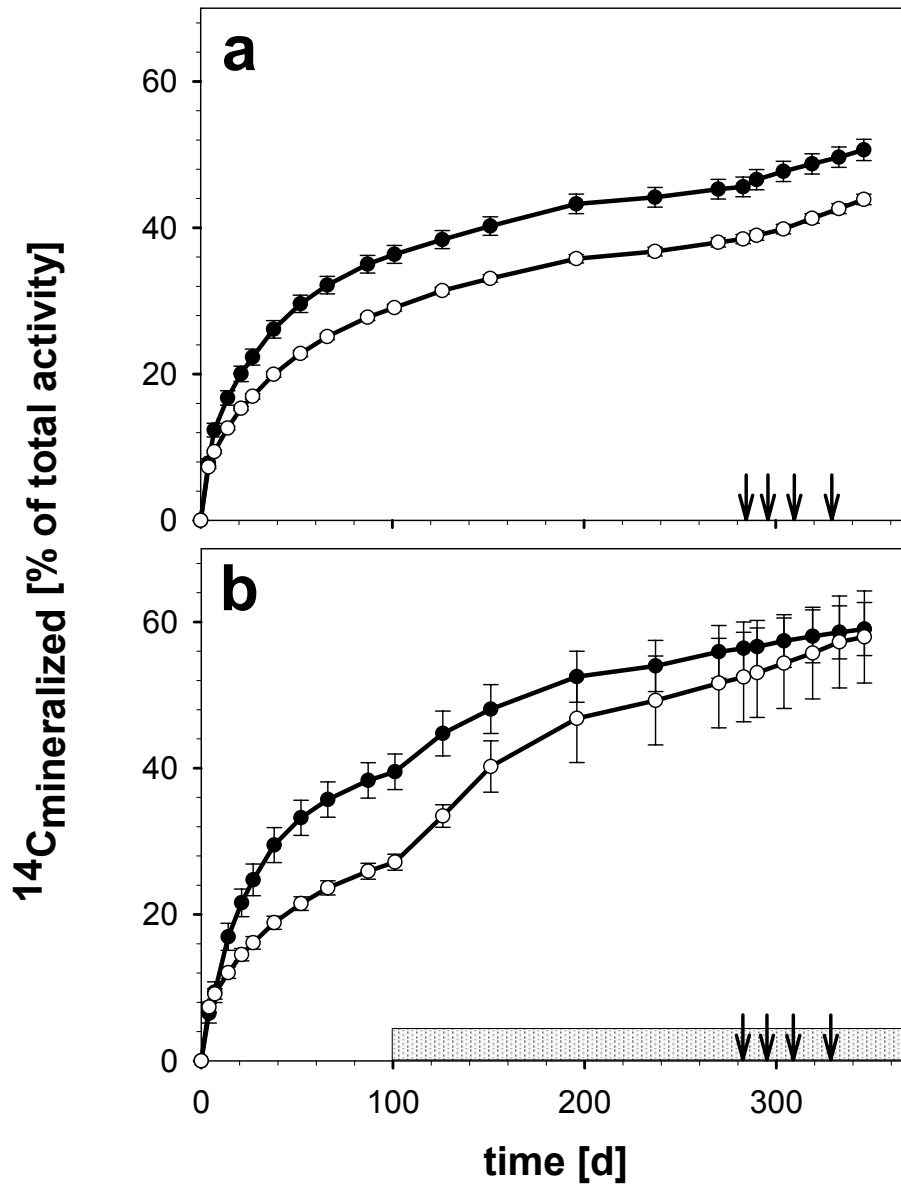


Fig. 26: Cumulative mineralization of intact ^{14}C -labeled *E. coli* cells (black circles) and cell envelope fragments (white circles) in soil incubation studies under (a) oxic and (b) O_2 depleted conditions. Arrows indicate time of nutrient and substrate addition (C, N, P) and the dotted areas water saturation.

211 d including two soil drying and rewetting cycles. The use of freeze-dried materials in previous experiments, which enable a faster turnover of cell envelope fragments and intact cells and the changes in the water regime, which were also revealed as an important factor in this study, may be explanations for the observed discrepancies.

In summary, cell envelope fragments were turned over more slowly than intact cells, which may promote their accumulation in soil. While a lower O₂ content had no clear effect, the water-logging increased the mineralization of the cell fragments to a large extent indicating that shrinking and swelling of cell envelopes may cause this effect.

4.2 Stabilization of microbial residues in soil

The results of the previous section have shown that the turnover of cell envelope fragments in soil was slower than those of intact bacterial cells, which may promote their accumulation. However, additional stabilization mechanisms may prevent biomass from degradation in soil. As already mentioned, the occlusion and incrustation due to co-precipitation can be considered as an additional stabilization mechanism and therefore, the protective effect was tested with ^{14}C -labeled biomass co-precipitated with Al and Fe oxyhydroxides. Because the redox potential is an important factor for Fe mobilization and precipitation and so for SOM stabilization and persistence, which also affects the co-precipitated organo-mineral associations (Schmidt et al., 2011), the samples were incubated under various levels of oxygen and water content. It was hypothesized, that the change in redox conditions may promote the dissolution of redox-sensitive organo-Fe oxyhydroxide associations leading to an enhanced mineralization.

The occlusion of cells and corresponding fragments with Fe oxyhydroxides caused a considerable decrease in mineralization rate vs. the control without the co-precipitates. After 98 d incubation, only $8.9 \pm 0.4\%$ of the ^{14}C was mineralized for the intact cells and $6.0 \pm 0.3\%$ for the cell fragments (Fig. 27a) under aerobic conditions. The mineralization was therefore four to five times lower than the control without the co-precipitates (Fig 26, page 63). Further incubation increased the mineralization up to $18.5 \pm 0.6\%$ (intact cells) and $12.6 \pm 0.7\%$ (cell envelope fragments) after 343 d incubation. The addition of nutrients had only a minor impact. The occlusion with Al oxyhydroxides also caused a decrease in degradation. After 101 d, the mineralization of cell fragments and intact cells were nearly the same (about 13%) (Fig. 27b) and thereby three times lower compared to the control. Further incubation increased the mineralization to 23% after 346 d; at this time it was therefore higher than in

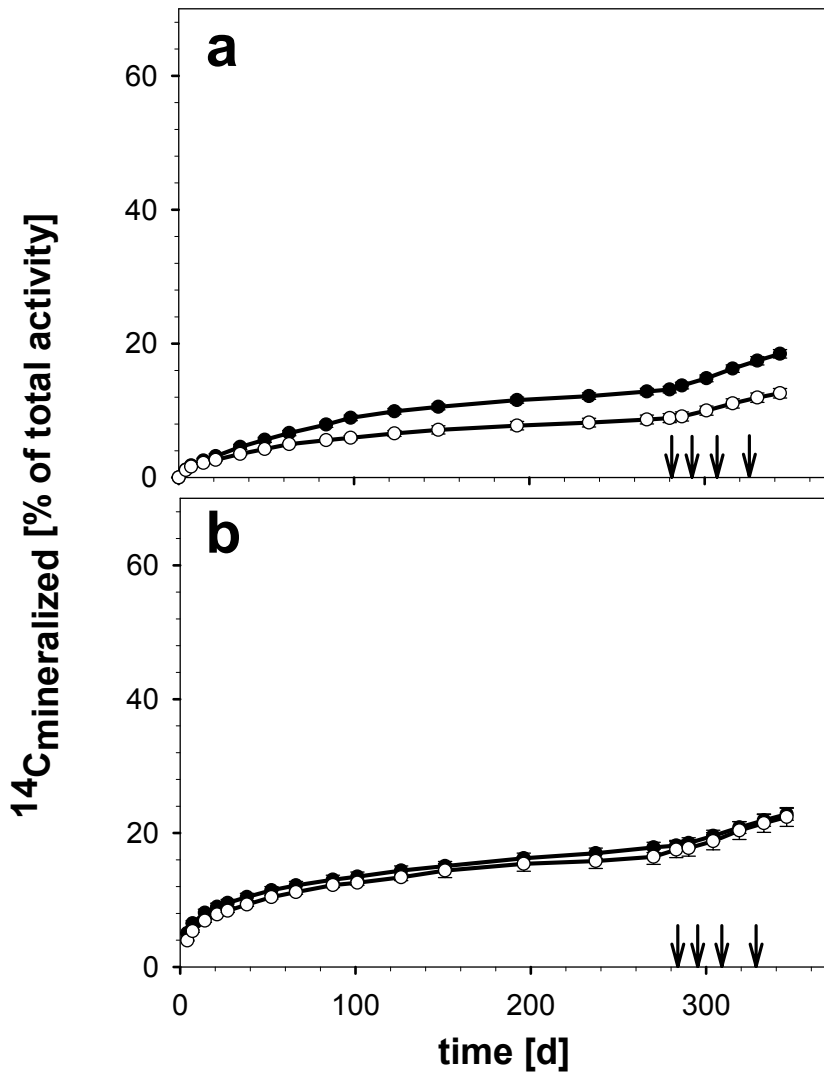


Fig. 27: Cumulative mineralization of intact ^{14}C -labeled *E. coli* cells (black circles) and cell envelope fragments (white circles) with (a) co-precipitation with Fe oxyhydroxide or (b) co-precipitation with Al oxyhydroxide, in soil incubation studies under aerobic conditions. Arrows indicate additional nutrient and substrate addition (C, N, P).

the Fe oxyhydroxides treatments. For all oxic incubation studies, the recovery ranged from 90 to 110 % (for residual activities and recoveries, see Appendix Tab. 8, page 92).

The incubations were also performed under O_2 depleted conditions with subsequent water saturation. Occlusion with Fe oxyhydroxides protected both the intact cells (mineralization:

$8.8 \pm 0.5\%$) and the cell envelope fragments (mineralization: $6.3 \pm 0.4\%$) to a large extent from degradation. The subsequent water saturation and further incubation had only a minor impact. In contrast to the oxic treatments, the addition of C and nutrients caused a drastic increase in mineralization extent (Fig. 28a). The mineralization increased to $36.7 \pm 1.3\%$ for the intact cells and $28.2 \pm 3.3\%$ for the cell fragments. The final redox potential of the test systems was -90 mV and the final pH between 8.2 and 8.4.

The occlusion with Al oxyhydroxides had a less pronounced stabilizing effect than the Fe treatment. After 101 d, the mineralization of the intact cells treatments was $18.3 \pm 0.8\%$, while that of the cell envelope fragments was $14.1 \pm 0.8\%$ (Fig. 28b). The subsequent water saturation had no clear effect on the mineralization, while there was a positive effect of the substrate and nutrient addition, increasing the mineralization of the intact cells to $32.8 \pm 1.3\%$ and of the cell fragments to $29.2 \pm 1.6\%$. The redox potential was between -50 and -60 mV and the pH ranged from 8.2 to 8.5. For all treatments, the recoveries were between 80 and 110% (see Appendix Tab. 8).

The results of the experiments confirmed the hypotheses that the occlusion and incrustation of microbial cell envelope fragments and intact bacterial cells by co-precipitation with Al and Fe oxyhydroxides has a protective effect against degradation. While the reduced oxygen contents had no clear effect, water saturation as well as nutrient and substrate addition accompanied by decreasing redox potentials increased the mineralization, in particular of samples with redox-sensitive Fe occlusions, emphasizing the importance of dissolution of Fe minerals as an important destabilization mechanism (Sollins et al., 1996). The occlusion with Al and Fe oxyhydroxides is therefore an effective stabilization mechanism for biomass residues and may be important for SOM stabilization in general. The protection against microbial attack afforded by the occlusion of organic matter into mineral aggregates may be the underlying mechanism, because it results in the inaccessibility of the material to

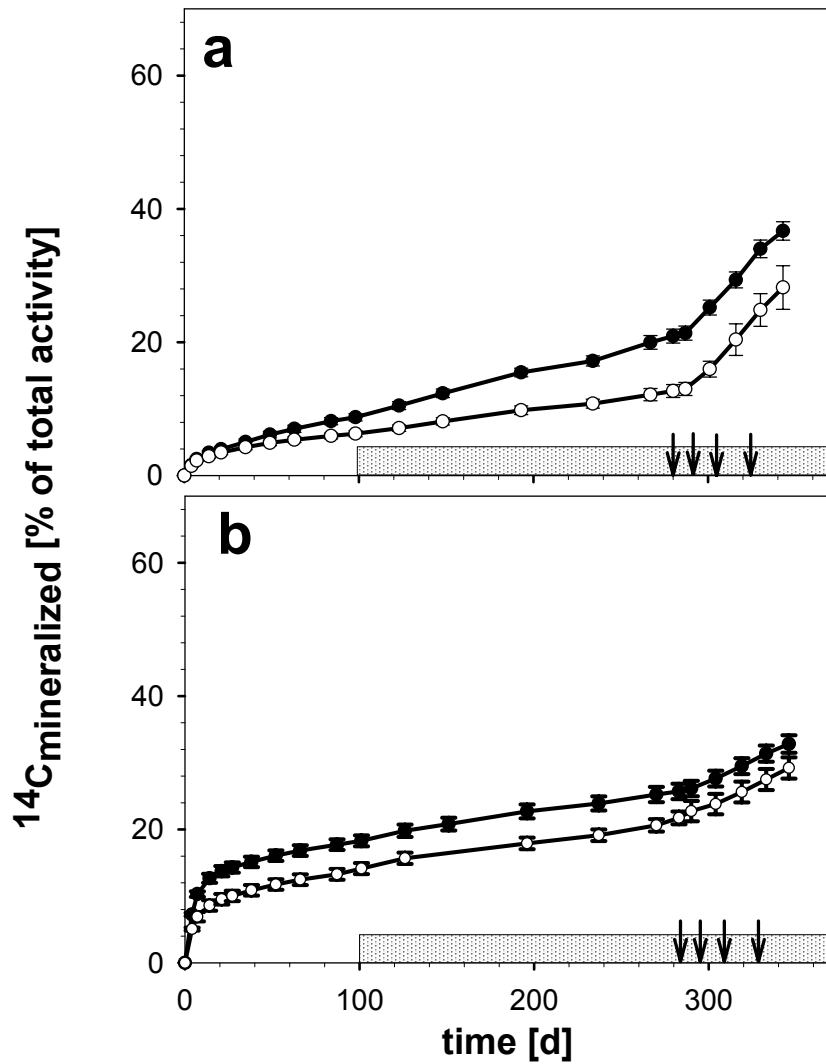


Fig. 28: Cumulative mineralization of intact ^{14}C -labeled *E. coli* cells (black circles) and cell envelope fragments (white circles) with (a) co-precipitation with Fe oxyhydroxide or (b) co-precipitation with Al oxyhydroxide, in soil incubation studies under O_2 depleted conditions. Arrows indicate time of nutrient and substrate addition (C, N, P) and the dotted areas water saturation.

hydrolyzing enzymes such as proteases (Eusterhues et al., 2014). The release of CO₂ after nutrient and substrate additions was pronounced in the water saturated systems with redox-sensitive Fe co-precipitates most. This was presumably due to the lowered redox potential resulting from microbial substrate consumption activity. An alternative explanation is the desorption of DOM from Al and Fe oxyhydroxide surfaces after the addition of phosphate in the buffer as shown in sorption experiments (Kaiser and Zech, 1997). However, the release of CO₂ would also be observable for the redox-insensitive Al oxyhydroxide treatment and under aerobic conditions, if competitive sorption were the main destabilization mechanism. Therefore, the reductive dissolution of the Fe oxyhydroxides plays an important role in destabilizing the cell envelopes in the Fe co-precipitates. The stabilizing effect on OM via co-precipitation has been shown by various authors, but mainly with the focus on DOM or EPS without the specific macromolecular aggregation of cell components. Scheel et al. (2007) showed that the precipitation of DOM with Al protected the organic matter significantly against microbial attack after 7 weeks. The same stabilizing effect was also observed for the degradation of EPS-Al precipitates in soil (Mikutta et al., 2011), although cell lysates rather than EPS in a microbiological definition were used. The stabilizing effect of the interaction of bulk OM such as leaf litter polysaccharides with Al hydroxide has already been shown by Miltner and Zech (1998), but it was mainly attributed to the adsorption of OM to mineral surfaces. In a recent study, the co-precipitation of a forest floor extract with FH stabilized the OM against degradation with fivefold lower metabolisation compared to the control after 68 d (Eusterhues et al., 2014). The biodegradation of lignin was completely prevented by this co-precipitation. At this point it must be stated that, in contrast to the present study, most of the previous incubation studies were performed in aqueous, DOM containing systems (Scheel et al., 2007; Mikutta et al., 2011; Eusterhues et al., 2014). The protection of intact cells and cell envelope fragments by occlusion with Al and Fe in particular due to co-precipitation presented here suggesting the relevance of this process in natural soils.

There is a general consensus that the protection of OM by sorptive interaction to mineral surfaces is the main mechanism explaining the stabilizing effect of organo-mineral interactions (Kögel-Knabner et al., 2008). The particular process of co-precipitation may occur mainly in temporarily flooded or groundwater affected soil, where changes in redox conditions, causing precipitation of Fe oxyhydroxides, take place. However, co-precipitation is assumed to occur in many sediments and soils (Eusterhues et al., 2014). Even in aerobic soil, changes in water content will result in filling or draining of pores. This can create anaerobic microsites, e.g., in the interior of aggregates (Pallud et al., 2010), and thus cause destabilization of redox-sensitive aggregates at these microsites.

A rather artificial experimental setup was chosen in order to study the effect of isolated factors for a better process understanding. Relevant mineral phases together with cell envelope fragments and intact bacterial cells were used, which have been shown to be a significant source of SOM (Kindler et al., 2006; Miltner et al., 2012; Schurig et al., 2013; Schütze et al., 2013). Although only one type of microorganism (but with the typical cell structure of Gram-negative bacteria) and two minerals were used, the general process is valid and can be transferred to natural systems. Therefore, the results provide new evidence that the occlusion of OM by co-precipitation with oxyhydroxides may be a significant process for the long-term stabilization at least of microbial residues in SOM.

From a mechanistic point of view, the observed stabilization must be caused by the physical separation of the biomolecules and macromolecular aggregates from potentially degrading enzymes such as hydrolases, proteases or xylanases. Before oxidation and precipitation, dissolved reduced metal ions will migrate into appropriate molecular spaces of the aggregates of various microbial cell wall types of fungi and Gram-negative or Gram-positive bacteria, as shown in Fig. 29 and precipitate there resulting in a strong protection against microbial attack. Certain differences in the ratio of occlusion and incrustation can be expected in

principle from the macromolecular structures of the various cell wall types. In addition to cell envelope fragments, all other particulate macromolecular aggregates such as ribosomes or fragments of the cytoskeleton can also be occluded.

For more differential understanding, the validity of the results needs to be confirmed for other types of microorganisms, e.g., fungi or Gram-positive bacteria, and for cytosolic compounds and other co-precipitates like Mn associations. Incubation experiments using ^{13}C and ^{15}N -labeled cells together with analysis of PLFA, amino acids and amino sugars would allow the fate and behavior of the protected microbial residues to be traced. Cutting-edge visualization methods, such as NanoSIMS, may provide more information on the exact composition of the cell-mineral co-precipitates as well as their spatial distribution in soil, and thereby on the stabilization mechanisms (Vogel et al., 2014).

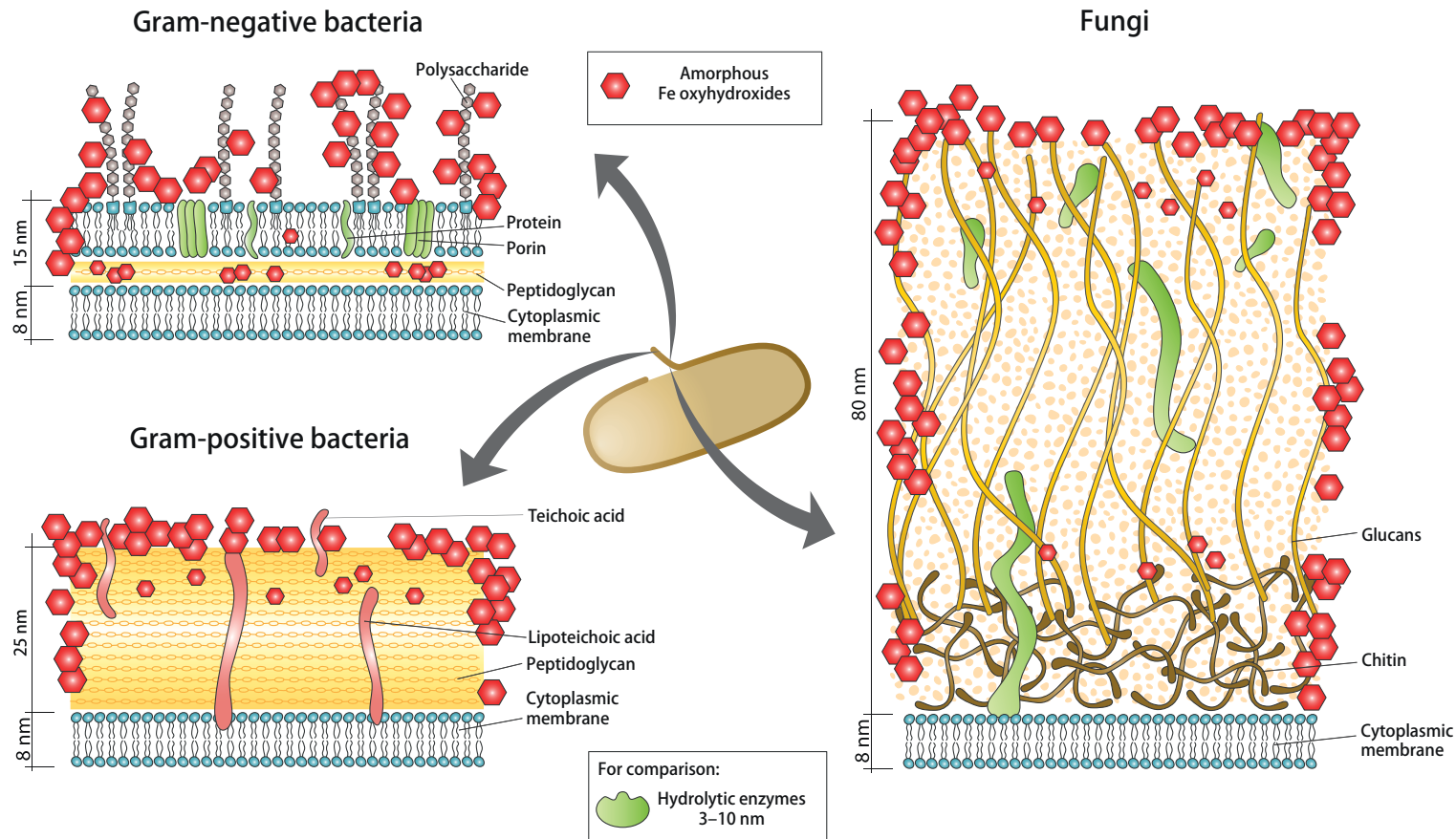


Fig. 29: Occlusion and incrustation of microbial residues, e.g., cell envelope fragments, by co-precipitation with Al and Fe oxyhydroxides as a mechanism for soil organic matter stabilization. Reduced dissolved metal ions can migrate into the cell wall structures or accumulate at the surfaces, where they precipitate leading to strongly restricted access of potential degrading hydrolytic enzymes to the biomass.

4.3 Impact of microbial residues on soil wettability

As shown before microbial cell envelope fragments accumulate and are stabilized in soil and thus contribute to SOM formation. Therefore, these processes may influence physical soil properties, like the wettability of the mineral phase. The hypothesis of the following section was that the interactions of cell envelope fragments, intact cells with minerals and stress-related adaptation mechanisms of bacteria change the surface wettability of the particles. Therefore, osmotic stress-induced changes of bacterial surfaces properties and their effect on the properties of organo-mineral associations were studied.

Fig. 30 shows representative SEM micrographs of the organo-mineral associations with MQ as mineral component. The morphological differences between the unstressed and by NaCl addition osmotically stressed cells were clearly visible (Fig. 30a–d). While unstressed cells showed a smooth surface and the rod-shape of vital cells, some of the stressed cells were flat and partly broken cell envelopes were visible. The cells were heterogeneously distributed over the quartz surface in the form of patchy microcolony-like structures. The same observations were made with another quartz (CQ) as mineral component (see Appendix Fig. 37, page 93). The cell fragments, however, showed a spherical and patchy shape (Fig. 30) and were, in contrast to the intact cells, more homogeneously distributed on the mineral surface. Generally and as expected, the surface coverage was higher with increasing cell concentration. The wetting properties of both quartz sands (MQ and CQ) were significantly influenced by attached bacteria (Fig. 31). Both types of quartz sand showed a negligible CA between 0 and 11° without and with 10^8 cells g^{-1} mineral. With increasing number of cells, the wettability significantly decreased until the surface was nearly hydrophobic with a CA of about 88° (10^{10} stressed cells g^{-1} MQ). In general, the CA of MQ was slightly larger than that of CQ. The CA of unstressed *P. putida* cells was about 42°, while the stress significantly increased the CA to 65°. This significant difference was reflected in the CA of the

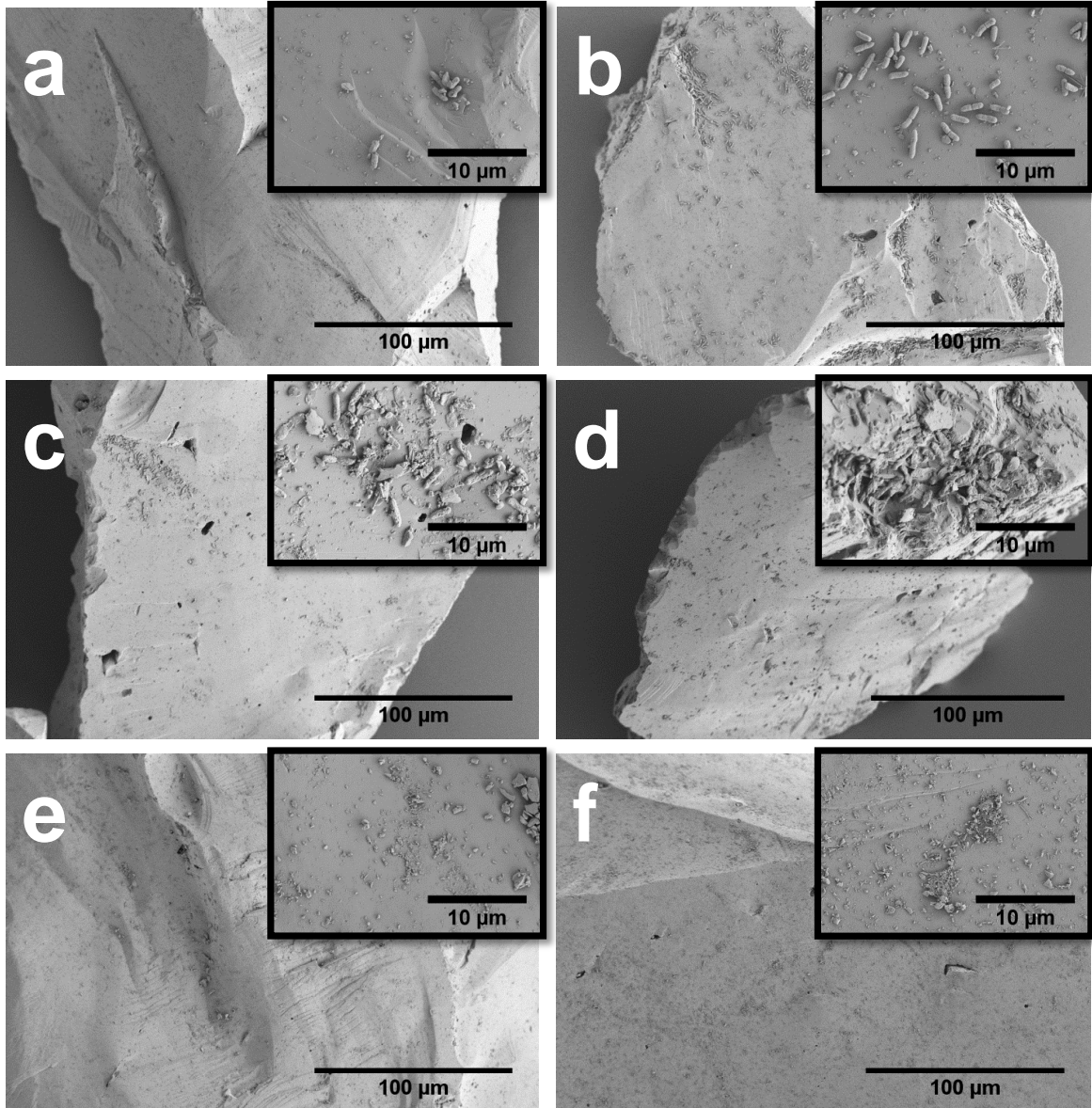


Fig. 30: Scanning electron micrographs of unstressed *P. putida* cells (a, b), osmotically stressed cells (c, d) and cell envelope fragments (e, f) attached to medium-grained quartz surfaces. In micrographs a, c and e, the concentration is 10^8 cells g^{-1} and in b, d and f, the concentration is 10^9 cells g^{-1} quartz. The smaller micrographs were taken at a higher magnification.

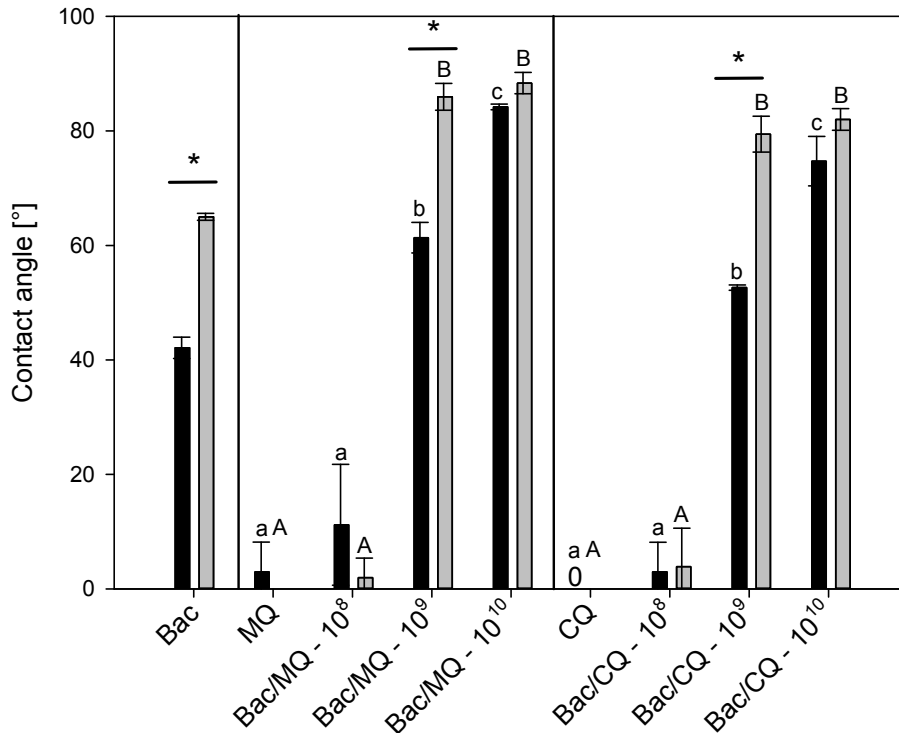


Fig. 31: Contact angle of *P. putida* (Bac) and medium-grained quartz (MQ) and coarse-grained quartz (CQ)/*P. putida* (unstressed cells (black bars) and osmotically stressed cells (grey bars)) - associations after 2 h drying. Different letters indicate significant differences between cell concentrations (lower case letters apply to unstressed cells, upper case letters to stressed cells) and asterisks between unstressed and stressed cells of the same cell concentration ($P < 0.05$).

cell-mineral associations for 10^9 cells g^{-1} MQ (θ unstressed cells: 61° , θ stressed cells: 86°) and CQ (θ unstressed cells: 53° , θ stressed cells: 79°). For the higher cell concentrations, the stress effect was less pronounced.

From regression analysis, an exponential rise up to maximum could be identified for MQ and CQ for CA as a function of the surface covered by unstressed cells (Fig. 32a, c). For the stressed cell-mineral associations, a hyperbolic function could be fitted for MQ (Fig. 32b) and a sigmoidal function for CQ (Fig. 32d), respectively. The fitting functions were chosen according their fitting quality.

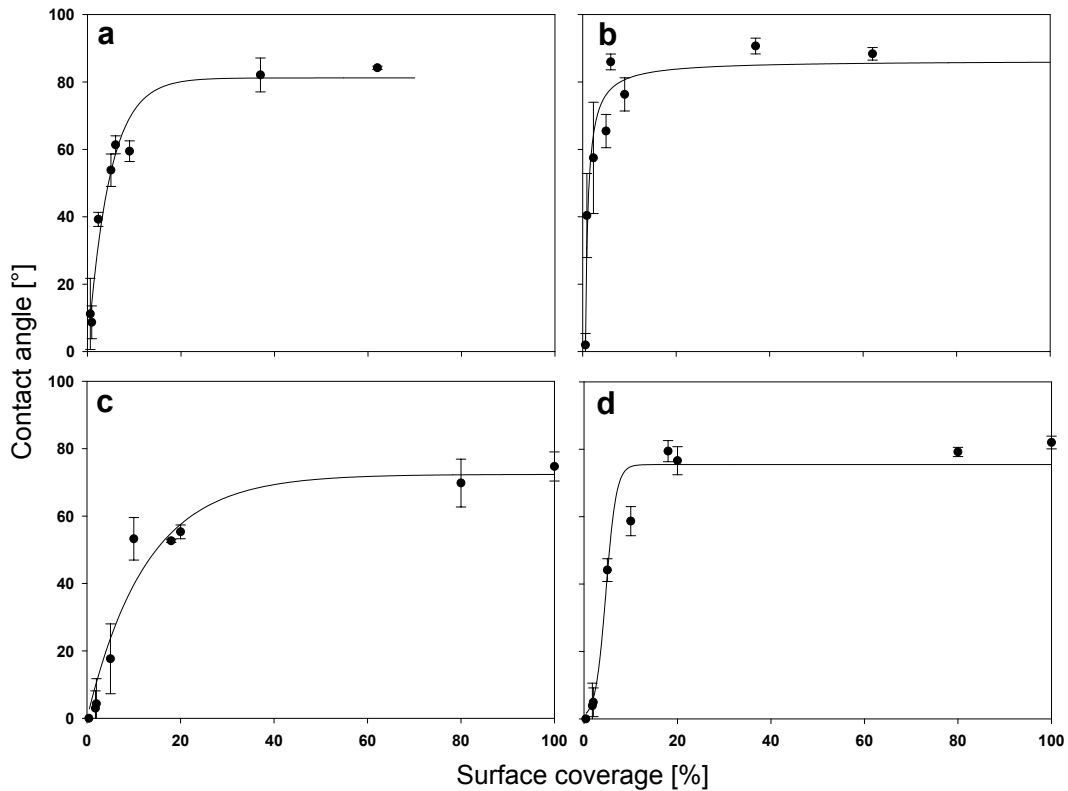


Fig. 32: Contact angle of *P. putida*/ mineral associations in relation to surface coverage with bacteria and corresponding fittings. (a) medium-grained quartz (MQ), unstressed cells; (b) MQ, osmotically stressed cells; (c) coarse-grained quartz (CQ), unstressed cells; (d) CQ, osmotically stressed cells.

The difference in CA between unstressed and stressed cells was observed for cell-mineral associations with 10^9 cells g^{-1} mineral while a higher concentration (i.e., 10^{10} cells g^{-1} mineral) did not additionally increase the effect. The increase of the CA up to a maximum indicates that a coverage between 1 and 11 % had the most significant effect on wettability, while a further increase of coverage only had minor additional effects. The stressed cells caused a distinctly greater increase compared to the unstressed cells at similar surface coverage, emphasizing a clear effect of osmotic stress on SWR (Fig. 32).

Exposure of the bacteria to osmotic stress increased their CA similar to what was observed for *P. putida* DOT-T1E under osmotic stress induced by 2 M NaCl (Baumgarten et al., 2012a).

Similar observations were made by using solvents, e.g., 1-Decanol as a stressor (Neumann et al., 2006). In contrast, silver nanoparticles and silver ions had no influence on the surface properties of *P. putida* mt-2 (Hachicho et al., 2014). The findings of the present study, that bacteria influence the wetting properties of minerals are in accordance with reports by Deo and Natarajan (1997, 1998), that the interaction of *Bacillus polymyxa* and *Paenibacillus polymyxa* with quartz decreased the wettability of the surfaces. A positive correlation between CA and surface coverage was also found for different size fractions of quartz sand treated with stearic acid (González-Peñaloza et al., 2013). However, previous results did not show the relevance of the physiological adaptation processes, e.g., decreased surface wettability of bacteria, for inducing increased water repellency.

As CQ and MQ are characterized by a low SSA, the microbial impact on the wettability of small-sized mineral particles (FQ and KA) was also analyzed (Fig. 33). The CA of pure KA (θ : 44°) was higher than that of FQ (θ : 15°). The attachment of cells significantly decreased the wettability of FQ up to a CA of 62° for 10^{10} unstressed cells g^{-1} mineral. For KA, no distinct effect could be observed. The difference between the CA of the bacterial cells was not reflected in the CA of the cell-mineral associations. The attachment of 10^{10} unstressed cells g^{-1} mineral FQ led to an approximately two times higher, but not significant, CA than the same amount of stressed cells (θ unstressed cells: 62° , θ stressed cells: 35°). An exponential relationship between surface coverage and CA as observed for the two types of quartz sand (MQ, CQ) can explain the observed low impact of bacterial attachment on the wettability of fine-grained minerals. Due to their high SSA (FQ: $1.06 \text{ m}^2 \text{ g}^{-1}$, KA: $8.92 \text{ m}^2 \text{ g}^{-1}$), the cell concentrations used were obviously too low for inducing an effect for KA. FQ was only affected at high bacteria concentrations. In this context it should be noted that the larger initial CA of KA and FQ compared to MQ and CQ presumably contributing to masking the microbially induced changes.

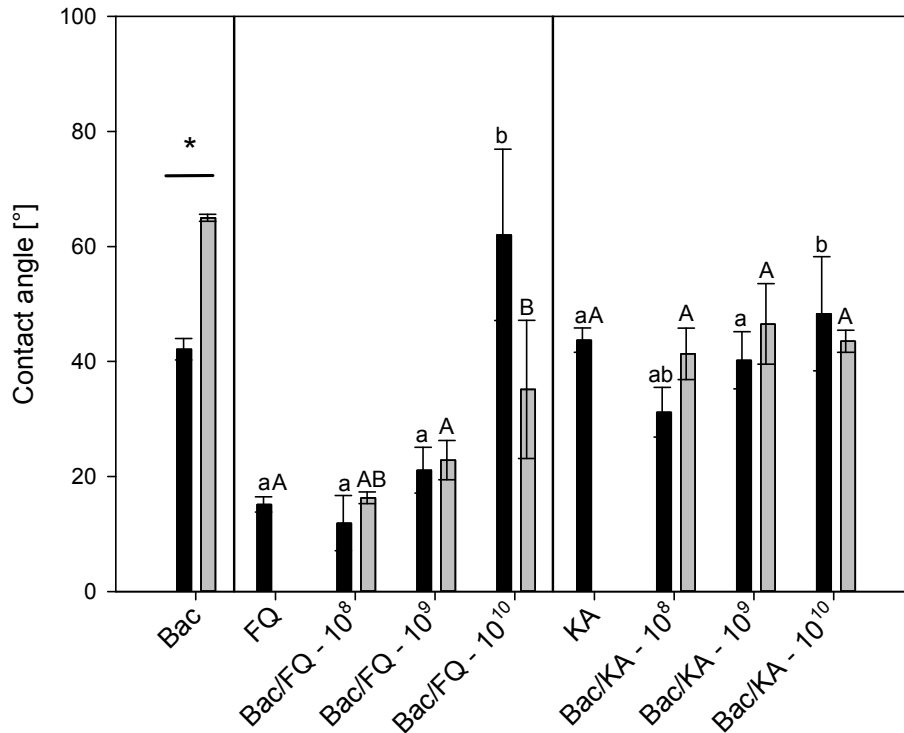


Fig. 33: Contact angle of *P. putida* (Bac) and fine-grained quartz (FQ) and kaolinite (KA)/*P. putida* (unstressed cells (black bars) and osmotically stressed cells (grey bars)) - associations after 2 h drying. Different letters indicate significant differences between cell concentrations (lower case letters apply to unstressed cells, upper case letters to stressed cells) and asterisks between unstressed and stressed cells of the same cell concentration ($P < 0.05$).

Due to the only marginal differences between both quartz sands and the generally large CA of the fine-grained minerals, MQ was selected as the mineral matrix for analyzing the effect of cell fragments, cytosolic compounds and BSA solution on wettability. Like for the intact cells, attachment of cell envelope fragments had no significant effect on the wettability at low concentrations (10^8 cells g^{-1} , Fig. 34). In contrast, the cytosol significantly increased the CA even at low concentrations (θ : 39°). At elevated concentrations, CA increased up to 101° for 10^9 cells g^{-1} , while higher concentrations (10^{10} cells g^{-1}) caused a slight increase for cell fragments and slightly smaller CA for cytosol (Fig. 34). The mixture of cytosol and cell fragments induced a wettability pattern which was similar to that of cytosol with

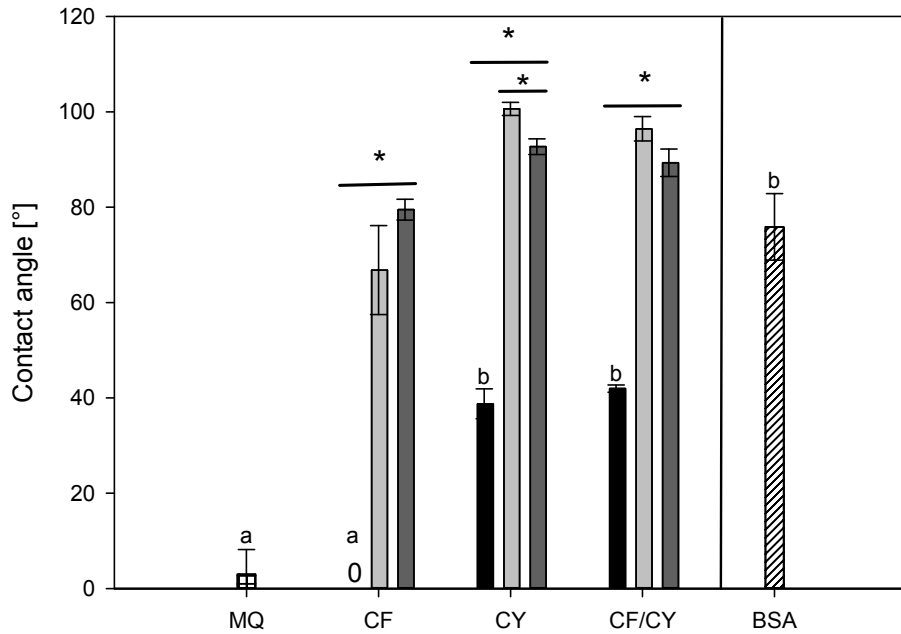


Fig. 34: Contact angle of *P. putida* cell envelope fragments (CF), cytosol (CY), mixture of cell envelope fragments and cytosol (CF/CY) and bovine serum albumin (BSA; hatched bar)/medium-grained quartz (MQ) - associations after 2 h drying. Different bacteria concentrations were used (10^8 : black bars; 10^9 : light grey bars; 10^{10} cells g⁻¹ mineral: dark grey bars). Different letters indicate significant differences between lowest cell concentration of each treatment and control (MQ) and asterisks between cell concentrations of the same treatment ($P < 0.05$).

a maximum CA of 96° at a concentration of 10^9 cells g⁻¹. The addition of BSA solution increased the CA of MQ to 76° , which suggests that proteins in the cytosol are important factors in determining wettability.

Cell envelope fragments and cytosol were able to strongly change the wettability of quartz. A study by Schurig et al. (2013) in the forefield of the Damma glacier (Switzerland) revealed that the coating of minerals with fragments of cell envelopes were correlated with the wettability of the particle surface. The ability of FA, which are important constituents of the cell fragments, to induce water repellency of acid washed sand has been described in various studies (Graber et al., 2009; Mainwaring et al., 2013). The stability of cytosolic substances and cell fragments of dying *Streptomyces* spp. was recently shown by Schütze

et al. (2013). For that reason, the accumulation of fragments and the release of cytosol may influence the wettability of natural soils. The BSA solution was found to induce a similar effect as cytosol, which suggests that proteins may influence the wettability in general as it was also described by Bialopiotrowicz and Janczuk (2001). Other types of proteins, like glycoproteins were also found to be positively correlated with the formation of SWR (Young et al., 2012). By using fragments and cytosol in a mixture, the cytosolic compounds could be identified as most important for determining the wetting properties. This may be due to a more homogenous distribution of the cytosol and a coating of cell envelope fragments by cytosolic substances.

Condensation experiments in an ESEM were performed to characterize the bacterial impact on the micro-scale wettability of mineral surfaces. ESEM micrographs with MQ as mineral component are shown in Fig. 35. Samples containing 10^8 cells g^{-1} mineral, i.e., unstressed, stressed, cell fragments and cytosol, were completely wettable, i.e., the water condensed homogeneously on the surfaces (Fig. 35a, c, e, g), while the 10^9 cells g^{-1} samples showed distinct formation of droplets during condensation (Fig. 35b, d, f, h). The attachment of stressed cells led to the formation of droplets with a higher CA (θ : 85°) compared to the unstressed cells (θ : 66°). For CQ, the same trends in micro-scale wettability were found (see Appendix Fig. 38, page 94). Interaction with the cell fragments (Fig. 35f) and the cytosol (Fig. 35h) led to the formation of droplets for 10^9 cells g^{-1} samples with CA of 69° and 76° , respectively.

Decreased wettability due to attachment of cells and cell fragments was also detected on the micro-scale by ESEM condensation experiments. This is in accordance with the observations of Polson et al. (2010) and Schurig et al. (2013) where bacterial and fungal attachment on quartz changed the micro-scale wettability from hydrophilic to hydrophobic. The ESEM micrographs of the hydrophobic material of the present study show a distinct drop formation

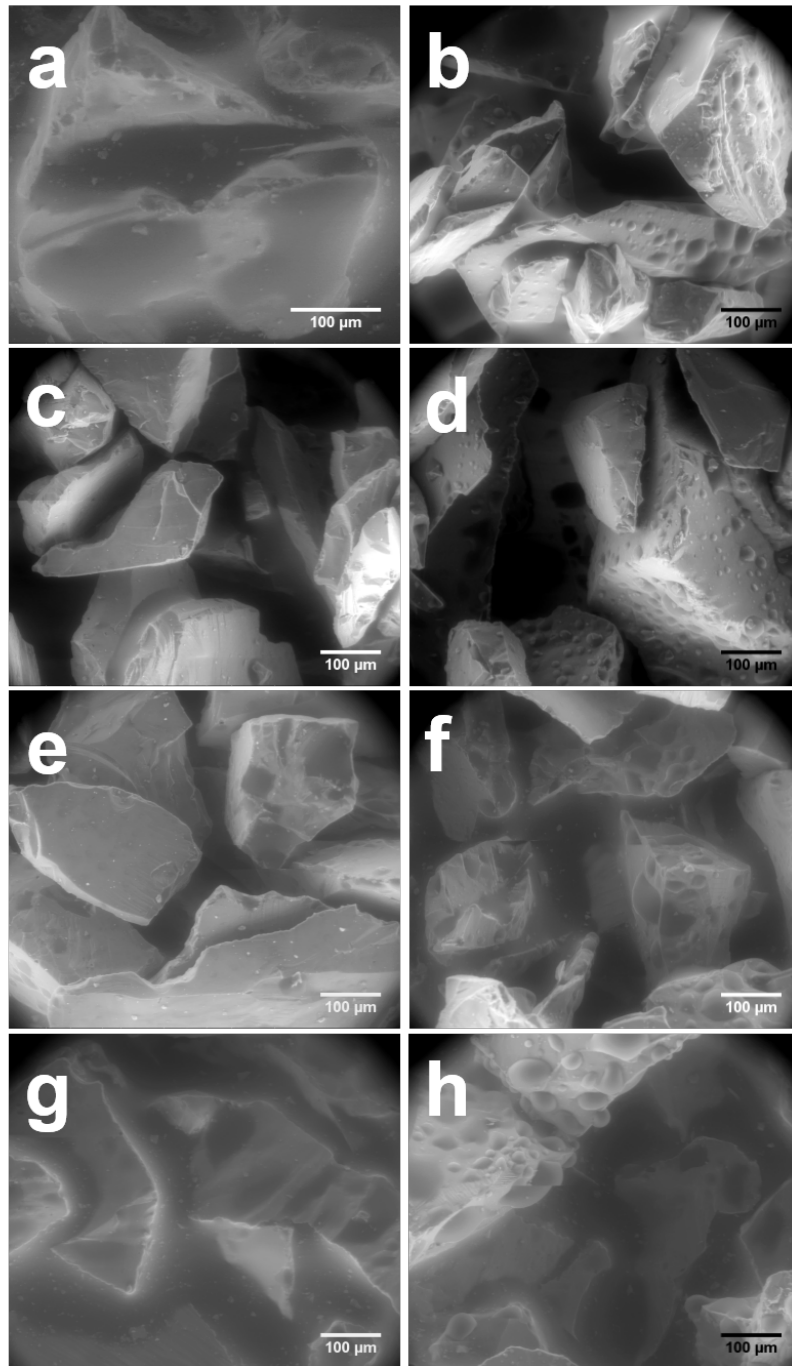


Fig. 35: Micrographs from condensation experiments in an environmental scanning electron microscope with unstressed *P. putida* cells (a, b), osmotically stressed cells (c, d), cell fragments (e, f) and cytosol (g, h) as organic coatings. The mineral phase is medium-grained quartz. In micrographs a, c, e and g, the concentration is 10^8 cells g^{-1} and in b, d, f and h, the concentration is 10^9 cells g^{-1} mineral.

with no direct connection between the drops. This leads to zones on the mineral surface where water is excluded and thus may have an impact on the micro-scale water distribution (Goebel et al., 2007). Furthermore, the micro-scale water repellency and associated variability may also have an influence on water transport (Hallett et al., 2004; Goebel et al., 2011). For that reason, attachment of bacteria and their residues may also have important consequences in case of the small-size fraction minerals used in these experiments, although the changes in the macroscopic CA were negligible.

Nevertheless, in the present experiments an effect on wettability was only detected for concentrations of 10^9 cells g^{-1} mineral or higher which corresponds to a surface coverage of approximately 10 %. This coverage seems not realistic for natural soils, where coverage of soil particles with living microorganisms is on average less than one percent (Chenu and Stotzky, 2002). However, if microbial residues are generally contributing to SOM, cell envelope fragments equivalent to 10^9 cells g^{-1} would be very common. The SEM micrographs of Miltner et al. (2012) and Schurig et al. (2013) showed a high density of microbial cell envelope fragments on mineral surfaces and therefore the amounts of cell fragments used in this study even seem to be underestimated compared to natural soils. In addition, soils are highly heterogeneous with respect to the spatial distribution of microorganisms. There are hotspots and large bacterial patches, which may affect the wettability (Nunan et al., 2002). In soil, high densities of microorganisms are often arranged in biofilms, whose effects on wettability were shown by Schaumann et al. (2007). The matrix of the biofilms consists of EPS, into which microorganisms are embedded (Wingender et al., 1999). Biofilms are often found in water saturated systems and in soil systems when complex substrates have been provided in high amounts supporting exponential growth of bacteria. The EPS of such biofilms are typically forming spider-web like structures in SEM micrographs (Miltner et al., 2012). However, this kind of biofilms was not observed in the present study. Hence, the effect of EPS was not tested in the experiments, but their formation during the 2 h desiccation

period cannot be completely excluded. The formation of EPS during desiccation was shown by Roberson and Firestone (1992) for *Pseudomonas* spp. in soil systems, but the incubation time was considerably longer than in the present study.

The findings support the evidence for a microbial origin of SWR (Hallett and Young, 1999; Or et al., 2007). However, so far, no mechanistic understanding of the role of microorganisms, their residues and stress response for the development of SWR is given in the literature. In the present study, it could be clearly shown that bacteria, their residues and osmotic stress related response can directly affect the wettability of minerals. The previously mentioned accumulation of microbial cell envelope fragments and their contribution to SOM formation therefore will have an important effect on the wettability of soil aggregates and soils in general. It was shown that not only specific substances like long chain FA (Horne and McIntosh, 2000), but also the microorganisms themselves as well as their cell residues, which always will accompany growth and decay, are able to induce or increase SWR. This would also explain the observations of Hallett and Young (1999) and Lamparter et al. (2014), who found a close relationship between increased microbial activity and changes in SWR. The contribution of cell residues to SWR formation may also, in part, explain the observations by Hallett et al. (2001b), where the use of bacterial biocide induced high levels of SWR. The induced death and decay of bacteria is accompanied by the release of cytosolic compounds and formation of cell envelope fragments, which may be responsible for the observed increase in SWR.

Furthermore, the findings can contribute to explain various other effects with respect to SWR. During desiccation, soil wettability changes from wettable to water repellent at the so called critical soil water content (Dekker and Ritsema, 1994; Doerr et al., 2000; Dekker et al., 2001). Due to the amphiphilic structure of many cytosolic components and the cell envelope fragments, the hydrophobic domains of in particular membrane lipids can be ori-

ented away from the mineral surface during drying and may form a hydrophobic coating on the mineral surface. The higher concentration of ions and the corresponding osmotic stress on microorganisms at lower water contents may also decrease their surface wettability. The drying and the induced osmotic stress may also partly explain the observed formation of fire-induced water SWR, where the high temperatures cause a drying of soil even in domains where temperatures do not rise sufficiently burn OM (Letey, 2001). The coating by cytosolic substances, cell envelope fragments and bacterial cells can be the reason for subcritical SWR, where infiltration is interrupted due to hydrophobic spots (Tillman et al., 1989; Hallett et al., 2001a). This is supported by the micro-scale hydrophobicity observed in the ESEM condensation experiments. Small water repellent spots also induced a shift in surface wettability from hydrophilic to hydrophobic in the study by Ustohal et al. (1998). In addition, the development of SWR after irrigation with treated sewage effluent is a widely observed phenomenon (Wallach et al., 2005). Assuming a high input of microorganisms (10^5 – 10^6 cells mL⁻¹) not adapted to soil and various salts with the wastewater, the subsequent adaptation to osmotic stress of the added microorganisms as well as their death and decay may increase SWR. Development of SWR after nutrient addition with following high respiration rates was also observed by Hallett and Young (1999). In addition, the ability of cell envelope fragments to induce SWR may also explain the long-term stabilization of cell residues in SOM (Miltner et al., 2012). During transient drying of a soil, cell envelope fragments may become covered by cell membrane lipids and thereby turn into dry micro spots, which cannot be biodegraded due to reduced water activity.

Only pure minerals as model compounds and only one type of bacterium was used in the present study. Therefore, it will be necessary to study the observed effects with other microorganisms like Gram-positive bacteria and to validate the findings for natural soils. Nevertheless, the principal process in non-complex systems was demonstrated and the proof of principle provided by the results of the experiments. Atomic force microscopy

according to Cheng et al. (2009) to characterize the nano-scale hydrophobicity of the organo-mineral associations would be a helpful tool to get further insights into small-scale surface properties.

In these experiments, the macro-scale and micro-scale wettability of mineral surfaces was affected by the coverage with bacteria and biomolecules, in particular cell envelope fragments and proteins. The surfaces of two quartz sands (small SSA), different in texture (coarse vs. medium) and pre-treatment (no pre-treatment, washed and calcined) decreased in wettability due to the interaction with biomass of *P. putida* mt-2 (i.e., intact cells, cell envelope fragments and cytosol). The extent of the induced water repellency was dependent on cell number and stress adaptation of the bacteria.

5 Conclusions and Synthesis

5.1 Formation and turnover of cell envelope fragments

Using test systems characterized by an increasing complexity, it was possible to elucidate and characterize the formation and turnover of cell envelope fragments in soils in detail. While the decay of cells and the formation of humic substances was observable in pure cultures, the formation of cell envelope fragments was only observed on PDL coated slides or in the presence of an additional mineral phase. The fragmentation process was observable for actinomycetes in artificial soils, while the high complexity and heterogeneity prevented the visualization of cell fragments from other bacteria. However, evidence for the death and decay of microorganisms and the subsequent formation of cell envelope fragments was given by analyzing the PLFA and tFA. Cell envelope fragments are not the only products of cell growth and decay. By incubating different bacteria in liquid culture, humic substances were revealed to be partly of microbial origin. Growth and decay of microorganisms also take place in soil; these processes thus may be valid for soils. The results from incubation studies with ^{14}C -labeled biomass have shown that cell envelope fragments degrade more slowly than intact cells in soil, which may promote their accumulation in soil leading to a significant contribution to SOM formation, which was also stressed by other studies (Schimel et al., 2007; Miltner et al., 2012; Schurig et al., 2013; Schütze et al., 2013).

5.2 Stabilization of microbial residues

By incubating co-precipitates of intact cells and cell envelope fragments with Fe and Al oxyhydroxides in soil, the occlusion and incrustation by co-precipitation was revealed as an important mechanism for the stabilization of microbial residues. It is therefore suggested

studying this mechanism further and integrating it into existing models describing organo-mineral associations (Kleber et al., 2007). For example, other minerals, in particular Mn oxides, and residues of other types of microorganism need to be investigated. The results of the present study also highlight the importance of the interaction between redox conditions and redox-sensitive organo-mineral associations for the stabilization and destabilization of microbial residues, as well as the general relevance of the chemical and physical structure, including the spatial arrangement of compounds in organic input material. As cell envelope fragments are important SOM precursors, the processes and mechanisms revealed here may have an impact on soil C cycling and thus on SOM accumulation and CO₂ release from soil.

5.3 Impact of microbial residues on soil wettability

By determining macro- and micro-scale CA, evidence was found for changes in macroscopic and microscopic wettability of model minerals induced by bacteria, cell envelopes and cytosol. This effect was modulated by bacterial response to osmotic stress. From these findings, a mechanistic process that may help understanding the development of SWR induced by microorganisms, their residues and specific responses to stress was derived. Various related phenomena, like subcritical water repellency and the development of SWR after irrigation with sewage effluents may also be explained by the findings of this study. The results emphasize that macromolecular biogenic structures are more important for SWR than single classes of substances like FA or waxes. Overall, the results of these experiments stress the significant impact of microorganisms and their residues on soil wetting properties.

5.4 Synthesis

The main findings of this thesis, i.e., the formation of microbial residues and their stabilization by occlusion and incrustation due to co-precipitation and the impact of the redox potential on this process, as well as the influence of residues on the wettability of soil minerals, can be included in the cell envelope formation cycle, which was hypothesized by Miltner et al. (2012) (Fig. 36). After growing and starving of bacteria, the decay with subsequent formation of cell envelope fragments takes place, as shown in this thesis. Afterward, the fragments are either stabilized by sorptive interactions with mineral surfaces or by occlusion and incrustation by co-precipitation with minerals. These processes are dependent on redox conditions. While the first mechanisms mainly occur under aerobic conditions, the co-precipitation mainly takes place in temporarily flooded or groundwater affected soils with high concentrations of Fe, Al or Mn ions and fluctuating redox conditions or in anaerobic microsites of oxic soils. The stabilized cell fragments contribute to SOM and have impact on soil surface properties like wettability. However, the co-precipitates are stable under oxic conditions, while O₂ depleted conditions can lead to a dissolution of the protecting occluding mineral phase and to the release of the formerly stabilized fragments, which then can act as a food source for other microorganisms.

The model experiments presented in this thesis thus support a significant contribution of cell envelope fragments to SOM formation. They are formed during cycles of microbial growth, death and decay and stabilized in soil. Furthermore, they strongly affect important soil particle surface properties such as wettability and thus control soil functions.

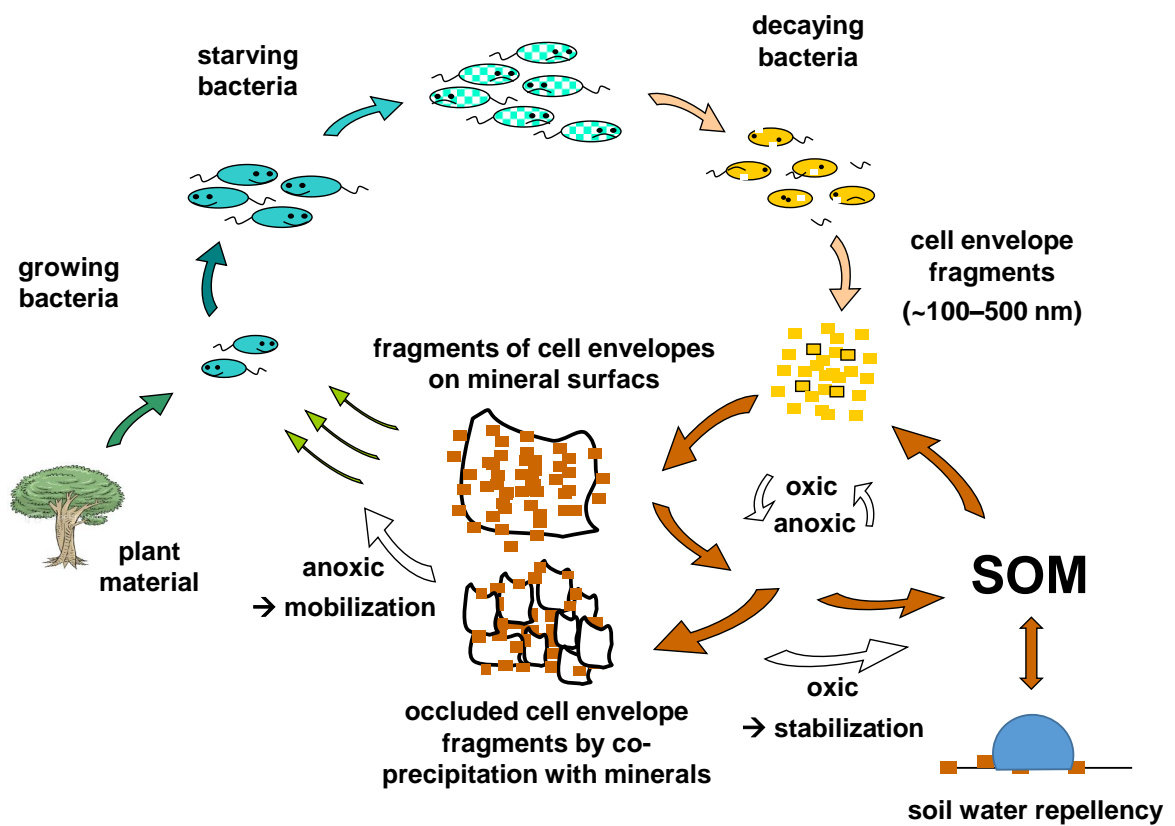


Fig. 36: Modified cell envelope fragments formation cycle from Miltner et al. (2012). The occlusion of cell envelope fragments is next to sorption of those on mineral surfaces an important stabilization mechanism, which is dependent on oxic and anoxic conditions in soil. The stabilized residues have influence on physical surface properties like soil water repellency.

Appendix

Tab. 8: Residual activities (% of total activity) and recovery rates of the incubation experiments with ^{14}C -labeled *E. coli* (n/a: not applicable).

Occlusion O ₂ regime	No occlusion		Fe oxyhydroxide		Al oxyhydroxide	
	Aerobic	O ₂ depleted	Aerobic	O ₂ depleted	Aerobic	O ₂ depleted
[%]						
Intact cells						
Day 0	n/a	n/a	n/a	n/a	n/a	n/a
Day 98/101	61.8 ± 4.8	64.8 ± 2.9	84 ± 4	85.1 ± 2.6	81.1 ± 1.9	76 ± 4
Day 343/346	50.8 ± 3.4	33 ± 12	74.6 ± 2.6	45 ± 3	76 ± 6	86 ± 9
Recovery	101	92	93	82	98	87
Cell fragments						
Day 0	n/a	n/a	n/a	n/a	n/a	n/a
Day 98/101	70.8 ± 2.7	70 ± 6	90 ± 6	94.3 ± 1.9	96 ± 6	84.5 ± 1.9
Day 343/346	53.9 ± 1.2	35 ± 14	95 ± 7	58 ± 12	85 ± 9	68 ± 4
Recovery	98	93	108	86	107	97

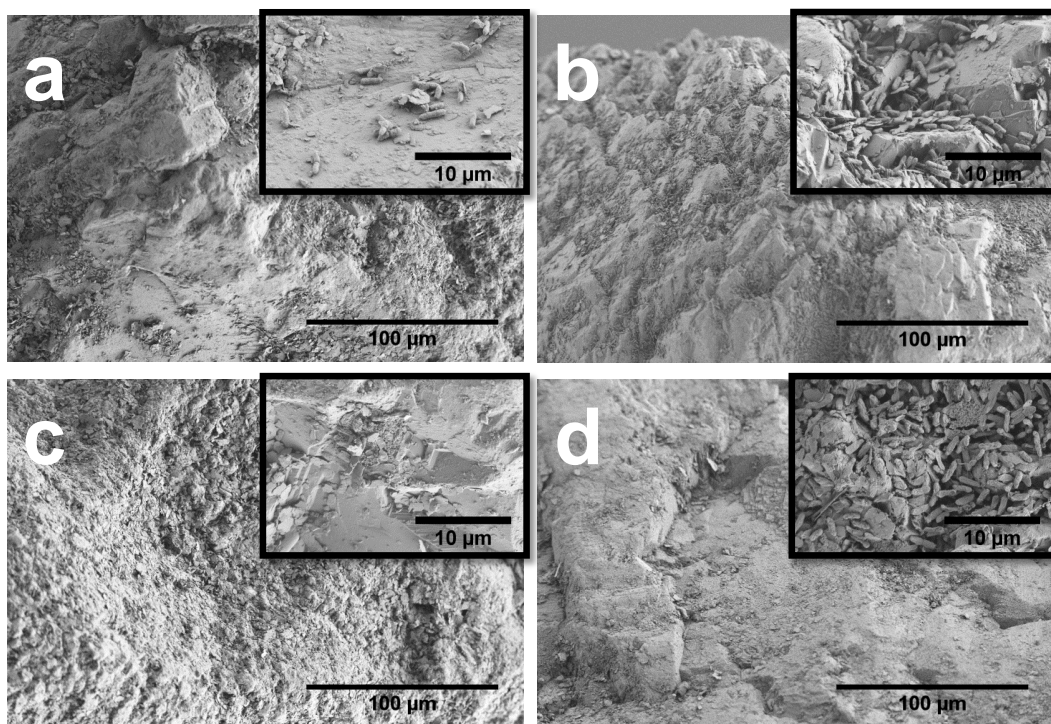


Fig. 37: Scanning electron micrographs of unstressed *P. putida* cells (a, b), and stressed cells (c, d). The mineral phase is coarse-grained quartz. In micrographs a and c, the concentration is 10^8 cells g^{-1} and in b and d, the concentration is 10^9 cells g^{-1} mineral. The smaller micrographs were taken with a higher magnification.

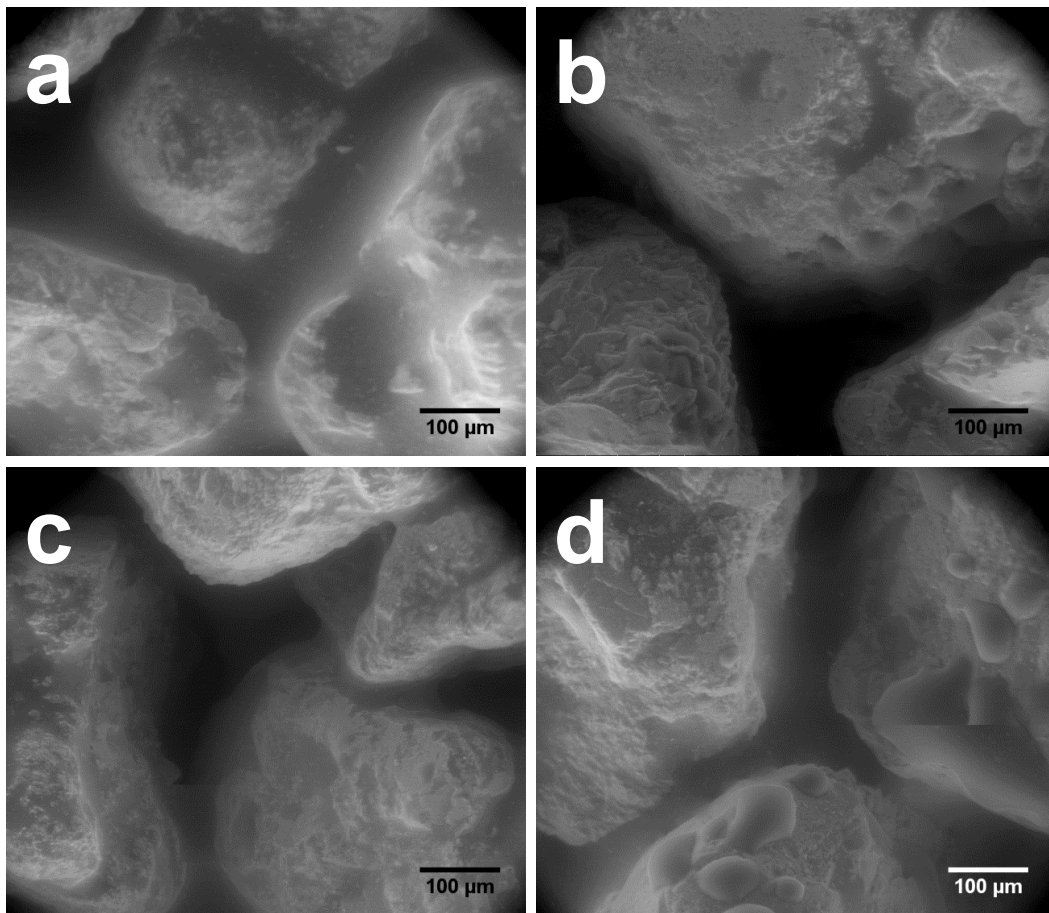


Fig. 38: Micrographs from condensation experiments in an environmental scanning electron microscope with unstressed *P. putida* cells (a, b) and stressed cells (c, d) as organic coatings. The mineral phase is coarse quartz. In micrographs a and c, the concentration is 10^8 cells g^{-1} and in b and d, the concentration is 10^9 cells g^{-1} mineral.

Bibliography

- Al-Tahhan, R. A., Sandrin, T. R., Bodour, A. A., Maier, R. M., 2000. Rhamnolipid-induced removal of lipopolysaccharide from *Pseudomonas aeruginosa*: effect on cell surface properties and interaction with hydrophobic substrates. *Applied and Environmental Microbiology* 66 (8), 3262–3268.
- Alvarez, H. M., Silva, R. A., Cesari, A. C., Zamit, A. L., Peressutti, S. R., Reichelt, R., Keller, U., Malkus, U., Rasch, C., Maskow, T., Mayer, F., Steinbüchel, A., 2004. Physiological and morphological responses of the soil bacterium *Rhodococcus opacus* strain PD630 to water stress. *FEMS Microbiology Ecology* 50 (2), 75–86.
- Babin, D., Ding, G.-C., Pronk, G. J., Heister, K., Kögel-Knabner, I., Smalla, K., 2013. Metal oxides, clay minerals and charcoal determine the composition of microbial communities in matured artificial soils and their response to phenanthrene. *FEMS Microbiology Ecology* 86 (1), 3–14.
- Bachmann, J., Ellies, A., Hartge, K. H., 2000. Development and application of a new sessile drop contact angle method to assess soil water repellency. *Journal of Hydrology* 231, 66–75.
- Baldock, J. A., Nelson, P. N., 2000. Soil organic matter. In: Sumner, M. E. (Ed.), *Handbook of soil science*. CRC Press, Boca Raton, USA, pp. B25–B84.
- Barrios, E., 2007. Soil biota, ecosystem services and land productivity. *Ecological Economics* 64 (2), 269–285.
- Batjes, N. H., 1996. Total carbon and nitrogen in the soils of the world. *European Journal of Soil Science* 47 (2), 151–163.

- Baumgarten, T., Sperling, S., Seifert, J., von Bergen, M., Steiniger, F., Wick, L. Y., Heipieper, H. J., 2012a. Membrane vesicle formation as a multiple-stress response mechanism enhances *Pseudomonas putida* DOT-T1E cell surface hydrophobicity and biofilm formation. *Applied and Environmental Microbiology* 78 (17), 6217–6224.
- Baumgarten, T., Vazquez, J., Bastisch, C., Veron, W., Feuilleley, Marc G. J., Nietzsche, S., Wick, L. Y., Heipieper, H. J., 2012b. Alkanols and chlorophenols cause different physiological adaptive responses on the level of cell surface properties and membrane vesicle formation in *Pseudomonas putida* DOT-T1E. *Applied Microbiology and Biotechnology* 93 (2), 837–845.
- Bellamy, P. H., Loveland, P. J., Bradley, R. I., Lark, R. M., Kirk, Guy J. D., 2005. Carbon losses from all soils across England and Wales 1978–2003. *Nature* 437 (7056), 245–248.
- Bialopiotrowicz, T., Janczuk, B., 2001. Wettability and surface free energy of bovine serum albumin films. *Journal of Surfactants and Detergents* 4 (3), 287–292.
- Bisdom, E. B., Dekker, L. W., Schoute, J. F., 1993. Water repellency of sieve fractions from sandy soils and relationships with organic material and soil structure. *Geoderma* 56 (1), 105–118.
- Blackwell, P. S., 2000. Management of water repellency in Australia, and risks associated with preferential flow, pesticide concentration and leaching. *Journal of Hydrology* 231, 384–395.
- Blair, N., Faulkner, R. D., Till, A. R., Korschens, M., Schulz, E., 2006. Long-term management impacts on soil C, N and physical fertility. *Soil and Tillage Research* 91 (1-2), 39–47.
- Bligh, E. G., Dyer, W. J., 1959. A rapid method of total lipid extraction and purification. *Canadian Journal of Biochemistry and Physiology* 37 (8), 911–917.

-
- Boudot, J.-P., 1992. Relative efficiency of complexed aluminum noncrystalline Al hydroxide, allophane and imogolite in retarding the biodegradation of citric acid. *Geoderma* 52 (1-2), 29–39.
- Burns, R. G., DeForest, J. L., Marxsen, J., Sinsabaugh, R. L., Stromberger, M. E., Wallenstein, M. D., Weintraub, M. N., Zoppini, A., 2013. Soil enzymes in a changing environment: Current knowledge and future directions. *Soil Biology and Biochemistry* 58 (0), 216 – 234.
- Cheng, S., Bryant, R., Doerr, S. H., Wright, C. J., Williams, P. R., 2009. Investigation of surface properties of soil particles and model materials with contrasting hydrophobicity using atomic force microscopy. *Environmental Science & Technology* 43 (17), 6500–6506.
- Chenu, C., Stotzky, G., 2002. Interactions between microorganisms and soil particles: An overview. In: Huang, P. M., Bollag, J. M., Senesi, N. (Eds.), *Interactions between soil particles and microorganisms*. Vol. 8 of IUPAC series on analytical and physical chemistry of environmental systems. Johny Wiley & Sons, Chinchester, UK, pp. 3–40.
- Churaev, N. V., 2000. *Liquid and vapor flows in porous bodies: Surface phenomena*. Vol. 13 of *Topics in Chemical Engineering*. Gordon & Breach Science Publishers, Boca Raton, USA.
- Claus, H., Gleixner, G., Filip, Z., 1999. Formation of humic-like substances in mixed and pure cultures of aquatic microorganisms. *Acta hydrochimica et hydrobiologica* 27 (4), 200–207.
- Cortez, J., 1989. Effect of drying and rewetting on mineralization and distribution of bacterial constituents in soil fractions. *Biology and Fertility of Soils* 7 (2), 142–151.

- DeAngelis, K. M., Silver, W. L., Thompson, A. W., Firestone, M. K., 2010. Microbial communities acclimate to recurring changes in soil redox potential status. *Environmental Microbiology* 12 (12), 3137–3149.
- Dekker, L. W., Doerr, S. H., Oostindie, K., Ziogas, A. K., Ritsema, C. J., 2001. Water repellency and critical soil water content in a dune sand. *Soil Science Society of America Journal* 65, 1667–1674.
- Dekker, L. W., Ritsema, C. J., 1994. How water moves in a water repellent sandy soil: 1. potential and actual water repellency. *Water Resources Research* 30 (9), 2507–2517.
- Dekker, L. W., Ritsema, C. J., 2000. Wetting patterns and moisture variability in water repellent Dutch soils. *Journal of Hydrology* 231–232, 148–164.
- Dekker, L. W., Ritsema, C. J., Wendroth, O., Jarvis, N., Oostindie, K., Pohl, W., Larsson, M., Gaudet, J.-P., 1999. Moisture distributions and wetting rates of soils at experimental fields in the Netherlands, France, Sweden and Germany. *Journal of Hydrology* 215 (1), 4–22.
- Deo, N., Natarajan, K. A., 1997. Interaction of *Bacillus polymyxa* with some oxide minerals with reference to mineral beneficiation and environmental control. *Minerals Engineering* 10 (12), 1339–1354.
- Deo, N., Natarajan, K. A., 1998. Studies on interaction of *Paenibacillus polymyxa* with iron ore minerals in relation to beneficiation. *International Journal of Mineral Processing* 55 (1), 41–60.
- Doerr, S. H., Shakesby, R. A., Walsh, R. P., 2000. Soil water repellency: its causes, characteristics and hydro-geomorphological significance. *Earth-Science Reviews* 51 (1), 33–65.

-
- DSMZ, 2014. List of recommended media for microorganisms. <http://www.dsmz.de/catalogues/catalogue-microorganisms/culture-technology/list-of-media-for-microorganisms.html> Accessed 19 August 2014.
- Dümig, A., Smittenberg, R., Kögel-Knabner, I., 2011. Concurrent evolution of organic and mineral components during initial soil development after retreat of the Damma glacier, Switzerland. *Geoderma* 163 (1-2), 83–94.
- Eusterhues, K., Neidhardt, J., Hädrich, A., Küsel, K., Totsche, K. U., 2014. Biodegradation of ferrihydrite-associated organic matter. *Biogeochemistry* 119 (1-3), 45–50.
- Falkowski, P., 2000. The global carbon cycle: A test of our knowledge of earth as a system. *Science* 290 (5490), 291–296.
- Feeney, D. S., Crawford, J. W., Daniell, T., Hallett, P. D., Nunan, N., Ritz, K., Rivers, M., Young, I. M., 2006. Three-dimensional microorganization of the soil–root–microbe system. *Microbial Ecology* 52 (1), 151–158.
- Franco, C. M., Clarke, P. J., Tate, M. E., Oades, J. M., 2000. Hydrophobic properties and chemical characterisation of natural water repellent materials in Australian sands. *Journal of Hydrology* 231-232, 47–58.
- Frostegård, A., Tunlid, A., Bååth, E., 1991. Microbial biomass measured as total lipid phosphate in soils of different organic content. *Journal of Microbiological Methods* 14 (3), 151–163.
- Goebel, M.-O., Bachmann, J., Reichstein, M., Janssens, I. A., Guggenberger, G., 2011. Soil water repellency and its implications for organic matter decomposition—is there a link to extreme climatic events? *Global Change Biology* 17 (8), 2640–2656.

- Goebel, M.-O., Bachmann, J., Woche, S. K., Fischer, W. R., 2005. Soil wettability, aggregate stability, and the decomposition of soil organic matter. *Geoderma* 128 (1), 80–93.
- Goebel, M.-O., Woche, S. K., Bachmann, J., Lamparter, A., Fischer, W. R., 2007. Significance of wettability-induced changes in microscopic water distribution for soil organic matter decomposition. *Soil Science Society of America Journal* 71 (5), 1593–1599.
- González-Peñaloza, F. A., Zavala, L. M., Jordán, A., Bellinfante, N., Bárcenas-Moreno, G., Mataix-Solera, J., Granged, A. J., Granja-Martins, F. M., Neto-Paixão, H. M., 2013. Water repellency as conditioned by particle size and drying in hydrophobized sand. *Geoderma* 209-210, 31–40.
- Graber, E. R., Tagger, S., Wallach, R., 2009. Role of divalent fatty acid salts in soil water repellency. *Soil Science Society of America Journal* 73 (2), 541–549.
- Green, C. T., Scow, K. M., 2000. Analysis of phospholipid fatty acids (PLFA) to characterize microbial communities in aquifers. *Hydrogeology Journal* 8 (1), 126–141.
- Gregorich, E., Voroney, R., Kachanoski, R., 1991. Turnover of carbon through the microbial biomass in soils with different texture. *Soil Biology and Biochemistry* 23 (8), 799 – 805.
- Guckert, J., Hood, M., White, D., 1986. Phospholipid ester-linked fatty acid profile changes during nutrient deprivation of *Vibrio cholerae*: increases in the trans/cis ratio and proportions of cyclopropyl fatty acids. *Applied and Environmental Microbiology* 52 (4), 794–801.
- Guenet, B., Leloup, J., Hartmann, C., Barot, S., Abbadie, L., 2011. A new protocol for an artificial soil to analyse soil microbiological processes. *Applied Soil Ecology* 48 (2), 243 – 246.

- Guggenberger, G., Frey, S. D., Six, J., Paustian, K., Elliott, E. T., 1999. Bacterial and fungal cell-wall residues in conventional and no-tillage agroecosystems. *Soil Science Society of America Journal* 63 (5), 1188–1198.
- Hachicho, N., Hoffmann, P., Ahlert, K., Heipieper, H. J., 2014. Effect of silver nanoparticles and silver ions on growth and adaptive response mechanisms of *Pseudomonas putida* mt-2. *FEMS Microbiology Letters* 355 (1), 71–77.
- Hallett, P. D., Baumgartl, T., Young, I. M., 2001a. Subcritical water repellency of aggregates from a range of soil management practices. *Soil Science Society of America Journal* 65 (1), 184–190.
- Hallett, P. D., Nunan, N., Douglas, J. T., Young, I. M., 2004. Millimeter-scale spatial variability in soil water sorptivity. *Soil Science Society of America Journal* 68 (2), 352–358.
- Hallett, P. D., Ritz, K., Wheatley, R. E., 2001b. Microbial derived water repellency in golf course soils. *International Turfgrass Society Research Journal* 9, 518–524.
- Hallett, P. D., Young, I. M., 1999. Changes to water repellence of soil aggregates caused by substrate-induced microbial activity. *European Journal of Soil Science* 50 (1), 35–40.
- Hartmans, S., Smits, J. P., Van der Werf, M.J., Volkering, F., Bont, J. A. d., 1989. Metabolism of styrene oxide and 2-phenylethanol in the styrene-degrading *Xanthobacter* strain 124X. *Applied and Environmental Microbiology* 55 (11), 2850–2855.
- Hayes, M. H. B., Swift, R. S., 1990. Genesis, isolation, composition and structures of soil humic substances. In: Boodt, M. F., Hayes, M. H. B., Herbillon, A., Strooper, E. B. A., Tuck, J. J. (Eds.), *Soil Colloids and Their Associations in Aggregates*. Vol. 214 of NATO ASI Series. Springer US, Boston, USA, pp. 245–305.

- Heimann, M., Reichstein, M., 2008. Terrestrial ecosystem carbon dynamics and climate feedbacks. *Nature* 451 (7176), 289–292.
- Horne, D. J., McIntosh, J. C., 2000. Hydrophobic compounds in sands in New Zealand-- extraction, characterisation and proposed mechanisms for repellency expression. *Journal of Hydrology* 231, 35–46.
- Hurrass, J., Schaumann, G. E., 2006. Properties of soil organic matter and aqueous extracts of actually water repellent and wettable soil samples. *Geoderma* 132 (1), 222–239.
- Huysman, F., Verstraete, W., 1993. Effect of cell surface characteristics on the adhesion of bacteria to soil particles. *Biology and Fertility of Soils* 16 (1), 21–26.
- ISO, 2003. Soil quality - Determination of abundance and activity of the soil microflora using respiration curves. No. 17155. Geneva, Switzerland.
- ISO, 2005. Bodenbeschaffenheit - Bestimmung des pH-Wertes. No. 10390. Geneva, Switzerland.
- Kaiser, K., Guggenberger, G., 2000. The role of DOM sorption to mineral surfaces in the preservation of organic matter in soils. *Organic Geochemistry* 31 (7-8), 711–725.
- Kaiser, K., Guggenberger, G., 2007. Sorptive stabilization of organic matter by microporous goethite: sorption into small pores vs. surface complexation. *European Journal of Soil Science* 58 (1), 45–59.
- Kaiser, K., Zech, W., 1997. Competitive sorption of dissolved organic matter fractions to soils and related mineral phases. *Soil Science Society of America Journal* 61 (1), 64.
- Kalbitz, K., Schwesig, D., Rethemeyer, J., Matzner, E., 2005. Stabilization of dissolved organic matter by sorption to the mineral soil. *Soil Biology and Biochemistry* 37 (7), 1319–1331.

-
- Kästner, M., 2000. "Humification" process or formation of refractory soil organic matter. In: Rehm, H.-J., Reed, G. (Eds.), *Biotechnology*. Vol. 14. Wiley-VCH Verlag GmbH, Weinheim, Germany, pp. 89–125.
- Kelleher, B. P., Simpson, A. J., 2006. Humic substances in soils: are they really chemically distinct? *Environmental Science & Technology* 40 (15), 4605–4611.
- Kindler, R., Miltner, A., Richnow, H.-H., Kästner, M., 2006. Fate of gram-negative bacterial biomass in soil – mineralization and contribution to SOM. *Soil Biology and Biochemistry* 38 (9), 2860–2870.
- Kleber, M., Johnson, M. G., 2010. Advances in understanding the molecular structure of soil organic matter. In: Sparks, D. (Ed.), *Advances in Agronomy*. Vol. 106 of *Advances in Agronomy*. Elsevier, pp. 77–142.
- Kleber, M., Sollins, P., Sutton, R., 2007. A conceptual model of organo-mineral interactions in soils: self-assembly of organic molecular fragments into zonal structures on mineral surfaces. *Biogeochemistry* 85 (1), 9–24.
- Kögel-Knabner, I., 2002. The macromolecular organic composition of plant and microbial residues as inputs to soil organic matter. *Soil Biology and Biochemistry* 34 (2), 139–162.
- Kögel-Knabner, I., Guggenberger, G., Kleber, M., Kandeler, E., Kalbitz, K., Scheu, S., Eusterhues, K., Leinweber, P., 2008. Organo-mineral associations in temperate soils: Integrating biology, mineralogy, and organic matter chemistry. *Journal of Plant Nutrition and Soil Science* 171 (1), 61–82.
- Kulp, A., Kuehn, M. J., 2010. Biological functions and biogenesis of secreted bacterial outer membrane vesicles. *Annual Review of Microbiology* 64 (1), 163–184.

- Lal, R., 2004a. Soil carbon sequestration impacts on global climate change and food security. *Science* 304 (5677), 1623–1627.
- Lal, R., 2004b. Soil carbon sequestration to mitigate climate change. *Geoderma* 123 (1-2), 1–22.
- Lamparter, A., Bachmann, J., Woche, S. K., Goebel, M.-O., 2014. Biogeochemical interfaces formation: wettability affected by organic matter sorption and microbial activity. *Vadose Zone Journal*, 10.2136/vzj2013.10.0175.
- Letey, J., 2001. Causes and consequences of fire-induced soil water repellency. *Hydrological Processes* 15 (15), 2867–2875.
- Liang, C., Balser, T. C., 2011. Microbial production of recalcitrant organic matter in global soils: implications for productivity and climate policy. *Nature Reviews Microbiology* 9 (1), 75.
- Liu, X., Eusterhues, K., Thieme, J., Ciobota, V., Höschel, C., Mueller, C. W., Küsel, K., Kögel-Knabner, I., Rösch, P., Popp, J., Totsche, K. U., 2013. STXM and NanoSIMS investigations on EPS fractions before and after adsorption to goethite. *Environmental Science & Technology* 47 (7), 3158–3166.
- Lopez, C. S., Heras, H., Garda, H., Ruzal, S., Sanchez-Rivas, C., Rivas, E., 2000. Biochemical and biophysical studies of *Bacillus subtilis* envelopes under hyperosmotic stress. *International Journal of Food Microbiology* 55 (1), 137–142.
- Lueders, T., Kindler, R., Miltner, A., Friedrich, M. W., Kaestner, M., 2006. Identification of bacterial micropredators distinctively active in a soil microbial food web. *Applied and Environmental Microbiology* 72 (8), 5342–5348.

-
- Madurai, S. L., Joseph, S. W., Mandal, A. B., Tsibouklis, J., Reddy, B. S., 2011. Intestine-specific, oral delivery of captopril/montmorillonite: Formulation and release kinetics. *Nanoscale Research Letters* 6 (1), 1–8.
- Mainwaring, K., Hallin, I. L., Douglas, P., Doerr, S. H., Morley, C. P., 2013. The role of naturally occurring organic compounds in causing soil water repellency. *European Journal of Soil Science* 64 (5), 667–680.
- Mainwaring, K. A., Morley, C. P., Doerr, S. H., Douglas, P., Llewellyn, C. T., Llewellyn, G., Matthews, I., Stein, B. K., 2004. Role of heavy polar organic compounds for water repellency of sandy soils. *Environmental Chemistry Letters* 2 (1), 35–39.
- Marschner, B., Brodowski, S., Dreves, A., Gleixner, G., Gude, A., Grootes, P. M., Hamer, U., Heim, A., Jandl, G., Ji, R., Kaiser, K., Kalbitz, K., Kramer, C., Leinweber, P., Rethemeyer, J., Schäffer, A., Schmidt, M. W. I., Schwark, L., Wiesenberg, Guido L. B., 2008. How relevant is recalcitrance for the stabilization of organic matter in soils? *Journal of Plant Nutrition and Soil Science* 171 (1), 91–110.
- Marumoto, T., Anderson, J., Domsch, K. H., 1982. Decomposition of ¹⁴C- and ¹⁵N-labelled microbial cells in soil. *Soil Biology and Biochemistry* 14 (5), 461–467.
- Marumoto, T., Kai, H., Yoshida, T., Harada, T., 1977. Drying effect on mineralizations of microbial cells and their cell walls in soil and contribution of microbial cell walls as a source of decomposable soil organic matter due to drying. *Soil Science and Plant Nutrition* 23 (1), 9–19.
- Ma'Shum, M., Tate, M. E., Jones, G. P., Oades, J. M., 1988. Extraction and characterization of water-repellent materials from Australian soils. *Journal of Soil Science* 39 (1), 99–110.

- Mayer, L. M., 1994. Surface area control of organic carbon accumulation in continental shelf sediments. *Geochimica et Cosmochimica Acta* 58 (4), 1271–1284.
- Mayes, M., Jagadamma, S., Ambaye, H., Petridis, L., Lauter, V., 2013. Neutron reflectometry reveals the internal structure of organic compounds deposited on aluminum oxide. *Geoderma* 192, 182–188.
- McEldowney, S., Fletcher, M., 1986. Variability of the influence of physicochemical factors affecting bacterial adhesion to polystyrene substrata. *Applied and Environmental Microbiology* 52 (3), 460–465.
- Mihelic, J. R., Luthy, R. G., 1988. Degradation of polycyclic aromatic hydrocarbon compounds under various redox conditions in soil-water systems. *Applied and Environmental Microbiology* 54 (5), 1182–1187.
- Mikutta, R., Zang, U., Chorover, J., Haumaier, L., Kalbitz, K., 2011. Stabilization of extracellular polymeric substances (*Bacillus subtilis*) by adsorption to and coprecipitation with al forms. *Geochimica et Cosmochimica Acta* 75 (11), 3135–3154.
- Miltner, A., Bombach, P., Schmidt-Brücken, B., Kästner, M., 2012. SOM genesis: microbial biomass as a significant source. *Biogeochemistry* 111 (1-3), 41–55.
- Miltner, A., Kindler, R., Knicker, H., Richnow, H.-H., Kästner, M., 2009. Fate of microbial biomass-derived amino acids in soil and their contribution to soil organic matter. *Organic Geochemistry* 40 (9), 978–985.
- Miltner, A., Richnow, H.-H., Kopinke, F.-D., Kästner, M., 2004. Assimilation of CO₂ by soil microorganisms and transformation into soil organic matter. *Organic Geochemistry* 35 (9), 1015–1024.

-
- Miltner, A., Zech, W., 1998. Carbohydrate decomposition in beech litter as influenced by aluminium, iron and manganese oxides. *Soil Biology and Biochemistry* 30 (1), 1–7.
- Miltner, A., Zech, W., 1999. Microbial degradation and resynthesis of proteins during incubation of beech leaf litter in the presence of mineral phases. *Biology and Fertility of Soils* 30 (1-2), 48–51.
- Nakas, J. P., Klein, D. A., 1979. Decomposition of microbial cell components in a semi-arid grassland soil. *Applied and Environmental Microbiology* 38 (3), 454–460.
- Neumann, G., Cornelissen, S., van Breukelen, F., Hunger, S., Lippold, H., Loffhagen, N., Wick, L. Y., Heipieper, H. J., 2006. Energetics and surface properties of *Pseudomonas putida* DOT-T1E in a two-phase fermentation system with 1-decanol as second phase. *Applied and Environmental Microbiology* 72 (6), 4232–4238.
- Nunan, N., Wu, K., Young, I. M., Crawford, J. W., Ritz, K., 2002. In situ spatial patterns of soil bacterial populations, mapped at multiple scales, in an arable soil. *Microbial Ecology* 44 (4), 296–305.
- Oades, J. M., 1989. An introduction to organic matter in mineral soils. In: Dixon, J. B., Weed, S. B., Dinauer, R. C. (Eds.), *Minerals in Soil Environments*. SSSA Book Series. Soil Science Society of America, Oakland, USA, pp. 89–159.
- Okada, K., Nagashima, T., Kameshima, Y., Yasumori, A., Tsukada, T., 2002. Relationship between formation, conditions, properties, and crystallite size of boehmite. *Journal of Colloid and Interface Science* 253 (2), 308–314.
- Omoike, A., Chorover, J., 2006. Adsorption to goethite of extracellular polymeric substances from *Bacillus subtilis*. *Geochimica et Cosmochimica Acta* 70 (4), 827–838.

- Or, D., Smets, B. F., Wraith, J. M., Dechesne, A., Friedman, S. P., 2007. Physical constraints affecting bacterial habitats and activity in unsaturated porous media – a review. *Advances in Water Resources* 30 (6-7), 1505–1527.
- Paim, S., Linhares, L. F., Mangrich, A. S., Martin, J. P., 1990. Characterization of fungal melanins and soil humic acids by chemical analysis and infrared spectroscopy. *Biology and Fertility of Soils* 10 (1), 72–76.
- Pallud, C., Masue-Slowey, Y., Fendorf, S., 2010. Aggregate-scale spatial heterogeneity in reductive transformation of ferrihydrite resulting from coupled biogeochemical and physical processes. *Biogeochemistry* 74 (10), 2811–2825.
- Pett-Ridge, J., Silver, W. L., Firestone, M. K., 2006. Redox fluctuations frame microbial community impacts on n-cycling rates in a humid tropical forest soil. *Biogeochemistry* 81 (1), 95–110.
- Polson, E. J., Buckman, J. O., Bowen, D., Todd, A. C., Gow, M. M., Cuthbert, S. J., 2010. An environmental-scanning-electron-microscope investigation into the effect of biofilm on the wettability of quartz. *SPE Journal* 15 (1), 223–227.
- Pronk, G. J., Heister, K., Ding, G.-C., Smalla, K., Kögel-Knabner, I., 2012. Development of biogeochemical interfaces in an artificial soil incubation experiment; aggregation and formation of organo-mineral associations. *Geoderma* 189–190, 585–594.
- Rabung, T., Pierret, M., Bauer, A., Geckeis, H., Bradbury, M., Baeyens, B., 2005. Sorption of Eu(III)/Cm(III) on Ca-montmorillonite and Na-illite. Part 1: Batch sorption and time-resolved laser fluorescence spectroscopy experiments. *Geochimica et Cosmochimica Acta* 69 (23), 5393 – 5402.

-
- Roberson, E. B., Chenu, C., Firestone, M. K., 1993. Microstructural changes in bacterial exopolysaccharides during desiccation. *Soil Biology and Biochemistry* 25 (9), 1299–1301.
- Roberson, E. B., Firestone, M. K., 1992. Relationship between desiccation and exopolysaccharide production in a soil *Pseudomonas* sp. *Applied and Environmental Microbiology* 58 (4), 1284–1291.
- Schaumann, G. E., Braun, B., Kirchner, D., Rotard, W., Szewzyk, U., Grohmann, E., 2007. Influence of biofilms on the water repellency of urban soil samples. *Hydrological Processes* 21 (17), 2276–2284.
- Scheel, T., Dörfler, C., Kalbitz, K., 2007. Precipitation of dissolved organic matter by aluminum stabilizes carbon in acidic forest soils. *Soil Science Society of America Journal* 71 (1), 64–74.
- Schimel, J., Balsler, T. C., Wallenstein, M., 2007. Microbial stress-response physiology and its implications for ecosystem function. *Ecology* 88 (6), 1386–1394.
- Schmidt, M. W. I., Torn, M. S., Abiven, S., Dittmar, T., Guggenberger, G., Janssens, I. A., Kleber, M., Kögel-Knabner, I., Lehmann, J., Manning, D. A. C., Nannipieri, P., Rasse, D. P., Weiner, S., Trumbore, S. E., 2011. Persistence of soil organic matter as an ecosystem property. *Nature* 478 (7367), 49–56.
- Schurig, C., Smittenberg, R. H., Berger, J., Kraft, F., Woche, S. K., Goebel, M.-O., Heipieper, H. J., Miltner, A., Kaestner, M., 2013. Microbial cell-envelope fragments and the formation of soil organic matter: a case study from a glacier forefield. *Biogeochemistry* 113 (1-3), 595–612.

- Schütze, E., Miltner, A., Nietzsche, S., Achtenhagen, J., Klose, M., Merten, D., Greyer, M., Roth, M., Kästner, M., Kothe, E., 2013. Live and death of streptomyces in soil-what happens to the biomass? *Journal of Plant Nutrition and Soil Science* 176 (5), 665–673.
- Schwertmann, U., Cornell, R. M., 2000. *Iron Oxides in the Laboratory*. Wiley-VCH Verlag GmbH, Weinheim, Germany.
- Simpson, A. J., Simpson, M. J., Smith, E., Kelleher, B. P., 2007. Microbially derived inputs to soil organic matter: Are current estimates too low? *Environmental Science & Technology* 41 (23), 8070–8076.
- Sleutel, S., Neve, S., Hofman, G., 2003. Estimates of carbon stock changes in belgian cropland. *Soil Use and Management* 19 (2), 166–171.
- Sollins, P., Homann, P., Caldwell, B. A., 1996. Stabilization and destabilization of soil organic matter: mechanisms and controls. *Geoderma* 74 (1-2), 65–105.
- Sollins, P., Swanston, C., Kramer, M., 2007. Stabilization and destabilization of soil organic matter – a new focus. *Biogeochemistry* 85 (1), 1–7.
- Stewart, C. E., Paustian, K., Conant, R. T., Plante, A. F., Six, J., 2007. Soil carbon saturation: concept, evidence and evaluation. *Biogeochemistry* 86 (1), 19–31.
- Studier, F., Moffatt, B. A., 1986. Use of bacteriophage t7 rna polymerase to direct selective high-level expression of cloned genes. *Journal of Molecular Biology* 189 (1), 113–130.
- Sutton, R., Sposito, G., 2005. Molecular structure in soil humic substances: The new view. *Environmental Science & Technology* 39 (23), 9009–9015.

-
- Swift, R., 1996. Organic matter characterization. In: Sparks, D., Page, A., Helmke, P., Loeppert, R. (Eds.), *Methods of Soil Analysis Part 3 - Chemical Methods*. Vol. 5.3 of SSSA Book Series. Soil Science Society of America, Oakland, USA, pp. 1011–1069.
- Thompson, A., Chadwick, O. A., Rancourt, D. G., Chorover, J., 2006. Iron-oxide crystallinity increases during soil redox oscillations. *Geochimica et Cosmochimica Acta* 70 (7), 1710–1727.
- Tillman, R. W., Scotter, Wallis, M. G., Clothier, B. E., 1989. Water repellency and its measurement by using intrinsic sorptivity. *Australian Journal of Soil Research* 27 (4), 637–644.
- Totsche, K. U., Rennert, T., Gerzabek, M. H., Koegel-Knabner, I., Smalla, K., Spiteller, M., Vogel, H.-J., 2010. Biogeochemical interfaces in soil: The interdisciplinary challenge for soil science. *Journal of Plant Nutrition and Soil Science* 173 (1), 88–99.
- Tranvik, L. J., 1993. Microbial transformation of labile dissolved organic matter into humic-like matter in seawater. *FEMS Microbiology Ecology* 12 (3), 177–183.
- Ustohal, P., Stauffer, F., Dracos, T., 1998. Measurement and modeling of hydraulic characteristics of unsaturated porous media with mixed wettability. *Journal of contaminant hydrology* 33 (1-2), 5–37.
- van Loosdrecht, M. C., Lyklema, J., Norde, W., Schraa, G., Zehnder, A. J., 1987. The role of bacterial cell wall hydrophobicity in adhesion. *Applied and Environmental Microbiology* 53 (8), 1893–1897.
- van Veen, J. A., Ladd, J. N., Martin, J. K., Amato, M., 1987. Turnover of carbon, nitrogen and phosphorus through the microbial biomass in soils incubated with ¹⁴C-, ¹⁵N- and ³²P-labelled bacterial cells. *Soil Biology and Biochemistry* 19 (5), 559–565.

- Vogel, C., Mueller, C. W., Höschen, C., Buegger, F., Heister, K., Schulz, S., Schloter, M., Kögel-Knabner, I., 2014. Submicron structures provide preferential spots for carbon and nitrogen sequestration in soils. *Nature Communications* 5.
- von Lützow, M., Kögel-Knabner, I., Ekschmitt, K., Matzner, E., Guggenberger, G., Marschner, B., Flessa, H., 2006. Stabilization of organic matter in temperate soils: mechanisms and their relevance under different soil conditions - a review. *European Journal of Soil Science* 57 (4), 426–445.
- von Lützow, M., Kögel-Knabner, I., Ludwig, B., Matzner, E., Flessa, H., Ekschmitt, K., Guggenberger, G., Marschner, B., Kalbitz, K., 2008. Stabilization mechanisms of organic matter in four temperate soils: Development and application of a conceptual model. *Journal of Plant Nutrition and Soil Science* 171 (1), 111–124.
- Wallach, R., Ben-Arie, O., Graber, E. R., 2005. Soil water repellency induced by long-term irrigation with treated sewage effluent. *Journal of Environmental Quality* 34 (5), 1910.
- Wei, H., Guenet, B., Vicca, S., Nunan, N., Asard, H., AbdElgawad, H., Shen, W., Janssens, I. A., 2014. High clay content accelerates the decomposition of fresh organic matter in artificial soils. *Soil Biology and Biochemistry* 77 (0), 100 – 108.
- Wershaw, R., 1993. Model for humus in soils and sediments. *Environmental Science & Technology* 27 (5), 814–816.
- Wershaw, R. L., 2004. Evaluation of conceptual models of natural organic matter (humus) from a consideration of the chemical and biochemical processes of humification. Vol. 2004-5121 of Scientific investigations report. U.S. Dept. of the Interior, U.S. Geological Survey and U.S. Geological Survey, Information Services [distributor], Reston Denver, USA.

-
- Wick, L. Y., Pasche, N., Bernasconi, S. M., Pelz, O., Harms, H., 2003. Characterization of multiple-substrate utilization by anthracene-degrading *Mycobacterium frederiksbergense* LB501T. *Applied and Environmental Microbiology* 69 (10), 6133–6142.
- Wingender, J., Neu, T. R., Flemming, H. C. (Eds.), 1999. *Microbial extracellular polymeric substances: Characterization, structure and function*. Springer, Berlin Heidelberg, Germany.
- Young, I. M., Crawford, J. W., 2004. Interactions and self-organization in the soil-microbe complex. *Science* 304 (5677), 1634–1637.
- Young, I. M., Feeney, D. S., O'Donnell, A. G., Goulding, K., 2012. Fungi in century old managed soils could hold key to the development of soil water repellency. *Soil Biology and Biochemistry* 45, 125–127.
- Zausig, J., Stepniewski, W., Horn, R., 1993. Oxygen concentration and redox potential gradients in unsaturated model soil aggregates. *Soil Science Society of America Journal* 57 (4), 908–916.
- Zelles, L., 1997. Phospholipid fatty acid profiles in selected members of soil microbial communities. *Chemosphere* 35 (1-2), 275–294.
- Zhang, W., Ricketts, T. H., Kremen, C., Carney, K., Swinton, S. M., 2007. Ecosystem services and dis-services to agriculture. *Ecological Economics* 64 (2), 253–260.

Publications and Presentations

Parts of this thesis, that have been published or are submitted for publication in peer-reviewed journals

Achtenhagen, J., Miltner, A., Kaestner, M., 2014. Stabilization of microbial cells and their residues in soils - Co-precipitation with Fe and Al oxyhydroxides as an important factor. *Biogeochemistry*, in preparation.

Achtenhagen, J., Goebel, M.-O., Miltner, A., Woche, S. K., Kästner, M., 2014. Bacterial impact on the wetting properties of soil minerals. *Biogeochemistry*, DOI: 10.1007/s10533-014-0040-9.

Further peer-reviewed publications

Ludwig, M., Achtenhagen, J., Miltner, A., Eckhardt, K. U., Leinweber, C., Emmerling, C., Thiele-Bruhn, S., 2014. Microbial contribution to SOM quantity and quality in density fractions of temperate arable soils. *Soil Biology and Biochemistry*, submitted.

Schütze, E., Miltner, A., Nietzsche, S., Achtenhagen, J., Klose, M., Merten, D., Greyer, M., Roth, M., Kästner, M., Kothe, E., 2013. Live and death of streptomyces in soil – what happens to the biomass? *Journal of Plant Nutrition and Soil Science* 176 (5), 665–673.

Achtenhagen J., Kreuzig R., 2011. Laboratory tests on the impact of superabsorbent polymers on transformation and sorption of xenobiotics in soil taking ¹⁴C-imazalil as an example. *Science of the Total Environment* 409 (24), 5454–5458.

Conferences

Achtenhagen, J., Goebel, M.-O., Miltner, A., Woche, S. K., Kästner, M. Bacterial impact on the wetting properties of soil minerals. Oral Presentation. International Symposium of German Priority Programme SPP 1315 "Biogeochemical Interfaces in Soil", Leipzig, Germany, 2014.

Achtenhagen, J., Goebel, M.-O., Miltner, A., Woche, S. K., Kästner, M. Interactions of bacteria with minerals with respect to physical surface properties. Oral Presentation. Deutsche Bodenkundliche Gesellschaft, Jahrestagung, Rostock, Germany, 2013.

Achtenhagen, J., Goebel, M.-O., Miltner, A., Woche, S. K., Kästner, M. Interactions of bacteria with minerals and their effect on physical surface properties. Poster Presentation. Vereinigung für Allgemeine und Angewandte Mikrobiologie, Jahrestagung, Bremen, Germany, 2013.

Achtenhagen, J., Miltner, A., Kästner, M. Poster Presentation. Contribution of cell wall envelopes to soil organic matter formation. Eurosoil, Bari, Italy, 2012.

Danksagung (Acknowledgements)

Als erstes möchte ich Prof. Dr. Matthias Kästner danken, der mir die Arbeit an dieser Dissertation ermöglichte. Danke für die stetige Motivation sowie die fortwährende fachliche und seelische Unterstützung auch in Zeiten, in denen es einmal nicht so lief. Prof. Dr. Ingrid Kögel-Knabner (Technische Universität München) danke ich für die Übernahme des Erstgutachtens und Prof. Dr. Jürgen Geist (TU München) für die Übernahme des Vorsitzes der Prüfungskommission. Ich danke der Deutschen Forschungsgemeinschaft (DFG) (Schwerpunktprogramm 1315 "Biogeochemical Interfaces in Soil", MI 598/2-2), sowie dem UFZ und HIGRADE für die Finanzierung meiner Promotion.

Meiner Betreuerin Dr. Anja Miltner gilt ein besonderer Dank für die fachliche und moralische Unterstützung während der Anfertigung der Promotion.

Mein besonderer Dank geht an Andrea Prager vom Leibniz-Institut für Oberflächenmodifizierung Leipzig (IOM) für die Hilfe bei den unzähligen SEM-Messungen. Weiterhin danke ich Lukas Y. Wick und Jana Reichenbach vom Department Umweltmikrobiologie (UFZ) für den Zugang zum Goniometer. Marc-Oliver Göbel und Susann K. Woche von der Leibniz Universität Hannover danke ich für die fruchtbare Zusammenarbeit, sowie Kontaktwinkel- und ESEM-Messungen. Susan Walter vom UFZ danke ich für die Mithilfe bei der Erstellung der Inkrustierungs-Abbildung. Der Forschungsstelle Leipzig des Helmholtz-Zentrums Dresden-Rossendorf danke ich für den Zugang zum ^{14}C -Labor.

Unendlicher Dank geht an Iris, Christian, Micha, Henrike und Stephi für all den Spaß, Schabernack und Freude im und außerhalb des Labors, sowie den unzähligen Praktikanten, Bachelor- und Masterstudenten, die in den Jahren an der Mittagsrunde teilnahmen und die Zeit der Promotion im nu vergingen ließ.

Ich danke dem gesamten Department für Umweltbiotechnologie für die freundliche Atmosphäre und im Besonderen Kerstin Ethner, Ines Mäusezahl, Kerstin Puschendorf und Claudia Pietsch für die Unterstützung im Labor.

Meiner Familie und meiner Freundin danke ich für die fortwährende seelische und moralische Unterstützung während der Promotionszeit.

Curriculum Vitae

Persönliche Daten

Name	Jan Achtenhagen
Geburtsdatum	29.03.1986
Geburtsort	Rostock
Geburtsland	Deutschland

Bildungsweg

01/2011 – vorauss. Ende 2014 Promotion zum Dr. rer. nat.

Angefertigt am Helmholtz Zentrum für Umweltforschung UFZ Leipzig

Promotionsführende Einrichtung: Technische Universität München

Thema der Promotion

“Dynamic (redox) interfaces in soil - Carbon turnover of microbial residues and their impact on soil properties”

10/2008 – 11/2010 Studium der Geoökologie

Technische Universität Braunschweig

Abschluss: Master of Science

Thema der Masterarbeit:

“Labortests zum Einfluss von Hydrogelen auf das Rückstandsverhalten von Pestiziden im Boden”

- 10/2005–10/2008 Studium der Umweltwissenschaften
Universität Bielefeld
Abschluss: Bachelor of Science
Thema der Bachelorarbeit:
“Entgiftung von Glucosinolaten im Meerrettichblattkäfer, *Phaedon cochleariae*”
- 06/2005 Allgemeine Hochschulreife
Ernst-Barlach-Gymnasium Rostock